STABILIZER DESIGN FOR DYNAMIC STABILITY CONTROL OF MULTIMACHINE POWER SYSTEMS

By

Qinghua Li

B. Sc., Jiangxi Polytechnic University, PRC, 1982

A THESIS SUBMITTED IN PARTIAL FULFILLMENT OF

THE REQUIREMENTS FOR THE DEGREE OF

DOCTOR OF PHILOSOPHY

in

THE FACULTY OF GRADUATE STUDIES

ELECTRICAL ENGINEERING

We accept this thesis as conforming

to the required standard

THE UNIVERSITY OF BRITISH COLUMBIA

December 1991

In presenting this thesis in partial fulfilment of the requirements for an advanced degree at the University of British Columbia, I agree that the Library shall make it freely available for reference and study. I further agree that permission for extensive copying of this thesis for scholarly purposes may be granted by the head of my department or by his or her representatives. It is understood that copying or publication of this thesis for financial gain shall not be allowed without my written permission.

(Signature)

Department of Electrical Engineering

The University of British Columbia
Vancouver, Canada

Date December 20, 1991

DE-6 (2/88)

Abstract

The development of new techniques for stabilizer design has been receiving considerable attention of power system industry. In this thesis, several new stabilizer design techniques are developed for the improvement of dynamic stability of multimachine power systems.

Three kinds of dynamic stability problems are dealt with: the low–frequency oscillations, the stability of power systems with wide–range changing operating conditions and the multi–mode torsional oscillations of a two–machine system. Therefore, different stabilizer design techniques are developed.

First, mathematical models are developed for dynamic studies and stabilizer design of multimachine power systems. Methods are also developed to select the number and the locations of stabilizers for the entire power system.

A new pole–placement technique is developed for a decentralized Power System Stabilizer (PSS) design to control low–frequency oscillations. The computation is economic. The technique is applied to the stabilizer designs of a three–machine system and a nine–machine system. Simulation results show that PSSs thus designed are very effective to control low–frequency oscillations.

A direct self–tuning regulator (STR) design method is developed for power systems with wide–range changing operating conditions. The indirect STR of Clarke based on the Generalized Predictive Control (GPC) method is improved so that the initial step control parameters are directly estimated and that the subsequent control parameters are recursively computed. The techniques developed are applied to the STR design of a nine–machine system. Comprehensive tests show that the STRs designed can effectively

stabilize the power system with wide–range changing operating conditions while well–designed PSSs fail to do so.

Finally, another pole–placement technique is developed for the excitation control of multi–mode torsional oscillations of a power system due to the subsynchronous resonance of a capacitor–compensated transmission line. This is a decentralized linear feedback design. The new technique is applied to the stabilizer design of the Second Benchmark Model of IEEE, System 2. Test results show that stabilizers designed can effectively control the torsional oscillations of the system over a wide–range of capacitor compensations.

Table of Contents

List of Tables

List of Figures

Acknowledgement

I would like to thank my research supervisor Dr. Yao–nan Yu for his invaluable guidance and encouragement throughout the course of this research. I am also indebted for the financial support of Grant A3626 from the Natural Science and Engineering Council, Canada.

I would like to express my gratitude to the Electrical Engineering Department and the UBC Computing Centre for computing support.

Finally, I would like to thank my parents and my wife, Yunwei, for their support throughout my graduate program.

Chapter 1

INTRODUCTION

1.1 Motivation

Increasing electrical energy demand results in higher transmission voltages, more and larger generating units, and more complex interconnections in a power system. New devices such as fast–response excitation system, series capacitor compensated transmission and HVDC transmission are also introduced. As a result, many new problems arise, for example, dynamic and transient stability, subsynchronous resonance, reliability, security, and voltage instability. A great deal of research is going on to solve these problems. This thesis is mainly concerned with the stabilizer design to improve the dynamic stability of power systems, especially multimachine power systems.

The dynamic stability of a multimachine power system will be considered in the more general context that after a disturbance in the system such as a change in load, a change in voltage regulator reference, or a change in governor reference, generators in the system must settle down to the synchronous speed. Supplementary stabilizers are usually required for a poorly damped or negatively damped power system to improve its dynamic stability. Control signals generated by these stabilizers may be applied through the excitation loops and/or the governor loops of the generating units that have poorly damped or negatively damped mechanical modes.

One dynamic stability problem is the low-frequency oscillation of a power system, which is usually stabilized by Power System Stabilizer (PSS). PSS has been developed

for power system for many years. However, designing PSSs for multimachine systems remains a challenging problem because the stabilizers must be decentralized in structure and only locally measurable signals are used for feedback.

There are two prerequisite decisions to be made prior to multimachine PSS design: 1) how many stabilizers are required and 2) where they should be located. Obviously, the stabilizers must be located at the most strategic locations so that the number of stabilizers can be minimized. However, methods of finding the strategic locations require improvement.

The power system operating conditions are not necessarily constant. Indeed, they are constantly changing for a large power system. The self–tuning regulator (STR) has been used in industries other than power system for many years. It may also be beneficial for power systems to have STR–type stabilizers.

There is another type of dynamic stability problem in a power system, the multi–mode torsional oscillations of turbine–generator shaft due to the subsynchronous resonance (SSR) of series–capacitor compensated transmission network. Designing stabilizers for a power system with SSR, especially for a multimachine system, is also a challenging problem of dynamic stability control. The IEEE SSR Working Group has published System 2, Benchmark Model II for the study of such phenomena.

1.2 Objectives of the Thesis

The main objectives of the thesis are:

1. To develop mathematical models for multimachine dynamic stability analyses, stabilizer designs and nonlinear high–order digital simulations.

2. To develop a precise technique to determine the number and location of stabilizers for multimachine system stabilizer design.

3. To develop a pole-placement technique for decentralized PSS design in order to stabilize multimachine power systems with low–frequency oscillations.

4. To develop an efficient algorithm for a direct multiple-input multiple–output (MIMO) self–tuning stabilizer design in order to control multimachine power systems with wide–range changing operating conditions.

5. To develop a direct pole–placement method for a decentralized linear feedback control design in order to stabilize the multi–mode shaft torsional oscillations of a two-machine system.

1.3 Outline of the Thesis

In Chapter 2, a basic multimachine power system model for dynamic stability studies is developed. The transmission network equations are related to individual machine equations in d-q coordinates. Based on this model, a linearized model for eigenvalue analysis and stabilizer designs, and a discretized model for nonlinear digital simulations are derived.

Methods to determine the number and site of stabilizers are developed in Chapter 3. Besides the participation factor method of linear analysis, a speed deviation index method based on nonlinear simulation is proposed. Numerical examples are included.

For the PSS design of multimachine power systems, a new pole–placement technique with less computation than the existing methods is developed in Chapter 4. The design procedures are illustrated by two example systems: a three–machine system [21] and a nine–machine system [3]. The effectiveness of the proposed design method is demonstrated.

A new design technique of a direct MIMO self–tuning regulator (STR) for a multimachine power system with wide-range changing operating conditions is developed in

Chapter 5. This is an extension of the principle of Clarke's indirect SISO GPC [29] with two improvements: the direct estimate of initial step control parameters and the recursive computation of subsequent control parameters. A nine–machine system is chosen as an example for the design. The system with designed STRs is thoroughly tested over wide–range changing operating conditions.

The problem of multimachine multi-mechanical mode torsional oscillations due to subsynchronous resonance (SSR) has been posed as System 2 of the Second Benchmark Model (SBM) by IEEE SSR Working Group [43]. The system has two nonidentical machines and a series–capacitor compensated transmission network. Decentralized linear feedback stabilizers are designed for the excitation control of torsional oscillations of the system in Chapter 6. For the design, a detailed mathematical model of the system is derived and a new direct pole–placement design method is developed. Participation factors are used to find the most effective variables for feedback. Computer simulations of the system are carried out to examine the performance of the designed stabilizers.

Conclusions and achievements of the thesis are summarized in Chapter 7. Further developments of the thesis area are also recommended.

Chapter 2

SYSTEM MODELS FOR STABILIZER DESIGN AND SIMULATION

For stabilizer design and simulation of a multimachine power system, mathematical modeling is desirable. Power system component models are presented in Section 2.1 and a complete system model is presented in Section 2.2. From the complete system model, a linearized model for eigenvalue analysis and stabilizer design is derived in Section 2.3 and a discretized model for computer simulation test in Section 2.4.

2.1 Component Models of a Power System

2.1.1 Synchronous Generator

The torque equations for a synchronous generator may be written as

$$\dot{\omega} = \frac{1}{M}(T_m - T_e - D\omega) \tag{2.1}$$

$$\dot{\delta} = \omega_b(\omega - 1.0) \tag{2.2}$$

where

ω	:	generator rotor speed
ω_b	:	base speed
δ	:	rotor angle
T_m, T_e	:	mechanical input and electric output torques
M, D	:	inertial constant and damping coefficient

and the dot over a variable denotes the derivative with respect to time. All values are in per unit, except δ in rad, ω_b in 2πf rad/s, and M in second.

Assuming one damper winding per rotor axis, the voltage equations for the generator rotor windings [1] are

$$\dot{e}_q^{'} = \frac{1}{T_{d0}^{'}}[E_{FD} - e_q^{'} - i_d(x_d - x_d^{'})] \tag{2.3}$$

$$\dot{e}_q^{''} = \frac{1}{T_{d0}^{''}}[-e_q^{''} - i_d(x_d^{'} - x_d^{''}) + e_q^{'} + T_{d0}^{''}\dot{e}_q^{'}] \tag{2.4}$$

$$\dot{e}_d^{''} = \frac{1}{T_{q0}^{''}}[-e_d^{''} + i_q(x_q - x_q^{''})] \tag{2.5}$$

where

$e_q^{'}$	:	q transient voltage of a field winding F
$e_q^{''}$	:	q subtransient voltage of a D damper winding
$e_d^{''}$	:	d subtransient voltage of a Q damper winding
x_d, $x_d^{'}$, $x_d^{''}$	:	d–axis synchronous, transient and subtransient reactances
x_q, $x_q^{''}$	:	q–axis synchronous and subtransient reactances
$T_{d0}^{'}$, $T_{d0}^{''}$	:	armature–open–circuited d–axis transient and subtransient time constants
$T_{q0}^{''}$	:	armature–open–circuited q–axis subtransient time constant
E_{FD}	:	field voltage as seen from the armature
i_d, i_q	:	d–axis and q–axis components of armature current

All values are in per unit, except time constants in seconds.

For low–frequency oscillation and dynamic stability studies, the stator armature and the transmission network are usually described by algebraic equations since, in most cases, their eigenmode frequencies are very high and the decay is very fast. Therefore, the armature voltage equations may be written as

$$\begin{bmatrix} v_d \\ v_q \end{bmatrix} = \begin{bmatrix} e_d^{''} \\ e_q^{''} \end{bmatrix} + \begin{bmatrix} -R_a & x_q^{''} \\ -x_d^{''} & -R_a \end{bmatrix} \begin{bmatrix} i_d \\ i_q \end{bmatrix} \tag{2.6}$$

A subscript "k" should be given to signify the k–th generator, but is dropped here for clarity.

2.1.2 Excitation System

Assuming a fast–response exciter and voltage regulator system, the differential equation for the excitation system may be written as

$$\dot{E}_{FD} = \frac{1}{T_A}[K_A u_E - K_A(v_t - v_{ref}) - (E_{FD} - E_{FD0})] \tag{2.7}$$

with the following constraints

$$E_{min.} \leq E_{FD} \leq E_{max.}$$

where T_A denotes a time constant, K_A an overall gain, v_t the generator terminal voltage, v_{ref} a reference voltage, and u_E a supplementary excitation control signal, if any. $E_{max.}$ and $E_{min.}$ are the constraints for E_{FD}. The block diagram for the excitation system is shown in Fig. 2.1

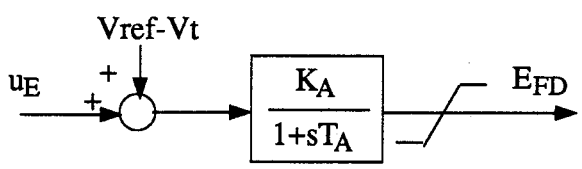

Figure 2.1: A Fast Excitation System

2.1.3 Governor Systems

Two types of governors are considered, a mechanical–hydraulic governor for a hydro–electric plant and an electrical–hydraulic governor for a thermo–electric plant. The differential equations of the hydro turbine and governor system [2] for the hydro–electric

plant are given by

$$
\begin{aligned}
\dot{G}1 &= \frac{1}{T_p}(u_G + \omega_{ref} - \omega - G2 - \sigma G1) \\
\dot{G}2 &= \frac{-G2}{T_r} + \delta_T \dot{G}1 \\
\dot{G}3 &= \frac{G1 - G3}{T_g} \\
\dot{T}_m &= \frac{(G3 - T_m + G_0)}{0.5T_\omega} - \frac{\dot{G}3}{0.5}
\end{aligned}
\tag{2.8}
$$

with the following governor speed and opening constraints

$$
GS_{min.} \leq \frac{G1 - G3}{T_g} \leq GS_{max.}
$$

$$
GO_{min.} \leq (G3 + G_0) \leq GO_{max.}
$$

In these equations, $G1$ represents the output of an actuator, $G2$ that of a dashpot, $G3$ that of a gate servo, G_0 the initial value of gate opening, and T_m the mechanical torque output of the hydro turbine. U_G is a supplementary governor control signal, if any. $GS_{min.}$, $GS_{max.}$, $GO_{min.}$ and $GO_{max.}$ are the gate speed and opening constraints. The block diagram for the governor–turbine system is shown in Fig. 2.2 (a)

The differential equations of a non-reheat steam turbine and governor system for the thermo–electric plant are given by

$$
\begin{aligned}
\dot{G} &= \frac{(u_G + \omega_{ref} - \omega)k_g - G}{T_{sm}} \\
\dot{T}_m &= \frac{(G + G_0 - T_m)}{T_{CH}}
\end{aligned}
\tag{2.9}
$$

with the following governor speed and opening constraints

$$
GS_{min.} \leq \dot{G} \leq GS_{max.}
$$

$$
GO_{min.} \leq (G + G_0) \leq GO_{max.}
$$

In these equations, G represents the output of a gate servo and T_m the mechanical torque output of the steam turbine. U_G is a supplementary governor control signal, if

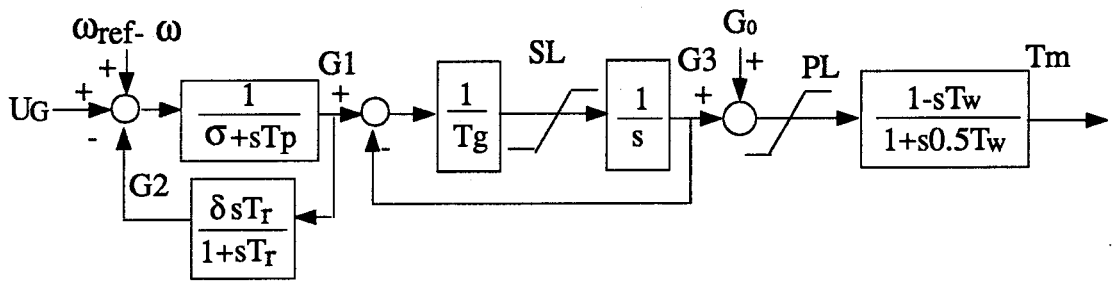

(a) Hydro Turbine and Governor

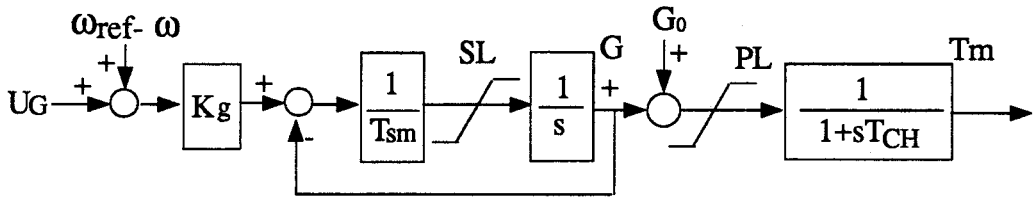

(b) Steam Turbine and Governor

Figure 2.2: Hydro Turbine, Steam Turbine, and Governors

any. $GS_{min.}$, $GS_{max.}$, $GO_{min.}$ and $GO_{max.}$ are the gate speed and opening constraints. The block diagram for the governor–turbine system is shown in Fig. 2.2 (b)

2.1.4 Power System Stabilizer

A conventional Power System Stabilizer (PSS) is shown in Fig. 2.3. It has two lead–lag components and one reset block. The differential equations for the PSS are

$$\begin{aligned} \dot{x}_{ps1} &= -\frac{x_{ps1}}{T} + \dot{\omega} \\ \dot{x}_{ps2} &= -\frac{x_{ps2}}{T_2} + \frac{K_c}{T_2} x_{ps1} + \frac{K_c T_1}{T_2} \dot{x}_{ps1} \\ \dot{u}_E &= -\frac{u_E}{T_2} + \frac{1}{T_2} x_{ps2} + \frac{T_1}{T_2} \dot{x}_{ps2} \end{aligned} \tag{2.10}$$

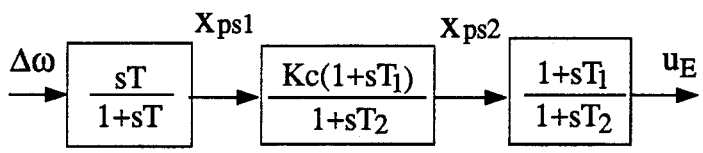

Figure 2.3: Transfer Function of PSS

2.1.5 Transmission Network

For low-frequency oscillation and dynamic stability studies, the transmission network is usually described by algebraic equations since its eigenmode frequency is very high and the decay is very fast. The equations of a transmission network of an m–machine power system are given by

$$[I_{D,Q}] = [Y][V_{D,Q}] \tag{2.11}$$

where $[I_{D,Q}]$ and $[V_{D,Q}]$ respectively includes the D and Q components of all generator armature currents and voltages

$$\begin{aligned}[I_{D,Q}] &= [i_{D1}, i_{Q1}, i_{D2}, i_{Q2}, \ldots, i_{Dm}, i_{Qm}]^T \\ [V_{D,Q}] &= [v_{D1}, v_{Q1}, v_{D2}, v_{Q2}, \ldots, v_{Dm}, v_{Qm}]^T\end{aligned}$$

$[Y]$ is the admittance matrix of the transmission network, which is obtained from the results of a load flow study by eliminating all non–generator buses

$$[Y] = \begin{bmatrix} [y_{11}] & [y_{12}] & \cdots & [y_{1m}] \\ [y_{21}] & [y_{22}] & \cdots & [y_{2m}] \\ \vdots & \vdots & \vdots & \vdots \\ [y_{m1}] & [y_{m2}] & \cdots & [y_{mm}] \end{bmatrix}$$

where

$$[y_{ij}] = \begin{bmatrix} G_{ij} & -B_{ij} \\ B_{ij} & G_{ij} \end{bmatrix}$$

and G_{ij} denotes the real component and B_{ij} the imaginary component of the admittance y_{ij}.

2.2 Complete Model of an M–machine System

Let all differential equations for the k-th machine obtained in section 2.1 be expressed as

$$[\frac{d\mathbf{Y_k}}{dt}] = [F(\mathbf{Y_k},\ i_{dk},\ i_{qk},\ v_{tk})] \tag{2.12}$$

where $\mathbf{Y_k}$ is a vector containing all state variables and i_{dk}, i_{qk} and v_{tk} are non–state variables. The terminal voltage v_{tk} may be expressed as

$$v_{tk} = \sqrt{v_{dk}^2 + v_{qk}^2} \quad or \quad v_{tk} = \sqrt{v_{Dk}^2 + v_{Qk}^2}$$

Let an additional subscript k be added to Eqs. (2.6) to signify the armature voltages of the k–th generator

$$\begin{bmatrix} v_{dk} \\ v_{qk} \end{bmatrix} = \begin{bmatrix} e''_{dk} \\ e''_{qk} \end{bmatrix} + \begin{bmatrix} -R_{ak} & x''_{qk} \\ -x''_{dk} & -R_{ak} \end{bmatrix} \begin{bmatrix} i_{dk} \\ i_{qk} \end{bmatrix} \tag{2.13}$$

The armature currents for the k–th generator can be obtained from Eq. (2.11)

$$\begin{bmatrix} i_{Dk} \\ i_{Qk} \end{bmatrix} = \begin{bmatrix} \sum_{j=1}^{m}(G_{kj}v_{Dj} - B_{kj}v_{Qj}) \\ \sum_{j=1}^{m}(B_{kj}v_{Dj} + G_{kj}v_{Qj}) \end{bmatrix} \tag{2.14}$$

While the armature current and voltage components in Eq. (2.14) are described by D–Q coordinate of the system network, those in Eqs. (2.12) and (2.13) are described by individual d–q coordinates of the k-th generator. Coordinate transformation must be carried out. Since there are more equations (2.12) and (2.13), which includes i_{dk} and i_{qk}, there will be less computation if the currents i_{Dk} and i_{Qk} of Eqs. (2.14) are transformed into the i_{dk} and i_{qk}. As for the armature voltage, since there are more v_D's and v_Q's in Eq. (2.14), it is preferred that only the voltages v_{dk} and v_{qk} of Eq. (2.13) be transformed to v_{Dk} and v_{Qk}. As result, Eq. (2.13) and Eq. (2.14) becomes

$$\begin{bmatrix} \sin\delta_k & -\cos\delta_k \\ \cos\delta_k & \sin\delta_k \end{bmatrix} \begin{bmatrix} v_{Dk} \\ v_{Qk} \end{bmatrix} = \begin{bmatrix} e''_{dk} \\ e''_{qk} \end{bmatrix} + \begin{bmatrix} -R_{ak} & x''_{qk} \\ -x''_{dk} & -R_{ak} \end{bmatrix} \begin{bmatrix} i_{dk} \\ i_{qk} \end{bmatrix} \tag{2.15}$$

and

$$\begin{bmatrix} \sin\delta_k & \cos\delta_k \\ -\cos\delta_k & \sin\delta_k \end{bmatrix} \begin{bmatrix} i_{dk} \\ i_{qk} \end{bmatrix} = \begin{bmatrix} \sum_{j=1}^{m}(G_{kj}v_{Dj} - B_{kj}v_{Qj}) \\ \sum_{j=1}^{m}(B_{kj}v_{Dj} + G_{kj}v_{Qj}) \end{bmatrix} \tag{2.16}$$

where δ_k is the rotor angle of the k–th generator and is one of the state variables in $\mathbf{Y_k}$ of (2.12). The four algebraic equations of Eqs. (2.15) and (2.16), which are required for the four non–state variables v_{Dk}, v_{Qk}, i_{dk}, and i_{qk}, and all differential equations of (2.12)

form a complete mathematical model for the k-th generator as follows

$$
\begin{aligned}
&[\tfrac{d\mathbf{Y_k}}{dt}] = [F(\mathbf{Y_k},\ i_{dk},\ i_{qk},\ v_{Dk},\ v_{Qk})] \\
&\begin{bmatrix} \sin\delta_k & -\cos\delta_k \\ \cos\delta_k & \sin\delta_k \end{bmatrix} \begin{bmatrix} v_{Dk} \\ v_{Qk} \end{bmatrix} = \begin{bmatrix} e''_{dk} \\ e''_{qk} \end{bmatrix} + \begin{bmatrix} -R_{ak} & x''_{qk} \\ -x''_{dk} & -R_{ak} \end{bmatrix} \begin{bmatrix} i_{dk} \\ i_{qk} \end{bmatrix} \\
&\begin{bmatrix} \sin\delta_k & \cos\delta_k \\ -\cos\delta_k & \sin\delta_k \end{bmatrix} \begin{bmatrix} i_{dk} \\ i_{qk} \end{bmatrix} = \begin{bmatrix} \sum_{j=1}^{m}(G_{kj}v_{Dj} - B_{kj}v_{Qj}) \\ \sum_{j=1}^{m}(B_{kj}v_{Dj} + G_{kj}v_{Qj}) \end{bmatrix}
\end{aligned}
\tag{2.17}
$$

For a power system of m machines, there are m sets of Eqs. (2.17). The last equation of Eqs. (2.17) shows the interconnection of all machines. This system model will be used for most dynamic stability studies in this thesis.

2.3 Linear Model for Eigenvalue study and Stabilizer Design

For eigenvalue analysis and controller design of a multimachine power system, a linear state model is used. The model consists of linearized first–order differential equations with state variables only. These equations are derived from the nonlinear differential equations obtained in the previous section. The non–state variables v_D, v_Q, i_d, and i_q must be eliminated.

For dynamic stability studies, the effects of rotor D and Q damper windings, e''_q and e''_d, are usually ignored. The reason for this is that a damper winding of a synchronous generator may be considered as a short–circuited winding of a transformer or an induction motor and the voltages induced in these windings at the low frequencies are negligibly small. The governor system is also ignored because its dynamic response is usually slow and hence the governor output may be treated as a constant. With these considerations, there are four differential equations remaining for each machine and the linearized equations may be rewritten in a matrix form as

$$\dot{x} = Ax + Cy \tag{2.18}$$

where

$$
\begin{aligned}
x &= [\Delta\delta, \Delta\omega, \Delta e_q^{'}, \Delta E_{FD}]^T \\
y &= [\Delta i_d, \Delta i_q]^T
\end{aligned}
$$

In Eq. (2.18), the currents Δi_d and Δi_q are written separately. They are the interacting variables of machines of the system. A is a 4×4 matrix and C a 4×2 matrix. $\Delta x = x(t) - x(0)$, and $x(0)$ is the given initial operating point of $x(t)$.

The multimachine linear model that has been developed for a decentralized optimal stabilizer design [3] can be derived in a slightly different way as follows. For a power system with m machines, there are m sets of Eqs. (2.18) and a subscript "k", k=1, 2, ..., m, may be added to signify the k–th machine. The m sets of equations may also be written in a matrix form as

$$
\begin{bmatrix} \dot{x}_1 \\ \dot{x}_2 \\ \vdots \\ \dot{x}_m \end{bmatrix} = \begin{bmatrix} A_1 & & & \mathbf{0} \\ & A_2 & & \\ & & \ddots & \\ \mathbf{0} & & & A_m \end{bmatrix} \begin{bmatrix} x_1 \\ x_2 \\ \vdots \\ x_m \end{bmatrix} + \begin{bmatrix} C_1 & & & \mathbf{0} \\ & C_2 & & \\ & & \ddots & \\ \mathbf{0} & & & C_m \end{bmatrix} \begin{bmatrix} \Delta i_{d1} \\ \Delta i_{q1} \\ \Delta i_{d2} \\ \Delta i_{q2} \\ \vdots \\ \Delta i_{dm} \\ \Delta i_{qm} \end{bmatrix} \tag{2.19}
$$

Next, the armature voltages and currents are non–state variables and they must be eliminated. Since the effects of the damper winding have been ignored, Eqs. (2.15) for armature voltages should be modified as

$$
\begin{bmatrix} \sin\delta_k & -\cos\delta_k \\ \cos\delta_k & \sin\delta_k \end{bmatrix} \begin{bmatrix} v_{Dk} \\ v_{Qk} \end{bmatrix} = \begin{bmatrix} 0 \\ 1 \end{bmatrix} e_{qk}^{'} + \begin{bmatrix} -R_{ak} & x_{qk} \\ -x_{dk}^{'} & -R_{ak} \end{bmatrix} \begin{bmatrix} i_{dk} \\ i_{qk} \end{bmatrix} \tag{2.20}
$$

Linearization of Eqs. (2.20) gives

$$[D_k]\,\Delta\delta_k + [E_k]\begin{bmatrix}\Delta v_{Dk}\\ \Delta v_{Qk}\end{bmatrix} = \begin{bmatrix}0\\1\end{bmatrix}\Delta e'_{qk} + \begin{bmatrix}-R_{ak} & x_{qk}\\ -x'_{dk} & -R_{ak}\end{bmatrix}\begin{bmatrix}\Delta i_{dk}\\ \Delta i_{qk}\end{bmatrix} \tag{2.21}$$

where

$$[D_k] = \begin{bmatrix}\cos\delta_{k0}v_{Dk0} + \sin\delta_{k0}v_{Qk0}\\ -sin\delta_{k0}v_{Dk0} + \cos\delta_{k0}v_{Qk0}\end{bmatrix}, \quad [E_k] = \begin{bmatrix}\sin\delta_{k0} & -\cos\delta_{k0}\\ \cos\delta_{k0} & \sin\delta_{k0}\end{bmatrix}$$

where a variable with a subscript 0 denotes its initial value and should be treated as known quantity. Next, linearization of the armature current equations (2.16) gives

$$[F_k]\,\Delta\delta_k + [H_k]\begin{bmatrix}\Delta i_{dk}\\ \Delta i_{qk}\end{bmatrix} = \begin{bmatrix}\sum_{j=1}^{m}(G_{kj}\Delta v_{Dj} - B_{kj}\Delta v_{Qj})\\ \sum_{j=1}^{m}(B_{kj}\Delta v_{Dj} + G_{kj}\Delta v_{Qj})\end{bmatrix} \tag{2.22}$$

where

$$[F_k] = \begin{bmatrix}\cos\delta_{k0}i_{dk0} - \sin\delta_{k0}i_{qk0}\\ \sin\delta_{k0}i_{dk0} + \cos\delta_{k0}i_{qk0}\end{bmatrix} \quad \text{and} \quad [H_k] = \begin{bmatrix}\sin\delta_{k0} & \cos\delta_{k0}\\ -\cos\delta_{k0} & \sin\delta_{k0}\end{bmatrix}$$

Eqs. (2.21) and (2.22) respectively can be rewritten as

$$\begin{bmatrix}\Delta v_{Dk}\\ \Delta v_{Qk}\end{bmatrix} = [J_k]_{2\times2}\begin{bmatrix}\Delta i_{dk}\\ \Delta i_{qk}\end{bmatrix} + [L_k]_{2\times4}\,[x_k] \tag{2.23}$$

and

$$\begin{bmatrix}\Delta i_{dk}\\ \Delta i_{qk}\end{bmatrix} = [M_k]_{2\times2m}\,[\Delta v_{D1}, \Delta v_{Q1}, \Delta v_{D2}, \Delta v_{Q2}, \ldots, \Delta v_{Dm}, \Delta v_{Qm}]^T + [N_k]_{2\times4}\,[x_k] \tag{2.24}$$

There are m sets of Eqs. (2.24) for m machines and they can be assembled into a matrix

equation

$$\begin{bmatrix} \Delta i_{d1} \\ \Delta i_{q1} \\ \Delta i_{d2} \\ \Delta i_{q2} \\ \vdots \\ \Delta i_{dm} \\ \Delta i_{qm} \end{bmatrix} = \begin{bmatrix} M_1 \\ M_2 \\ \vdots \\ M_m \end{bmatrix} \begin{bmatrix} \Delta v_{D1} \\ \Delta v_{Q1} \\ \Delta v_{D2} \\ \Delta v_{Q2} \\ \vdots \\ \Delta v_{Dm} \\ \Delta v_{Qm} \end{bmatrix} + \begin{bmatrix} N_1 & & & \mathbf{0} \\ & N_2 & & \\ & & \ddots & \\ \mathbf{0} & & & N_m \end{bmatrix} \begin{bmatrix} x_1 \\ x_2 \\ \vdots \\ x_m \end{bmatrix} \tag{2.25}$$

There are also m sets of Eqs. (2.23) for m machines and they can be substituted into Eqs. (2.25) to eliminate the voltage vector. With the substitution, Eqs. (2.25) becomes

$$\begin{bmatrix} \Delta i_{d1} \\ \Delta i_{q1} \\ \Delta i_{d2} \\ \Delta i_{q2} \\ \vdots \\ \Delta i_{dm} \\ \Delta i_{qm} \end{bmatrix} = [P]_{2m \times 4m} \begin{bmatrix} x_1 \\ x_2 \\ \vdots \\ x_m \end{bmatrix} \tag{2.26}$$

Substituting Eq. (2.26) into Eq. (2.19) gives

$$\begin{bmatrix} \dot{x}_1 \\ \dot{x}_2 \\ \vdots \\ \dot{x}_m \end{bmatrix} = \begin{bmatrix} A_{11} & A_{12} & \dots & A_{1m} \\ A_{21} & A_{22} & \dots & A_{2m} \\ \vdots & & & \vdots \\ A_{m1} & A_{m2} & \dots & A_{mm} \end{bmatrix} \begin{bmatrix} x_1 \\ x_2 \\ \vdots \\ x_m \end{bmatrix} \tag{2.27}$$

For conciseness, Eq. (2.27) is usually written as

$$[\dot{x}] = [A][x] \tag{2.28}$$

where $[x]$ is a $4m \times 1$ state vector representing the perturbation of the system state from its chosen operating point. $[A]$ is a $4m \times 4m$ system matrix depending on the system parameters as well as the system operating condition. Eq. (2.28) is the linear model of the open–loop m–machine power system, which will be used for eigenvalue analysis and stabilizer design in Chapter 3 and Chapter 4.

2.4 Discretized Model for Computer Simulation

For dynamic stability studies of power systems, the dynamic responses of the power systems with and without supplementary stabilizer are usually investigated by digital computer simulations. The major task of simulations is to simultaneously solve all differential and algebraic equations of Section 2.2. Let the two differential and algebraic equation sets be written in matrix form, respectively as

$$[\frac{d\mathbf{Y(t)}}{dt}] = [F(\mathbf{Y(t)}, \mathbf{Z(t)})] \tag{2.29}$$

$$[\Phi(\mathbf{Y(t)}, \mathbf{Z(t)})] = [\mathbf{0}] \tag{2.30}$$

where $\mathbf{Y}$ is a vector containing all state variables and $\mathbf{Z}$ is a vector containing all non–state variables (i_d, i_q, v_D, and v_Q of all generators).

Usually, the differential equations, Eqs. (2.29), are solved using some integration techniques including the Runge–Kutta method while the algebraic equations, Eqs. (2.30), are solved by a numerical method. Hence, the equations are solved in two separate loops and the interface error between the two loops must be dealt with. This is not desirable. A better method is to use the trapezoidal rule of integration to transform Eqs. (2.29) into a set of algebraic equations so that all equations to be solved are algebraic equations and can be solved simultaneously.

2.4.1 Trapezoidal Rule of Integration

Consider a differential equation of Eq. (2.29)

$$\frac{dy(t)}{dt} = f[Y(t), Z(t)] \tag{2.31}$$

Since the time responses of $y(t)$ are computed on a digital computer at discrete intervals of time (step size Δt), the numerical solution of Eq. (2.31) at time t may be expressed in integral form as

$$y(t) - y(t - \Delta t) = \int_{t-\Delta t}^{t} f[Y(\tau), Z(\tau)]d\tau \tag{2.32}$$

Since the RHS of Eq. (2.32) may equal the trapezoidal area of

$$\frac{\Delta t}{2}\{f[Y(t - \Delta t), Z(t - \Delta t)] + f[Y(t), Z(t)]\}$$

we have

$$y(t) = \frac{\Delta t}{2} f[Y(t), Z(t)] + y_0 \tag{2.33}$$

with y_0 known from the solution at the preceding time step,

$$y_0 = y(t - \Delta t) + \frac{\Delta t}{2} f[Y(t - \Delta t), Z(t - \Delta t)] \tag{2.34}$$

The trapezoidal rule has been discussed in detail in Electromagnetic Transients Program (EMTP) [4]. The error introduced by the trapezoidal rule of integration is negligible for a very small step size Δt.

The following is an example. Consider Eq. (2.4)

$$\dot{e}_q'' = \frac{1}{T_{d0}''}[-e_q'' - i_d(x_d' - x_d'') + e_q' + T_{d0}''\dot{e}_q']$$

It may be rewritten as

$$\frac{d}{dt}(e_q'' - e_q') = \frac{1}{T_{d0}''}[-e_q'' - i_d(x_d' - x_d'') + e_q']$$

Therefore

$$\begin{aligned} y(t) &= e_q^{''} - e_q^{'} \\ f[Y(t), Z(t)] &= \frac{1}{T_{d0}^{''}}[-e_q^{''} - i_d(x_d^{'} - x_d^{''}) + e_q^{'}] \end{aligned}$$

From the trapezoidal rule Eqs. (2.33) and (2.34), we have

$$e_q^{''} - e_q^{'} = \frac{\Delta t}{2T_{d0}^{''}}[-e_q^{''} - i_d(x_d^{'} - x_d^{''}) + e_q^{'}] + y_0 \tag{2.35}$$

and

$$y_0 = e_q^{''} - e_q^{'} + \frac{\Delta t}{2T_{d0}^{''}}[-e_q^{''} - i_d(x_d^{'} - x_d^{''}) + e_q^{'}] \tag{2.36}$$

where y_0 is calculated from the values of variables at $time = t - \Delta t$ and hence is treated as known quantities at $time = t$. Rearranging Eq (2.35) and (2.36) yields

$$e_q^{''} = e_q^{'} - a_{e''q} i_d(x_d^{'} - x_d^{''}) + b_{e''q}$$

where

$$\begin{aligned} a_{e''q} &= \frac{\Delta t}{2T_{d0}^{''} + \Delta t} \\ b_{e''q} &= e_q^{''} - e_q^{'} + a_{e''q}[2(e_q^{'} - e_q^{''}) - i_d(x_d^{'} - x_d^{''})] \end{aligned}$$

The $b_{e''q}$ includes the values of variables at $time = t - \Delta t$. Hence, besides a, b is the known coefficient at $time = t$

2.4.2 Obtaining Algebraic Equations from Differential Equations

In this subsection, the differential equations of a power system will be transformed to algebraic equations according to the trapezoidal rule of integration. The resultant a and b coefficients of these algebraic equations obtained are listed in detail in Table 2.1. Note that the computation of b coefficients requires the values of some variables at $time = t - \Delta t$,

which must be updated after every Δt. However, both a and b coefficients are always treated as known quantities at $time = t$.

Applying the trapezoidal rule of integration, the following algebraic equations are obtained.

Governor for a hydro–electric plant. From differential equations (2.8) we have

$$\begin{aligned} G1 &= a_{g1}(\omega_{ref} - \omega - G2 + u_G) + b_{g1} \\ G2 &= a_{g2}G1 + b_{g2} \\ G3 &= \frac{a_{g3}(G1 - G3)}{T_g} + b_{g3}\ , \qquad GS_{min.} \leq \frac{G1 - G3}{T_g} \leq GS_{max.} \\ T_m &= a_{tm1}G3 + a_{tm2}G_0 + b_{tm}\ , \qquad GO_{min.} \leq (G3 + G_0) \leq GO_{max.} \end{aligned} \tag{2.37}$$

Torque equations of the generator. From the differential equations (2.1) and (2.2) we have

$$\omega = a_\omega(T_m - T_e) + b_\omega\ , \qquad T_e = e_d^{''} i_d + e_q^{''} i_q - (x_d^{''} - x_q^{''}) i_d i_q \tag{2.38}$$

$$\delta = a_\delta(\omega - 1.0) + b_\delta \tag{2.39}$$

Power system stabilizer. From the differential equations (2.10), we have

$$\begin{aligned} x_{ps1} &= a_{ps1}\omega + b_{ps1} \\ x_{ps2} &= a_{ps2}x_{ps1} + b_{ps2} \\ u_E &= a_{ue}x_{ps2} + b_{ue} \end{aligned} \tag{2.40}$$

Excitation system, F winding and D damper winding. From the differential equations (2.7), (2.3) and (2.4), we have

$$\begin{aligned} E_{Fd} &= a_{efd}(u_E - \sqrt{v_D^2 + v_Q^2} + v_{ref}) + b_{efd}\ , \quad E_{min.} \leq E_{FD} \leq E_{max.} \\ e_q^{'} &= a_{e'q}[E_{FD} - i_d(x_d - x_d^{'})] + b_{e'q} \\ e_q^{''} &= e_q^{'} - a_{e''q} i_d (x_d^{'} - x_d^{''}) + b_{e''q} \end{aligned} \tag{2.41}$$

Table 2.1: a and b Coefficients

$a_{g1} = \frac{\Delta t}{2T_p+\sigma\Delta t}$	$b_{g1} = G1 + a_{g1}(\omega_{ref} - \omega - G2 - 2\sigma G1 + u_G)$
$a_{g2} = \frac{2T_r\delta_T}{2T_r+\Delta t}$	$b_{g2} = (\frac{2a_{g2}}{\delta_T} - 1)G2 - a_{g2}G1$
$a_{g3} = \frac{\Delta t}{2}$	$b_{g3} = G3 + \frac{a_{g3}(G1-G3)}{T_g}$
$a_{tm1} = \frac{\Delta t-2T_\omega}{T_\omega+\Delta t}$ $a_{tm2} = \frac{\Delta t}{T_\omega+\Delta t}$	$b_{tm} = (2a_{tm2} - a_{tm1})G3 + (1 - 2a_{tm2})T_m + a_{tm2}G_0$
$a_\omega = \frac{\Delta t}{2M+D\Delta t}$	$b_\omega = \omega + a_\omega(T_m - T_e - 2D\omega)$
$a_\delta = \frac{\Delta t\omega_b}{2}$	$b_\delta = \delta + a_\delta(\omega - 1.0)$
$a_{ps1} = \frac{2T}{2T+\Delta t}$	$b_{ps1} = \frac{2T-\Delta t}{2T+\Delta t}x_{ps1} - a_{ps1}\omega$
$a_{ps2} = \frac{K_c(2T_1+\Delta t)}{2T_2+\Delta t}$	$b_{ps2} = \frac{K_c(\Delta t-2T_1)}{2T_2+\Delta t}x_{ps1} + \frac{2T_2-\Delta t}{2T_2+\Delta t}x_{ps2}$
$a_{ue} = \frac{2T_1+\Delta t}{2T_2+\Delta t}$	$b_{ue} = \frac{\Delta t-2T_1}{2T_2+\Delta t}x_{ps2} + \frac{2T_2-\Delta t}{2T_2+\Delta t}u_E$
$a_{efd} = \frac{\Delta t K_A}{2T_A+\Delta t}$	$b_{efd} = E_{FD} + a_{efd}(u_E - \sqrt{v_D^2 + v_Q^2} + v_{ref} - \frac{2(E_{FD}-E_{FD0})}{K_A})$
$a_{e'q} = \frac{\Delta t}{2T'_{d0}+\Delta t}$	$b_{e'q} = e'_q + a_{e'q}[E_{FD} - 2e'_q - i_d(x_d - x'_d)]$
$a_{e''q} = \frac{\Delta t}{2T''_{d0}+\Delta t}$	$b_{e''q} = e''_q - e'_q + a_{e''q}[2(e'_q - e''_q) - i_d(x'_d - x''_d)]$
$a_{e''d} = \frac{\Delta t}{2T''_{q0}+\Delta t}$	$b_{e''d} = e''_d + a_{e''d}[i_q(x_q - x''_q) - 2e''_d]$

Q damper winding. Finally, from the differential equation (2.5) we have

$$e_d'' = a_{e''d} i_q (x_q - x_q'') + b_{e''d} \tag{2.42}$$

2.4.3 Reduced Equations

To save computation time, the number of equations involved in the numerical solution for the complete system will be minimized. First, Eqs. (2.38) and (2.39) can be reduced to a single equation by eliminating ω,

$$\delta = a_1(T_m - T_e) - b_1 \tag{2.43}$$

where

$$\begin{aligned} a_1 &= a_\delta a_\omega \\ b_1 &= a_\delta(1.0 - b_\omega) - b_\delta \\ T_e &= e_d'' i_d + e_q'' i_q - (x_d'' - x_q'') i_d i_q \end{aligned}$$

Next, Eq. (2.39) can be rewritten as

$$\omega = (1 + \delta/a_\delta - b_\delta/a_\delta) \tag{2.44}$$

Substituting Eq. (2.44) into the first equation of (2.37) and then eliminating the variables $G1$, $G2$, and $G3$ of (2.37) successively, we shall have

$$T_m = a_m \delta + b_m \tag{2.45}$$

with modified coefficients as

$$\begin{aligned} a_m &= a_{g1}' a_{g3}' a_{tm1} \ , & b_m &= a_{tm1}(a_{g3}' b_{g1}' + b_{g3}') + a_{tm2} G_0 + b_{tm} \\ a_{g1}' &= \frac{-a_{g1}}{a_\delta(a_{g1} a_{g2} + 1)} \ , & b_{g1}' &= \frac{a_{g1} b_\delta / a_\delta + b_{g1} - a_{g1}(b_{g2} - u_G)}{a_{g1} a_{g2} + 1} \\ a_{g3}' &= \frac{a_{g3}}{T_g + a_{g3}} \ , & b_{g3}' &= \frac{b_{g3} T_g}{T_g + a_{g3}} \end{aligned}$$

Inserting Eq. (2.45) into Eq. (2.43) gives

$$(1 - a_1 a_m)\delta + a_1[e_d^{''} i_d + e_q^{''} i_q - (x_d^{''} - x_q^{''}) i_d i_q] - a_1 b_m + b_1 = 0 \tag{2.46}$$

Thus, equations (2.37), (2.38) (2.39) have been reduced to a single equation i.e., Eq. (2.46).

Similarly, equations (2.40) and (2.41) can be reduced to a single algebraic equation. First, the ω in the first equation of Eq. (2.40) can be replaced with Eq. (2.44). Next, substituting x_{ps1} and x_{ps2} into the equation of u_E, we shall have

$$u_E = a_{ue}^{'} \delta + b_{ue}^{'} \tag{2.47}$$

where

$$\begin{aligned} a_{ue}^{'} &= \frac{a_{ue} a_{ps1} a_{ps2}}{a_\delta} \\ b_{ue}^{'} &= a_{ue}(a_{ps1} a_{ps2} + a_{ps2} b_{ps1} + b_{ps2}) + b_{ue} - a_{ue}^{'} b_\delta \end{aligned}$$

Inserting Eq. (2.47) into the first equation of Eq. (2.41) and then eliminating E_{FD} and $e_q^{'}$, we shall have

$$e_q^{''} - a_{21}\delta + a_{22} i_d + a_{23} v_t - b_2 = 0 \tag{2.48}$$

with modified coefficients,

$$\begin{aligned} a_{21} &= a_{e'q} a_{efd} a_{ue}^{'} \ , \quad a_{22} = a_{e'q}(x_d - x_d^{'}) + a_{e''q}(x_d^{'} - x_d^{''}) \\ a_{23} &= a_{e'q} a_{efd} \ , \quad b_2 = b_{e'q} + b_{e''q} + a_{e'q}(a_{efd} v_{ref} + a_{efd} b_{ue}^{'} + b_{efd}) \end{aligned}$$

Hence, all differential equations for each machine can be represented by only three algebraic equations, namely, Eqs. (2.46), (2.48), and (2.42). They are summarized as

$$\begin{aligned} &(1 - a_1 a_m)\delta + a_1[e_d^{''} i_d + e_q^{''} i_q - (x_d^{''} - x_q^{''}) i_d i_q] - a_1 b_m + b_1 = 0 \\ &e_q^{''} - a_{21}\delta + a_{22} i_d + a_{23}\sqrt{v_D^2 + v_Q^2} - b_2 = 0 \\ &e_d^{''} - a_{e''d} i_q (x_q - x_q^{''}) - b_{e''d} = 0 \end{aligned} \tag{2.49}$$

Eqs. (2.49) can be used for any machine. If a different type of governor is used or there exists a supplementary governor control, only a_m and b_m coefficients will change. For a different supplementary excitation control other than PSS, a_{21} and b_2 will change due to change in a'_{ue} and b'_{ue}. To take into account the upper and lower limits of variables, a and b coefficients may be modified. For example, once E_{FD} reaches its upper limit E_{max}, Eqs. (2.40) and the first equation of Eqs. (2.41) should be temporarily excluded. Also, E_{FD} in the second equation of Eqs. (2.41) should be set to E_{max}. This is equivalent to setting $a_{21} = a_{23} = 0$ and setting $b_2 = b_{e'q} + b_{e''q} + a_{e'q}E_{max.}$ in Eqs. (2.49). Hence, the form of Eqs. (2.49) holds for various control circuits of any one of machines in a multimachine system. This is very useful in computer programming for the dynamic stability studies where the behavior of each machine with and without various stabilizers will be simulated.

2.4.4 Complete System Equations for Simulations

As already mentioned in the previous subsection, all differential equations can be transformed into algebraic equations and subsequently be reduced to Eqs. (2.49). Replacing the differential equations of Eqs. (2.17) with Eqs. (2.49), we have

$$
\begin{aligned}
&(1 - a_{1k}a_{mk})\delta_k + a_{1k}[e''_{dk}i_{dk} + e''_{qk}i_{qk} - (x''_{dk} - x''_{qk})i_{dk}i_{qk}] - a_{1k}b_{mk} + b_{1k} = 0 \\
&e''_{qk} - a_{21k}\delta_k + a_{22k}i_{dk} + a_{23k}\sqrt{v_{Dk}^2 + v_{Qk}^2} - b_{2k} = 0 \\
&e''_{dk} - a_{e''dk}i_{qk}(x_{qk} - x''_{qk}) - b_{e''dk} = 0 \\
&\begin{bmatrix} \sin\delta_k & -\cos\delta_k \\ \cos\delta_k & \sin\delta_k \end{bmatrix} \begin{bmatrix} v_{Dk} \\ v_{Qk} \end{bmatrix} = \begin{bmatrix} e''_{dk} \\ e''_{qk} \end{bmatrix} + \begin{bmatrix} -R_{ak} & x''_{qk} \\ -x''_{dk} & -R_{ak} \end{bmatrix} \begin{bmatrix} i_{dk} \\ i_{qk} \end{bmatrix} \\
&\begin{bmatrix} \sin\delta_k & \cos\delta_k \\ -\cos\delta_k & \sin\delta_k \end{bmatrix} \begin{bmatrix} i_{dk} \\ i_{qk} \end{bmatrix} = \begin{bmatrix} \sum_{j=1}^{m}(G_{kj}v_{Dj} - B_{kj}v_{Qj}) \\ \sum_{j=1}^{m}(B_{kj}v_{Dj} + G_{kj}v_{Qj}) \end{bmatrix}
\end{aligned}
\tag{2.50}
$$

The subscript k is added to the first three equations to signify the k–th generator. For the simulation of a m–machine power system, there exists m sets of these equations for

all machines. Together they constitute a complete set of simultaneous equations. They are nonlinear algebraic equations and can be solved by the Newton–Raphson method.

Once the solutions for δ, e_q'', e_d'', and armature currents and voltages are obtained from simultaneous equations (2.50) at $time = t$, they are substituted into the algebraic equations in subsection 2.4.2 to solve for other state variables which were eliminated during the equation reductions. For instance, with δ known, the ω is obtained directly from Eq. (2.39). Thereafter, $G1$ is obtained from the first equation of Eq. (2.37), $G2$ from the second one of Eq. (2.37), and so on. Hence, the solutions for other state variables involve only substitutions. After the solutions for all variables, the lower and upper limits for some state variables must be applied and all b coefficients must be updated for the next computation of Eqs (2.50) at $time = t + \Delta t$.

Chapter 3

SELECTION OF NUMBER AND SITES OF STABILIZERS

3.1 Introduction

Power system stabilizers (PSSs) are designed as supplementary control devices in a power system for the improvement of its stability. To improve the stability of a large power system, all generators larger than a certain capacity are recommended to be equipped with PSSs. This may not be economic nor effective since not all large generators are situated at strategic locations. Therefore, in designing stabilizers for a multimachine power system, two prerequisite decisions must be made: 1) how many stabilizers are required and 2) on which machines these should be located.

Eigenvector methods ([5], [6]) were commonly used for the stabilizer site selection. Later, the participation factor method was proposed by Perez–Arriaga et al. ([7], [8]) and applied by Hsu and Chen [9] for one stabilizer siting. Participation factors are calculated from the eigenvectors of a system matrix $[A]$, which may be called the right vectors, and the eigenvectors of the transpose of the matrix $[A]$, which may be called the left vectors. Hsu and Chen's work was concerned with the location of only one stabilizer because the power system under study had only one unstable oscillating mode. For a large power system with many unstable modes, further research must be performed.

This chapter is aimed at presenting the results of this research on the number and site selection of stabilizers for an unstable nine–machine power system. Two methods are included; the participation factor method and the speed deviation index method. While

the participation factor method is based on a low–order linearized generator model, the speed deviation index method is based on a high–order nonlinear model. The index method defines a weighted speed deviation index from computer simulation results. The index can identify the most unstable generators which must consequently be equipped with stabilizers. In these simulations, coherently swinging groups of the system are also identified. The final selection of stabilizer number and sites, however, can only be made after examining the results of stabilizer design. For the stabilizer design, a pole-placement design technique is developed in the next chapter, but the results of several stabilizer designs are assessed in this chapter using a system stability index (SSI).

Many results of this chapter and the next chapter are published ([11], [12]).

3.2 A Nine–Machine System under Study

A nine–machine system [3], Fig. 3.1, is used for this study. The nine–machine system is chosen because a system with two or three machines is not large enough to display the nature of coherent group behaviour of a large power system. On the other hand, a system with too many machines will be crowded with results and thus it is hard to extract useful information from the results.

The system under study comprises nine synchronous generators interconnected by a transmission network. Machines 3 and 9 are hydro–electric plants with mechanical–hydraulic governors while the others are thermal–electric plants with electrical–hydraulic governors. An exciter and voltage regulator system of the fast–response type is assumed for each generator. The multimachine power system is initially unstable. The system data are as follows.

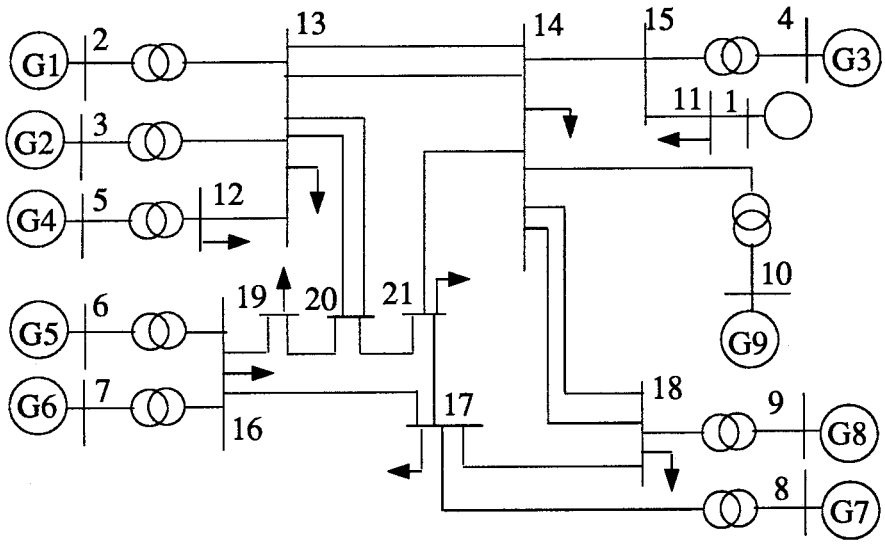

Figure 3.1: An Initially Unstable Nine–Machine System

Generator

No.	x_d	x_q	x'_d	x''_d	x''_q	M	D	T'_d	T''_d	T''_q
1	0.70	0.70	0.12	0.098	0.098	25.0	5.0	7.0	0.091	0.455
2	0.60	0.60	0.10	0.084	0.084	30.0	5.0	7.0	0.091	0.455
3	0.50	0.40	0.15	0.070	0.070	20.0	5.0	8.0	0.104	0.520
4	1.60	1.60	0.23	0.224	0.224	12.8	5.0	7.0	0.091	0.455
5	0.95	0.95	0.15	0.133	0.133	19.8	5.0	7.0	0.091	0.455
6	0.95	0.95	0.15	0.133	0.133	19.8	5.0	7.0	0.091	0.455
7	1.00	1.00	0.17	0.140	0.140	18.0	5.0	7.0	0.091	0.455
8	1.00	1.00	0.17	0.140	0.140	18.0	5.0	7.0	0.091	0.455
9	0.39	0.32	0.06	0.055	0.055	32.0	5.0	6.0	0.078	0.390

All data are in per unit except M, T'_d, T''_d, and T''_q in seconds.

Bus Load

$Bus\ \#$	P_g $(p.u.)$	V_t $(p.u.)$	$Bus\ \#$	P_{load} $(p.u.)$	Q_{load} $(p.u.)$
1	$(slack)$	1.06	11	2.5	0.2
2	3.0	1.04	12	1.5	0.1
3	3.5	1.035	13	2.4	0.2
4	2.0	1.03	14	4.5	0.5
5	1.0	1.035	15	0.0	0.0
6	2.5	1.04	16	3.5	0.2
7	2.5	1.04	17	2.0	0.2
8	2.0	1.01	18	2.0	0.0
9	2.0	1.015	19	1.5	0.0
10	3.5	1.06	20	0.0	0.0
			21	3.5	-1.7

Excitation System

T_A=0.10 s $\quad$ K_A=50.0 $p.u.$ $\quad$ *For machines 7, 8 and 9*

T_A=0.05 s $\quad$ K_A=100.0 $p.u.$ $\quad$ *For other machines*

$-0.7\ p.u. \geq E_{FD} \leq 0.7\ p.u.$ $\quad$ $-0.12\ p.u. \geq U_E \leq 0.12\ p.u.$

Hydro Turbine and Governor

σ=0.05 $p.u.$ $\quad$ δ=0.25 $p.u.$ $\quad$ T_g=0.5 s

T_p=0.02 s $\quad$ T_r=4.8 s $\quad$ T_ω=1.6 s

$-0.1\ p.u./s \geq SL \leq 0.1\ p.u./s$ $\quad$ $0.0 \geq PL \leq P_{max}$

$-0.15\ p.u. \geq U_G \leq 0.15\ p.u.$

Steam Turbine and Governor

T_{sm}=0.1 s T_{CH}=0.4 s K_g=20.0 $p.u.$

$-0.1\ p.u./s \geq SL \leq 0.1\ p.u./s$ $0.0 \geq PL \leq P_{max}$

$-0.15\ p.u. \geq U_G \leq 0.15\ p.u.$

Transmission Line

Bus I	*Bus J*	*R (p.u.)*	*X (p.u.)*	*Bus I*	*Bus J*	*R (p.u.)*	*X (p.u.)*
2	13	0.0	0.059	13	14	0.024	0.24
3	13	0.0	0.0135	20	13	0.0096	0.096
5	12	0.0	0.29	20	13	0.0096	0.096
12	13	0.0068	0.068	14	15	0.007	0.07
6	16	0.0	0.05	15	4	0.02	0.232
16	19	0.03	0.3	15	11	0.007	0.07
7	16	0.0	0.10	14	10	0.012	0.12
16	17	0.00145	0.0145	14	18	0.0204	0.204
19	20	0.0106	0.106	14	18	0.0204	0.204
20	21	0.0064	0.064	18	9	0.0	0.28
21	17	0.0161	0.161	17	18	0.0057	0.057
21	14	0.0025	0.025	17	8	0.032	0.32
13	14	0.024	0.24	11	1	0.0	0.032

3.3 Participation Factor

The participation factor was introduced in [7] for selective modal analysis (SMA). A brief introduction to the participation factor is given in Section 3.3.1. The calculated participation factors of the nine–machine system are presented in Section 3.3.2.

3.3.1 Definition of the Participation Factor and Concept

Consider a linear time-invariant system

$$[\dot{x}] = [A][x] \tag{3.1}$$

where $[x]$ is an n state vector and $[A]$ an $n \times n$ system matrix. There are n eigenvalues for the system, λ_i, $i = 1, \ldots, n$. For each eigenvalue λ_i, there is an eigenvector $[y_i]$ of $[A]$ satisfying

$$[A][y_i] = \lambda_i[y_i] \quad , [y_i] \neq 0 \tag{3.2}$$

It is well–known that both $[A]$ and $[A]^T$ have the same eigenvalues but the different eigenvectors. Let the eigenvector of $[A]^T$ for λ_i be $[u_i]$

$$[A]^T[u_i] = \lambda_i[u_i] \quad , [u_i] \neq 0 \tag{3.3}$$

or

$$[u_i]^T[A] = [u_i]^T\lambda_i \quad , [u_i] \neq 0 \tag{3.4}$$

Let $[y_i]$ be called the right eigenvector and $[u_i]$ the left eigenvector. Note that there are n entries for each eigenvector and the k–th entry of $[y_i]$ or $[u_i]$ belongs to the k–th state variable of $[x]$. A participation factor is defined in [7] as

$$p_{ki} = u_{ki}y_{ki} \tag{3.5}$$

where y_{ki} (u_{ki}) is the k–th entry of the i–th right (left) eigenvector $[y_i]$ ($[u_i]$).

Consider the time response of the system (3.1). For an initial condition $[x(0)]$, the solutions of the $[x(t)]$ are

$$[x(t)] = \sum_{j=1}^{n}[u_j]^T[x(0)]e^{\lambda_j t}[y_j] \tag{3.6}$$

If $[x(0)] = [y_i]$, Eq. (3.6) becomes

$$[x(t)] = \sum_{j=1}^{n} [u_j]^T [y_i] e^{\lambda_j t} [y_j] \tag{3.7}$$

Since $[u_j]$ and $[y_i]$ are orthogonal for $j \neq i$ [7], we have

$$[u_j]^T [y_i] \;=\; 0.0 \quad for \;\; j \neq i \tag{3.8}$$

Therefore, Eq. (3.7) becomes

$$\begin{aligned} [x(t)] &= [u_i]^T [y_i] e^{\lambda_i t} [y_i] \\ &= (p_{1i} + p_{2i} + \ldots + p_{ni}) e^{\lambda_i t} [y_i] \end{aligned} \tag{3.9}$$

Hence, when only the i–th eigenvalue is excited, p_{ki}, k =1, 2, ..., n measures the relative participation of the k–th state variable in the time response of the i–th eigenvalue mode. Based on this concept, participation factors of a system can be used to find the most sensitive state variable to the electromechanical eigenvalues of interest.

3.3.2 Participation Factors of the Nine–machine System

Based on the linearized state equation, Eq. (3.1), the system matrix of the nine–machine power system can be readily obtained by a Fortran program following the linear model procedure given in Chapter 2. Each machine is described by a fourth–order model in which state variables are arranged in a definite order of $\Delta\delta$, $\Delta\omega$, $\Delta e_q^{'}$, and ΔE_{FD}. There are 36 state variables in $[x]$ for the nine–machine system and the system matrix $[A]$ is a 36×36 matrix. The 36 eigenvalues of the system without supplementary stabilizers (open–loop system) are calculated and listed in Table 3.1. Eigenvalues 11–28 are electromechanical modes. These modes are identified with participation factors. When the participation factors of a pair of complex–conjugated eigenvalues have the maximum values for state variables $\Delta\delta$ and $\Delta\omega$ of a particular machine, this pair of eigenvalues is closely associated with the mechanical modes of that machine.

Table 3.1: Eigenvalues of the Open–Loop System

Number	Eigenvalues	
1	-17.5178	
2, 3	-9.9615 $\pm j$ 11.1700	
4	-15.8514	
5, 6	-10.5035 $\pm j$ 6.8676	
7, 8	-10.3454 $\pm j$ 6.4374	
9, 10	-10.2149 $\pm j$ 2.9120	
11, 12	-0.3354 $\pm j$ 9.1267	#
13, 14	-0.2188 $\pm j$ 8.6423	#
15, 16	-0.0947 $\pm j$ 7.2452	#
17, 18	-0.0627 $\pm j$ 7.0242	#
19, 20	-0.1970 $\pm j$ 6.5043	#
21, 22	0.5083 $\pm j$ 5.3235	#
23, 24	0.5260 $\pm j$ 5.4462	#
25, 26	0.2248 $\pm j$ 6.1273	#
27, 28	0.0922 $\pm j$ 2.8020	#
29, 30	-5.2957 $\pm j$ 5.2354	
31, 32	-6.1138 $\pm j$ 4.0579	
33, 34	-5.8807 $\pm j$ 4.0080	
35	-4.5908	
36	-2.6307	

# Denotes electromechanical mode eigenvalues

It is found from Table 3.1 that there are four unstable eigenmodes, or eigenvalue–pairs with a positive real part (eigenvalues 21–28). The participation factors of these unstable modes are listed in Table 3.2.

For the participation factors of each of the first three unstable modes, there are two largest values corresponding to $\Delta\delta$ and $\Delta\omega$ of a particular machine. It is found that they belong to machines 7, 8, and 3, respectively. This clearly suggests that the machines 7, 8 and 3 should be the first three to be designed with PSSs. But it is much less clear for the fourth unstable mode. Since the participation factors of machines 7, 8 and 9 of this unstable mode all have the largest value, whether a stabilizer designed on machines 7,

Table 3.2: Participation Factors of Unstable Modes

Eigenvalues of Unstable Modes (Eigenvalue No.)	Participation Factors Corresponding to State Variables: $\Delta\delta(i)$	$\Delta\omega(i)$	$\Delta e_q'(i)$	$\Delta E_{FD}(i)$	Machine Number (i)
	0.05	0.05	0.00	0.00	1
	0.05	0.05	0.00	0.00	2
	0.02	0.02	0.00	-0.00	3
	0.06	0.06	-0.00	0.00	4
0.5083 $\pm j$ 5.3235	-0.00	-0.00	0.01	0.00	5
(21 and 22)	-0.00	-0.00	0.00	0.00	6
	$\boxed{0.28}$	$\boxed{0.27}$	0.11	0.04	7
	-0.06	-0.05	-0.02	0.01	8
	0.03	0.03	-0.00	0.00	9
	-0.01	-0.01	0.00	-0.00	1
	-0.01	-0.01	0.00	-0.00	2
	-0.01	-0.01	-0.00	-0.00	3
	0.01	0.01	0.00	-0.00	4
0.5260 $\pm j$ 5.4462	0.00	0.00	-0.00	0.00	5
(23 and 24)	0.00	0.00	-0.00	0.00	6
	0.05	0.05	-0.02	0.01	7
	$\boxed{0.40}$	$\boxed{0.39}$	0.10	0.05	8
	-0.01	-0.01	0.00	0.00	9
	0.01	0.01	0.00	0.00	1
	0.01	0.01	0.00	0.00	2
	$\boxed{0.44}$	$\boxed{0.44}$	0.06	0.00	3
	0.02	0.03	-0.00	0.00	4
0.2248 $\pm j$ 6.1273	0.00	0.00	0.00	0.00	5
(25 and 26)	-0.00	-0.00	0.00	0.00	6
	-0.00	-0.00	0.00	-0.00	7
	-0.00	-0.00	0.00	-0.00	8
	-0.01	-0.01	0.00	0.00	9
	0.06	0.06	-0.00	-0.00	1
	0.06	0.06	0.01	-0.00	2
	0.02	0.02	0.00	-0.00	3
	0.04	0.04	-0.00	-0.00	4
0.0922 $\pm j$ 2.8020	0.05	0.05	0.01	-0.00	5
(27 and 28)	0.05	0.05	0.00	-0.00	6
	$\boxed{0.07}$	$\boxed{0.07}$	0.00	-0.00	7
	$\boxed{0.07}$	$\boxed{0.07}$	0.01	-0.00	8
	$\boxed{0.07}$	$\boxed{0.07}$	-0.00	-0.00	9

8, or 9 will effectively improve the fourth unstable mode is uncertain. Also, it is unclear whether three stabilizers on machines 3, 7, and 8 are sufficient to stabilize the entire system or a fourth stabilizer must be designed. Since the participation factor method is a linear analysis using a low–order linearized generator model, further analysis of the nine–machine system through nonlinear simulations using high–order nonlinear system models probably will provide a more accurate answer.

3.4 Nonlinear Simulations for Open-Loop System

To find a more accurate answer to the question of how many stabilizers are required and where they should be located, comprehensive time–domain simulations using a high–order nonlinear system model are performed by the computer simulation method described in Chapter 2. A three–phase fault is assumed to occur near the terminal bus of each of the machines in turn for the simulation tests. There are nine machines and nine different short–circuit tests. All time responses of angle, speed, torque, etc. are recorded. Therefore, there are numerous curves which can be plotted. Our primary concerns at the moment, however, are the angular swings and the speed deviations of the nine machines.

3.4.1 Coherent Groups

One of our interests is how these machines behave. Are they swinging coherently or individually? Typical results found from the short–circuit test at the terminal bus of generator 1 are shown in Figs. 3.2 through 3.5. The generator angular swings for all short–circuit tests show that there are six coherent groups and the results are summarized in Table 3.3.

Although swing curves from the comprehensive nonlinear simulation tests give a clear picture of how many coherent groups, they still cannot tell how many stabilizers are really

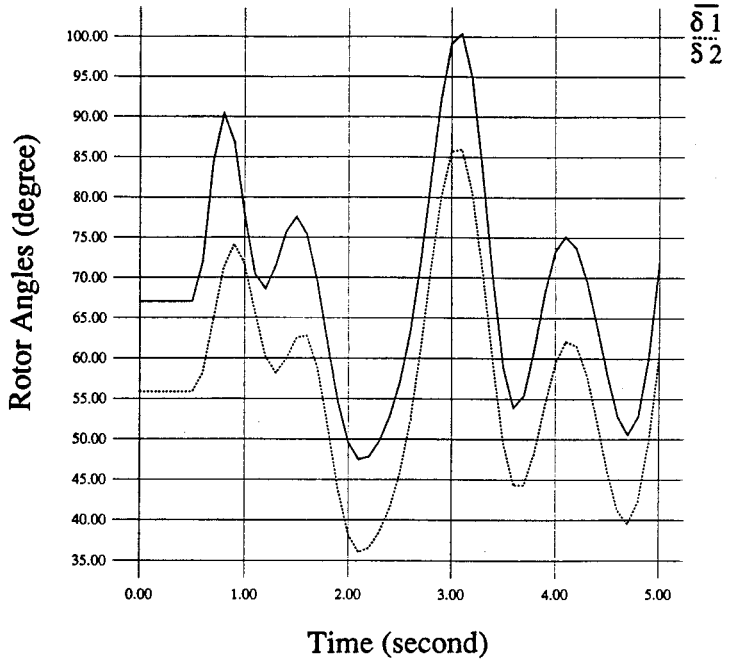

Figure 3.2: Angular Swings of Machines 1 and 2

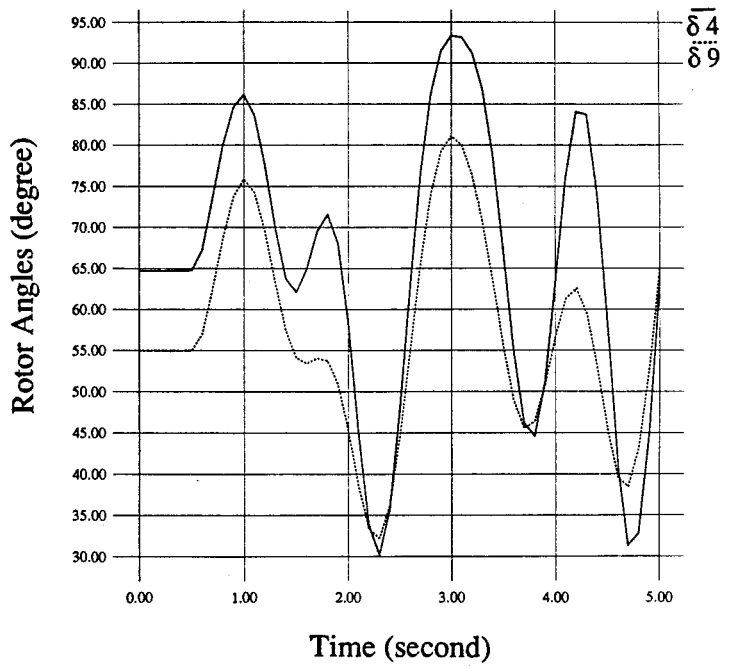

Figure 3.3: Angular Swings of Machines 4 and 9

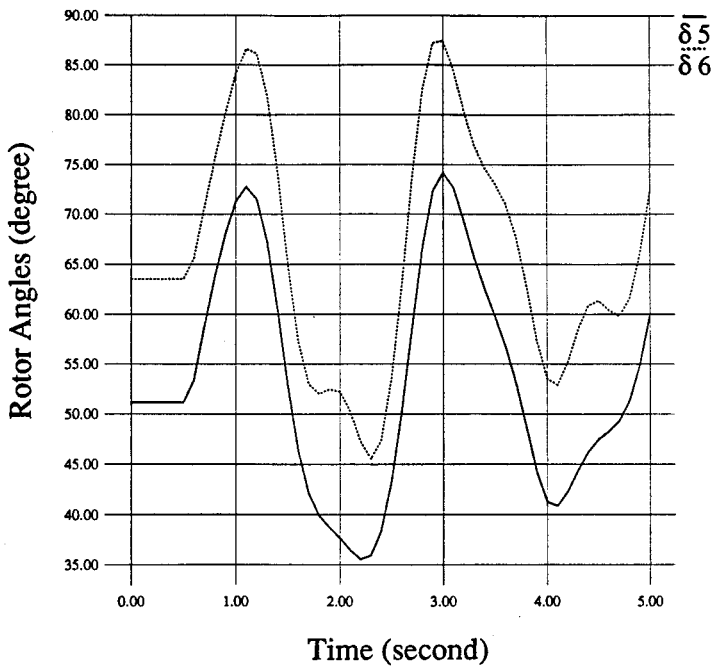

Figure 3.4: Angular Swings of Machines 5 and 6

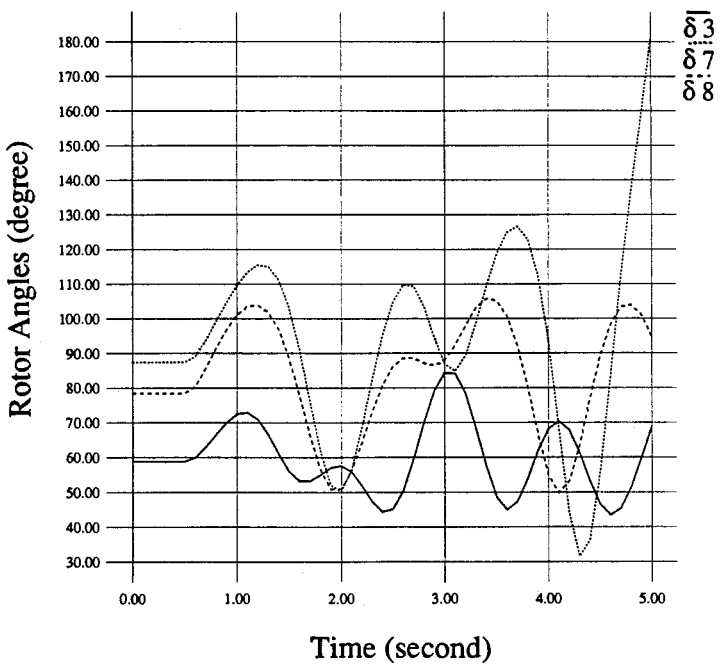

Figure 3.5: Angular Swings of Machines 3, 7 and 8

Table 3.3: Coherent Groups of a 9–machine System

Groups	1	2	3	4	5	6
Machine No.	1, 2	4, 9	5, 6	3	7	8

required for the stabilization of the system and where they should be located. Although Hiyama [10] suggested at least one stabilizer for each coherent group of a large power system, it remains to be examined.

3.4.2 Speed Deviation Analysis

Searching for the most unstable generators in a multimachine system may be helpful in deciding the stabilizer number and sites for the system. Although the stability performances of generators may be compared with each other by directly observing generator speed deviations from system simulations, the comparison of a great number of speed deviation curves of all machines for various simulation tests is very tedious. To avoid that, a speed deviation index (SDI) is defined for individual machine generator as follows

$$SDI = \frac{1}{k}\sum_{j=1}^{k}\int_{0}^{t} M\Delta\omega_j^2 dt \tag{3.10}$$

where $\Delta\omega_j$ is the speed deviation of a machine with respect to the system synchronous speed in the j–th test, M is the inertia constant of the machine used as a weighting factor, $M\Delta\omega_j^2$ has the same unit as kinetic energy, which is integrated over time from 0 to t, and k is the total number of simulation tests. This means that the SDI is defined by the average value of weighted speed deviations of a machine for all short–circuit tests over the simulation time. The SDI of a machine measures the degree of stability of the machine. The larger the SDI value of a machine is, the less stable the machine.

A three–phase short–circuit for 0.12 second is given to each generator terminal of the system in turn. There are nine simulation tests for the nine–machine system and

Table 3.4: Speed Deviation Indices of Machines for the Open–loop System

(Normalized with Respect to Their Maximum Value)

SDI	1.000	0.6713	0.1028	0.0666	0.0658	0.0630	0.0609	0.0404	0.0308
Mc. No.	7	8	3	2	9	1	4	6	5

each simulation lasts 5 seconds, i.e., $k = 9$ and $t = 5$ in Eq. (3.10). The SDI values of all machines are calculated for all simulation tests and normalized with respect to their largest value. They are listed in Table 3.4 for comparison.

Table 3.4 shows that there are three machines of G7, G8 and G3 which have relatively larger SDI values and another six machines which have relatively smaller SDI values. Therefore, machines 3, 7, and 8 are the first three candidates for stabilizer sites. The remaining questions are whether the three stabilizers are sufficient to ensure the stability of the entire system or a fourth stabilizer is required.

3.5 Stabilizer Designs

So far it has been found from both participation factors and speed deviation indices that the first three stabilizers must be designed for machines 3, 7, and 8. Whether three stabilizers on these machines are sufficient or not must be further investigated through actual stabilizer designs. For this, different combinations of machines for PSS locations are as follows:

Design No.	Machines with Stabilizer
1	3 7 8
2	3 7 8 1
3	3 7 8 2
4	3 7 8 4
5	3 7 8 5
6	3 7 8 6
7	3 7 8 9

A pole–placement technique developed in Chapter 4 is applied to these power system stabilizer (PSS) designs for the multimachine system. The design procedure and the designed PSS parameters will be presented in detail in the next chapter and are not described here. Our concerns at this moment are the dynamic performances of the nine–machine system with designed stabilizers in order to make the final decision of stabilizer number and sites. To assess the merit of a PSS design from the nonlinear simulation tests in time–domain, a system stability index (SSI) is introduced, which is defined as

$$SSI = \sum_{j=1}^{k} \int_0^t \sum_{i=1}^{n} M_i \Delta\omega_{ij}^2 dt \tag{3.11}$$

where n is the number of machines in the system, i the i–th machine, j the j–th test and k the number of simulation tests. For each PSS design, the speed deviations of all machines of the power system are integrated over the entire simulation duration, and the results are added for all short–circuit simulations to give a SSI value. The SSI value measures the degree of stability of the closed–loop power system for this design. The smaller the SSI value of the system is, the more stable the system.

Again, a three–phase short–circuit for 0.12 second is assumed to occur near a terminal bus of all generators in turn and the results are recorded for 10 seconds for each short–circuit test. There are nine machines and nine short–circuit test, i.e., $n = 9$, $k = 9$ and

Table 3.5: System Stability Indices of Various Designs

Design No.	Machines with PSS	SSI of the System
1	3 7 8	0.55331
2	3 7 8 1	0.54721
3	3 7 8 2	0.54680
4	3 7 8 4	0.55036
5	3 7 8 5	0.55091
6	3 7 8 6	0.54382
7	3 7 8 9	0.54988

$t = 10$ in Eq. (3.11). The nine simulation tests and calculations of SSI are repeated for each PSS design. For all simulation tests, the initially unstable nine–machine system becomes stable for all stabilizer designs. The results of calculated SSI are listed in Table 3.5.

The results in Table 3.5 indicate that the three–stabilizer design of G3, G7, and G8 is just as good as any of four–stabilizer designs. It is concluded that the three stabilizers are sufficient to stabilize the nine–machine system. Some simulation results of the closed–loop system for the three-stabilizer design will be given in the next chapter.

3.6 Conclusions

1. Both participation factor method of linear analysis and the speed deviation index (SDI) based on nonlinear simulations are helpful in deciding stabilizer number and sites for a multimachine system. Stabilizers should be installed on machines whose speed state variables have relatively larger participation factors of unstable modes or on machines having relatively larger speed deviation indices.

2. Coherent groups can be found from the nonlinear simulation tests, but it is not necessary to have a stabilizer for each coherent group.

3. For the initially unstable nine–machine system, three PSSs on machines 7, 8, and 3 are sufficient to ensure the stability of the system although there are four unstable modes and six coherent groups for the open–loop system.

Note that the third conclusion has been verified not only from the results of PSS designs in Chapter 4 but also from the results of a self–tuning stabilizer design in Chapter 5.

Chapter 4

PSS FOR MULTIMACHINE SYSTEMS WITH LOW–FREQUENCY OSCILLATIONS

Low–frequency electro-mechanical mode oscillations between interconnected synchronous generators in a large power system stem from the increase in size and in complexity of power systems. The oscillating frequencies range approximately from 0.2 to 2.5 Hz [13]. To improve damping of low–frequency oscillations, Power System Stabilizers (PSS) are designed. The use of PSSs has been popular in power industry [14]. However, the design of PSS parameters for a large power system is still a tough task since PSSs are usually installed on some large generators in the system and only local variables of these generators can be readily utilized as feedback signals. Due to the decentralized control structure and dynamic interaction between machines [15], much effort has been made in PSS design to coordinate all PSSs of a multimachine system to provide certain damping for low–frequency oscillating modes of the entire system ([16]–[18]). Progress also has been made in developing pole–placement methods for determining PSS parameters to yield exact damping to negatively or poorly damped low–frequency oscillating modes ([19]–[20]). Although these exact pole–placement techniques are useful for PSS design, they are still complicated and involve much computation. A simpler pole–placement technique with less computation is desirable.

This chapter presents a new pole–placement design technique for determining PSS parameters of multimachine power systems in order to move unstable or poorly damped low–frequency oscillating mode eigenvalues to desired locations on the complex plane.

The mathematical formulation of the design method is concise and systematic and the computational requirement is less than the previous methods ([19]–[20]). Two multimachine power systems are used as examples to illustrate the design procedure and to show the effectiveness of the proposed method.

4.1 A New Pole–Placement PSS Design Method

Consider a design of m stabilizers for a multimachine power system. The number of machines of the system may be equal to or larger than the number of the stabilizers. In the frequency domain, the linear state equation of the power system may be written as

$$[sx(s)] = [A][x(s)] + [B][u(s)] \tag{4.1}$$

where $[x]$ is an n state vector of all machines with the speed variables of m generators in leading positions, $[u]$ is an m control vector, $[A]$ is an $n \times n$ system matrix, and $[B]$ is an $n \times m$ control matrix. Assuming that the control signals of stabilizers are applied to the excitation systems of the m machines, Eq. (4.1) may be partitioned as

$$\begin{bmatrix} s\Delta\omega(s) \\ sy(s) \end{bmatrix} = \begin{bmatrix} A_{11} & A_{12} \\ A_{21} & A_{22} \end{bmatrix} \begin{bmatrix} \Delta\omega(s) \\ y(s) \end{bmatrix} + \begin{bmatrix} 0 \\ B_u \end{bmatrix} [u(s)] \tag{4.2}$$

where $[\Delta\omega(s)]$ consists of m speed elements of the m machines for which the stabilizers are designed and $[y(s)]$ the remaining state variables of $[x]$. $[B_u]$ is part of $[B]$, also consisting of mostly null elements except those associated with the transfer functions of excitation systems.

The speed variable of the j–th machine, $\Delta\omega_j$, is used as feedback input of the decentralized stabilizer on the j–th machine to produce a control signal

$$u_j(s) = h_j(s)\Delta\omega_j(s) \tag{4.3}$$

where

$$h_j(s) = \frac{sT_{rj}}{1+sT_{rj}} \frac{(1+sT_j)^2}{(1+sT_j')^2} K_j \quad ; \quad j = 1, \ 2, \ \ldots, \ m \tag{4.4}$$

and $h_j(s)$ is the transfer function of a Power System Stabilizer (PSS), with an additional reset block, on the j–th machine. The PSS time constant T_j' and the reset block time constant T_{rj} are usually preselected and treated as known quantities. The other PSS parameters of $h_j(s)$ are treated as the unknowns. For the m stabilizers of the power system, there are m Eq. (4.3) and they may be assembled into

$$[u(s)] = [H(s)][\Delta\omega(s)] \tag{4.5}$$

where [H] is an $m \times m$ matrix with only diagonal elements $h_j(s), j = 1, \ldots, m$. Therefore, the last term of Eq. (4.2) becomes

$$\begin{aligned} \begin{bmatrix} \mathbf{0} \\ B_u \end{bmatrix} [u(s)] &= \begin{bmatrix} \mathbf{0} \\ B_u \end{bmatrix} [H(s) \quad \mathbf{0}] \begin{bmatrix} \Delta\omega(s) \\ y(s) \end{bmatrix} \\ &= \begin{bmatrix} \mathbf{0} & \mathbf{0} \\ B_u H(s) & \mathbf{0} \end{bmatrix} \begin{bmatrix} \Delta\omega(s) \\ y(s) \end{bmatrix} \end{aligned} \tag{4.6}$$

Substituting Eq. (4.6) into Eq. (4.2) gives

$$\begin{aligned} [s\Delta\omega(s)] &= [A_{11}][\Delta\omega(s)] &&+[A_{12}][y(s)] \\ [sy(s)] &= [A_{21} + B_u H(s)][\Delta\omega(s)] &&+[A_{22}][y(s)] \end{aligned} \tag{4.7}$$

Eliminating $[y(s)]$ from Eq. (4.7) yields

$$[F(s)][\Delta\omega(s)] = [H(s)][\Delta\omega(s)] \tag{4.8}$$

where

$$[F(s)] = \left[A_{12}(sI - A_{22})^{-1} B_u\right]^{-1} [sI - A_{11} - A_{12}(sI - A_{22})^{-1} A_{21}] \tag{4.9}$$

and $[F(s)]$ is an $m \times m$ matrix.

To find the unknown parameters of $h_j(s)$ of the j–th stabilizer, let $h_j(s)$ be expressed explicitly first. Let the j–th speed variable of $[\Delta\omega(s)]$ of Eq. (4.8), $\Delta\omega_j(s)$, be moved to the first position. Hence, $[F(s)]$ and $[H(s)]$ must be reordered as $[F_j(s)]$ and $[H_j(s)]$ as follows

$$\begin{bmatrix} F_{j11}(s) & F_{j12}(s) \\ F_{j21}(s) & F_{j22}(s) \end{bmatrix} \begin{bmatrix} \Delta\omega_j(s) \\ x_j(s) \end{bmatrix} = \begin{bmatrix} h_j(s) & 0 \\ \mathbf{0} & H_{j2}(s) \end{bmatrix} \begin{bmatrix} \Delta\omega_j(s) \\ x_j(s) \end{bmatrix} \tag{4.10}$$

where $h_j(s)$ is separated from other PSS transfer functions and $H_{j2}(s)$ is an $(m-1) \times (m-1)$ matrix with the remaining $m-1$ stabilizer transfer functions as its diagonal elements. $[x_j(s)]$ is a vector with $m-1$ speed variables of $[\Delta\omega(s)]$ excluding $\Delta\omega_j(s)$. Eliminating $[x_j(s)]$ from Eq. (4.10), we shall have the explicit expression of $h_j(s)$.

$$h_j(s) = F_{j11}(s) + F_{j12}(s)[H_{j2}(s) - F_{j22}(s)]^{-1}F_{j21}(s) \tag{4.11}$$

The process of reordering Eq. (4.8) to obtain Eq. (4.11) must be repeated for $j = 1, \ldots, m$ so that m equations of Eq. (4.11) can be obtained for m stabilizers. Let PSS transfer functions of Eq. (4.11) be replaced by Eq. (4.4). Then, Eq. (4.11) may be rewritten in a general form

$$h_j(s, K_j, T_j) = f_j(s, K_1, T_1, \ldots, K_{j-1}, T_{j-1}, K_{j+1}, T_{j+1}, \ldots, K_m, T_m) \quad ; \quad j = 1,\ 2,\ \ldots,\ m \tag{4.12}$$

The remaining problem is to determine PSS time constant T_j and the gain K_j. This can be done in such a way that m pairs of open–loop unstable eigenvalues can be moved exactly to the desired locations for the closed–loop system. For this purpose, replacing s in every j–th equation of Eqs. (4.12) with the j-th desired eigenvalue λ_j or its conjugate

value λ_j^*, we have

$$
\begin{aligned}
h_1(\lambda_1, K_1, T_1) &= f_1(\lambda_1, K_2, T_2, K_3, T_3, \ldots K_m, T_m) \\
h_2(\lambda_2, K_2, T_2) &= f_2(\lambda_2, K_1, T_1, K_3, T_3, \ldots K_m, T_m) \\
\ldots \quad & \ldots \quad \ldots \\
h_j(\lambda_j, K_j, T_j) &= f_j(\lambda_j, K_1, T_1, \ldots, K_{j-1}, T_{j-1}, K_{j+1}, T_{j+1}, \ldots, K_m, T_m) \\
\ldots \quad & \ldots \quad \ldots \\
h_m(\lambda_m, K_m, T_m) &= f_m(\lambda_m, K_1, T_1, K_2, T_2, \ldots, K_{m-1}, T_{m-1})
\end{aligned}
\tag{4.13}
$$

Finally, the pole–placement design problem has been reduced to the solution of $2m$ PSS parameters K_j and T_j ($j = 1, \ldots, m$) from the algebraic equations (4.13).

Two major advantages of the new design method are clear at this moment. Firstly, it is obvious that the mathematical formulation involved for reducing system state equation to algebraic equations (4.13) is concise and systematic. Secondly, since h_j is explicitly expressed in the j–th equation of Eqs. (4.13) (or h_j is separated from the arguments of f_j), a relatively simple method, the Gauss–Seidel method or the fixed point method, can be used to solve for K_j and T_j, $j = 1, \ldots, m$. But, this cannot be done if all $h_j, j = 1, \ldots, m$ were implicitly expressed in a set of algebraic equation as in [20]. In such case, the Newton–Raphson method must be used to find the solution. But, the required computation of Jacobian matrix at each iteration is very time consuming.

4.2 PSS Designs Using the New Pole–Placement Method

This section discusses how to apply the proposed new pole–placement method to the PSSs designs for power systems. Two multimachine power systems are used as the design examples to show the design procedure and the effectiveness of the method.

4.2.1 Algorithm of Solving PSS Parameters by Gauss–Seidel Method

In this subsection, the Gauss–Seidel method is used to solve for the PSS parameters K_j and T_j ($j = 1, \ldots, m$) from Eqs. (4.13). The algorithm is as follows.

1. Specify a set of desired new electromechanical mode eigenvalues λ_j for closed–loop system and set $K_j(0)$, $T_j(0)$ for $j = 1, \ldots, m$.

   Specify error tolerances ε_K and ε_T.

   Set iteration index $I = 1$.

2. Solve $K_j(I)$ and $T_j(I)$, $j = 1, \ldots, m$ from

$$
\begin{aligned}
&h_1(\lambda_1, K_1(I), T_1(I)) \\
&\quad = f_1(\lambda_1, K_2(I-1), T_2(I-1), K_3(I-1), T_3(I-1), \ldots K_m(I-1), T_m(I-1)) \\
&h_2(\lambda_2, K_2(I), T_2(I)) \\
&\quad = f_2(\lambda_2, K_1(I), T_1(I), K_3(I-1), T_3(I-1), \ldots K_m(I-1), T_m(I-1)) \\
&\cdots \quad \cdots \quad \cdots \\
&h_j(\lambda_j, K_j(I), T_j(I)) \\
&\quad = f_j(\lambda_j, K_1(I), T_1(I), \ldots, K_{j-1}(I), T_{j-1}(I), \\
&\qquad\qquad K_{j+1}(I-1), T_{j+1}(I-1), \ldots, K_m(I-1), T_m(I-1)) \\
&\cdots \quad \cdots \quad \cdots \\
&h_m(\lambda_m, K_m(I), T_m(I)) \\
&\quad = f_m(\lambda_m, K_1(I), T_1(I), K_2(I), T_2(I), \ldots, K_{m-1}(I), T_{m-1}(I))
\end{aligned}
$$

   one by one.

3. Are $|K_j(I) - K_j(I-1)| < \varepsilon_K$ and $|T_j(I) - T_j(I-1)| < \varepsilon_T$ $\quad j = 1, 2, \ldots, m$?

4. Stop if both yes;

   Otherwise set $I = I + 1$ and goto step 2.

4.2.2 Selection of Eigenvalues for the Closed–Loop System

The natural frequency ω_n of an oscillating mode is equal to the absolute value of the corresponding eigenvalue. For the pole–placement design, new eigenvalue pairs $(\lambda_j,\ \lambda_j^*)$ are specified by designating a new damping factor for initially unstable mode eigenvalues with their natural frequency remaining unchanged. For example, if ζ is the desired new damping factor, we shall specify

$$\lambda_j,\ \lambda_j^* = -\zeta\omega_n \pm j\sqrt{1-\zeta^2}\omega_n$$

The purpose of selecting eigenvalues for closed–loop system in this way is to concentrate the control efforts of PSSs on improving the damping of specific low–frequency oscillating modes.

4.2.3 Design Example 1 — A Three–Machine Power System

To test the new pole–placement method for PSS design, a three–machine power system, Fig. 4.1, is chosen as the first example system. It consists of three machines and an infinite busbar. Each machine is equipped with a static exciter. The detailed data of the system can be found in ([21], [16]). The linearized system state equation is included in [16]

$$\dot{x} = Ax + Bu$$

but with state variables reordered here as

$$x = [\Delta\omega_1,\ \Delta\omega_2,\ \Delta\omega_3,\ \Delta\delta_1,\ \Delta\delta_2,\ \Delta\delta_3, \Delta e'_{q1},\ \Delta e'_{q2},\ \Delta e'_{q3},\ \Delta E_{FD1},\ \Delta E_{FD2},\ \Delta E_{FD3}]$$

and

$$u = [u_1,\ u_2,\ u_3]^T$$

$$A = \begin{bmatrix}
-0.039 & 0.004 & 0.02 & -0.147 & 0.022 & 0.046 & -0.013 & 0 & 0.003 & 0 & 0 & 0 \\
-0.034 & 0.032 & -0.028 & 0.004 & -0.149 & 0.079 & -0.0065 & -0.008 & 0 & 0 & 0 & 0 \\
-0.017 & -0.01 & -0.017 & 0.001 & 0.017 & -0.056 & -0.003 & 0 & -0.009 & 0 & 0 & 0 \\
377. & 0 & 0 & 0 & 0 & 0 & 0 & 0 & 0 & 0 & 0 & 0 \\
0 & 377. & 0 & 0 & 0 & 0 & 0 & 0 & 0 & 0 & 0 & 0 \\
0 & 0 & 377. & 0 & 0 & 0 & 0 & 0 & 0 & 0 & 0 & 0 \\
-3.393 & 0.754 & 1.131 & -0.266 & -0.087 & -0.250 & -0.922 & 0.024 & 0.072 & 1. & 0 & 0 \\
1.131 & -1.885 & 0.754 & 0.121 & -1.60 & 0.460 & 0.021 & -0.21 & 0.06 & 0 & 1. & 0 \\
0 & 0 & -1.131 & 0.083 & 0.220 & -1.20 & -0.002 & 0.011 & -0.197 & 0 & 0 & 1. \\
-309.14 & -91.99 & -1675 & -30.1 & 24.599 & 62.051 & -60.943 & -3.501 & -10.194 & -20. & 0 & 0 \\
-64.47 & -516.11 & -171.91 & -18.48 & 106.09 & 16.99 & -12.55 & -21.67 & -11.41 & 0 & -20. & 0 \\
-33.93 & -46.37 & -893.49 & -10.1 & 1.7 & 70.1 & -6.78 & -2.1 & -54.4 & 0 & 0 & -20.
\end{bmatrix}$$

$$B = \begin{bmatrix}
0 & 0 & 0 & 0 & 0 & 0 & 0 & 0 & 0 & 800 & 0 & 0 \\
0 & 0 & 0 & 0 & 0 & 0 & 0 & 0 & 0 & 0 & 900 & 0 \\
0 & 0 & 0 & 0 & 0 & 0 & 0 & 0 & 0 & 0 & 0 & 1000
\end{bmatrix}^T$$

The eigenvalues of the system without PSSs are calculated and listed in the first column of Table 4.2. There are three pairs of complex–conjugated eigenvalues with low natural frequency and poor damping. A new damping factor 0.3 is specified for all three poorly damped modes. The new eigenvalues are as follows:

Sites of PSSs	Old eigenvalues	Specified eigenvalues (λ_j)
Machine 1	$-0.0627 \pm j7.3692$	$-2.1800 \pm j6.9200$
Machine 2	$0.0953 \pm j7.8364$	$-2.3700 \pm j7.5300$
Machine 3	$0.2637 \pm j4.0915$	$-1.1700 \pm j3.7200$

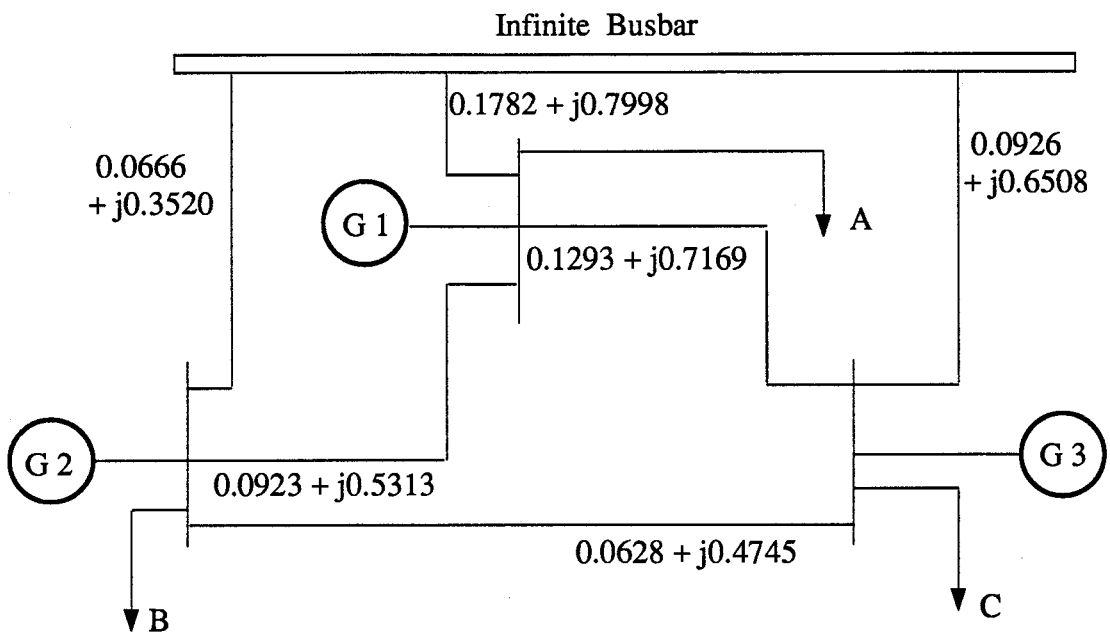

Figure 4.1: A Three–Machine Power System for PSS Design

Table 4.1: Tuned Parameters of PSSs

K_1	T_1	K_2	T_2	K_3	T_3
23.6881	0.1828	34.9859	0.2293	18.4519	0.1599

The parameters of the three PSSs are calculated with a Fortran program written according to the proposed design algorithm and the results are listed in Table 4.1. The eigenvalues of the closed–loop system with the designed PSSs are computed and listed in the second column of Table 4.2. As expected, the exact assignment of specified eigenvalues is achieved by the PSSs designed with the new pole–placement method.

4.2.4 Design Example 2 — A Nine–Machine Power System

The nine–machine power system described in Chapter 3 is chosen as a second example for PSS design with the new pole–placement method. The system configuration is shown

Table 4.2: Eigenvalue Comparison

System without PSSs	System with PSSs
-0.0627 $\pm j$ 7.3692	-2.1800 $\pm j$ 6.9200 *
0.0953 $\pm j$ 7.8364	-2.3700 $\pm j$ 7.5300 *
0.2637 $\pm j$ 4.0915	-1.1700 $\pm j$ 3.7200 *
-1.5112	-1.3226
-3.4305	-3.1685
-5.8914	-5.8332
-15.1893	-40.1939
-17.0519	-42.5035
-18.8713	-46.5227
	-11.7893 $\pm j$ 16.0235
	-13.5454 $\pm j$ 12.1889
	-15.5560 $\pm j$ 9.4230
	-0.2083
	-0.2048
	-0.2027

*: Exactly Assigned Eigenvalues

in Fig. 3.1 and the system data are given in Chapter 3. There are 36 eigenvalues for the nine–machine system without supplementary control as listed in Table 3.1. The electromechanical modes eigenvalues of the 36 eigenvalues are listed here in the first column of Table 4.4. There are four unstable eigenmodes (last four eigenvalue–pairs) and two poorly damped eigenmodes (the third and fourth eigenvalue–pairs) among the electromechanical modes.

It was mentioned in Chapter 3 that either three stabilizers for machines 3, 7, and 8 or four stabilizers for the three machines plus a fourth machine must be designed before the final decision of stabilizer number and sites. The different combinations of machines for PSS locations are listed as follows:

Design No.	Machines with PSS
1	3 7 8
2	3 7 8 1
3	3 7 8 2
4	3 7 8 4
5	3 7 8 5
6	3 7 8 6
7	3 7 8 9

The details of these designs are as follows. In the first example of PSS design in the previous subsection, a uniform damping $\zeta = 0.3$ was specified for all mechanical mode eigenvalues. The choice of damping factor here for the nine–machine system is not as simple as that in the first example since the four stabilizers are supposed not only to move four unstable mode eigenvalue pairs to new places on the complex plane but also to improve the dampings of two other poorly damped modes. Four stabilizers on machines 3, 7, 8, and 9 have been chosen to carry out designs in order to find proper damping factors for the four unstable eigenvalues. We began with a uniform damping $\zeta = 0.3$ for all four initially unstable modes for the design. The four stabilizers designed with the new pole–placement method did provide exact damping factor to the four unstable modes as intended, but failed to improve dampings of the other two poorly damped modes. Then we varied the dampings one at a time, but kept the other dampings unchanged and continued the design. Finally, we found that the best damping for the entire system can be obtained by specifying new non–uniform damping factors 0.8, 0.7, 0.3, and 0.4, respectively, for the four unstable mode eigenvalues. The specified eigenvalues are as follows:

Locations of PSSs	Old Eigenvalues	Specified Eigenvalues (Damping)
Machine 7	0.5083$\pm j$ 5.3235	-4.2782$\pm j$ 3.2087 (0.8)
Machine 8	0.5260$\pm j$ 5.4462	-3.8301$\pm j$ 3.9075 (0.7)
Machine 3	0.2248$\pm j$ 6.1273	-1.8394$\pm j$ 5.8490 (0.3)
A fourth machine	0.0922$\pm j$ 2.8020	-1.1214$\pm j$ 2.5695 (0.4)

For all designs, the reset block time constant T_r of Eq (4.4) is preselected as 5.0 s and one time constant T_j' of PSSs as 0.035 s. To find the unknown parameters K_j and T_j of the PSSs so that the unstable mode eigenvalues can be changed to those specified new values, a Fortran program is written according to the proposed pole–placement algorithm for all designs. The results of all designs are listed in Table 4.3.

The eigenvalues of the nine–machine power system with the designed stabilizers (closed–loop system) are then computed. Note that since each PSS has three state variables, there are 9 more state variables for the power system with three stabilizers and 12 more state variables for the system with four stabilizers. Therefore, there are 45 eigenvalues for the closed–loop system with three stabilizers and 48 eigenvalues for all closed–loop systems with four stabilizers. Only electromechanical mode eigenvalues of closed–loop systems for all designs are listed in Table 4.4 for comparison because other eigenvalues have much larger dampings and higher frequencies. The results show not

Table 4.3: PSS Parameters of Various Designs

Design No.	T_3	K_3	T_7	K_7	T_8	K_8	T_i	K_i
1	0.1029	18.0754	0.1039	28.2710	0.1239	31.3517		
2	0.1047	18.0116	0.1033	27.7738	0.1210	32.4351	0.1961	52.2946
3	0.1047	17.9839	0.1046	28.0538	0.1202	29.4844	0.2093	24.4412
4	0.1036	17.9782	0.1038	28.2490	0.1238	31.4645	0.2207	43.9847
5	0.1124	15.9459	0.1030	31.6431	0.1340	37.2103	0.1215	19.5734
6	0.1050	17.7158	0.0969	29.2139	0.0991	20.9985	0.1652	40.4407
7	0.1016	18.6228	0.1039	27.8718	0.1197	30.9386	0.1384	36.3307

Table 4.4: Electromechanical Mode Eigenvalue Comparison

System without PSSs	System with PSSs on Machine 3 7 8	System with PSSs on Machine 3 7 8 1	System with PSSs on Machine 3 7 8 2
-0.3354±j 9.1267	-0.3352±j 9.1273	-0.8393±j 7.4043	-0.8846±j 7.3731
-0.2188±j 8.6423	-0.2259±j 8.6496	-0.2309±j 8.6538	-0.2252±j 8.6497
-0.0947±j 7.2452	-0.1267±j 7.2762	-0.6384±j 7.9944	-0.2448±j 7.6732
-0.0627±j 7.0242	-0.1964±j 6.8179	-0.2902±j 6.1798	-0.3024±j 6.1700
-0.1970±j 6.5043	-0.2521±j 6.1470	-0.2131±j 6.8286	-0.2127±j 6.8316
0.5083±j 5.3235	-4.2782±j 3.2087 *	-4.2782±j 3.2087 *	-4.2782±j 3.2087 *
0.5260±j 5.4462	-3.8301±j 3.9075 *	-3.8301±j 3.9075 *	-3.8301±j 3.9075 *
0.2248±j 6.1273	-1.8394±j 5.8490 *	-1.8394±j 5.8490 *	-1.8394±j 5.8490 *
0.0922±j 2.8020	-0.5275±j 2.7844	-1.1214±j 2.5695 *	-1.1214±j 2.5695 *

* Denotes Exact Assignment of Eigenvalues

System with PSSs on Machine 3 7 8 4	System with PSSs on Machine 3 7 8 5	System with PSSs on Machine 3 7 8 6	System with PSSs on Machine 3 7 8 9
-0.3330±j 9.1156	-0.3356±j 9.1252	-0.3353±j 9.1267	-0.3342±j 9.1235
-0.2260±j 8.6497	-0.1260±j 7.3206	-0.5298±j 8.0959	-0.2249±j 8.6497
-0.8807±j 7.3808	-0.6402±j 7.3419	-0.1838±j 7.2780	-0.1118±j 7.1568
-0.1705±j 7.0351	-0.5448±j 6.8192	-0.3232±j 6.6798	-0.8450±j 7.3728
-0.1261±j 6.7231	-0.6727±j 6.1768	-0.4222±j 5.9310	-0.2690±j 6.1339
-4.2782±j 3.2087 *	-4.2782±j 3.2087 *	-4.2782±j 3.2087 *	-4.2782±j 3.2087 *
-3.8301±j 3.9075 *	-3.8301±j 3.9075 *	-3.8301±j 3.9075 *	-3.8301±j 3.9075 *
-1.8394±j 5.8490 *	-1.8394±j 5.8490 *	-1.8394±j 5.8490 *	-1.8394±j 5.8490 *
-1.1214±j 2.5695 *	-1.1214±j 2.5695 *	-1.1214±j 2.5695 *	-1.1214±j 2.5695 *

* Denotes Exact Assignment of Eigenvalues

only that the exact assignments of specified dampings to unstable modes can be achieved for all designs but also that the dampings of the other two poorly damped modes are improved.

To assess the actual performances of all designs, comprehensive nonlinear simulation tests are performed and system stability indices are calculated as already described in Chapter 3. Typical simulation results of the closed–loop system for three-stabilizer design are plotted in Fig. 4.2. The results show how three stabilizers on machines 3, 7, and 8 can effectively stabilize the nine–machine system under a severe disturbance. Note that the nine–machine system is initially unstable for the same short–circuit test as shown in Figs. 3.2 through 3.6

4.3 Conclusions

1. A new pole–placement technique is presented in this chapter for decentralized stabilizer design of multimachine power systems to damp low–frequency oscillations. A concise and systematic mathematical formulation is developed to reduce the system state equations to algebraic equations. The parameters of all PSSs in a multimachine power system can be determined simultaneously from the algebraic equations. Since PSS transfer functions are explicitly expressed in our algebraic equations, less computation is required for the determination of PSS parameters than the existing methods.

2. The effectiveness of the new pole–placement design technique has been demonstrated by various PSS designs of the two multimachine power systems. Exact assignment of any number of eigenvalues associated with low–frequency oscillating modes to new specified locations can be achieved for all designs.

3. Non–uniform damping factors can be assigned to the eigenvalues to be changed.

Assigning a relatively large damping factor to an unstable mechanical mode can also improve the damping of poorly damped mechanical modes nearby through the dynamic interaction of machines.

4. The pole–placement technique in this chapter is general and it can also be applied to the decentralized stabilizer design of other industries.

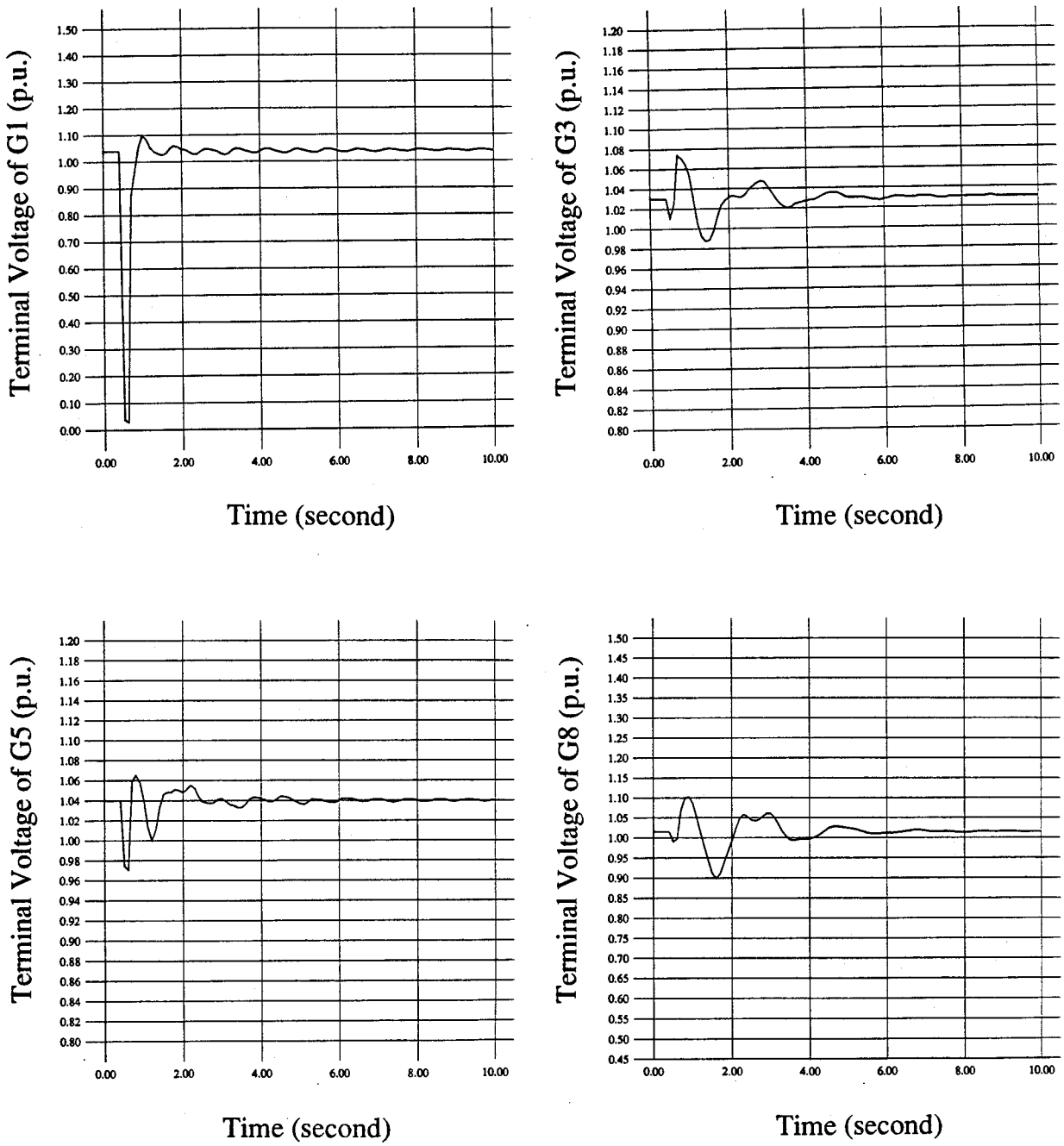

Figure 4.2: Responses to a Short–Circuit near G1 Bus. (a)

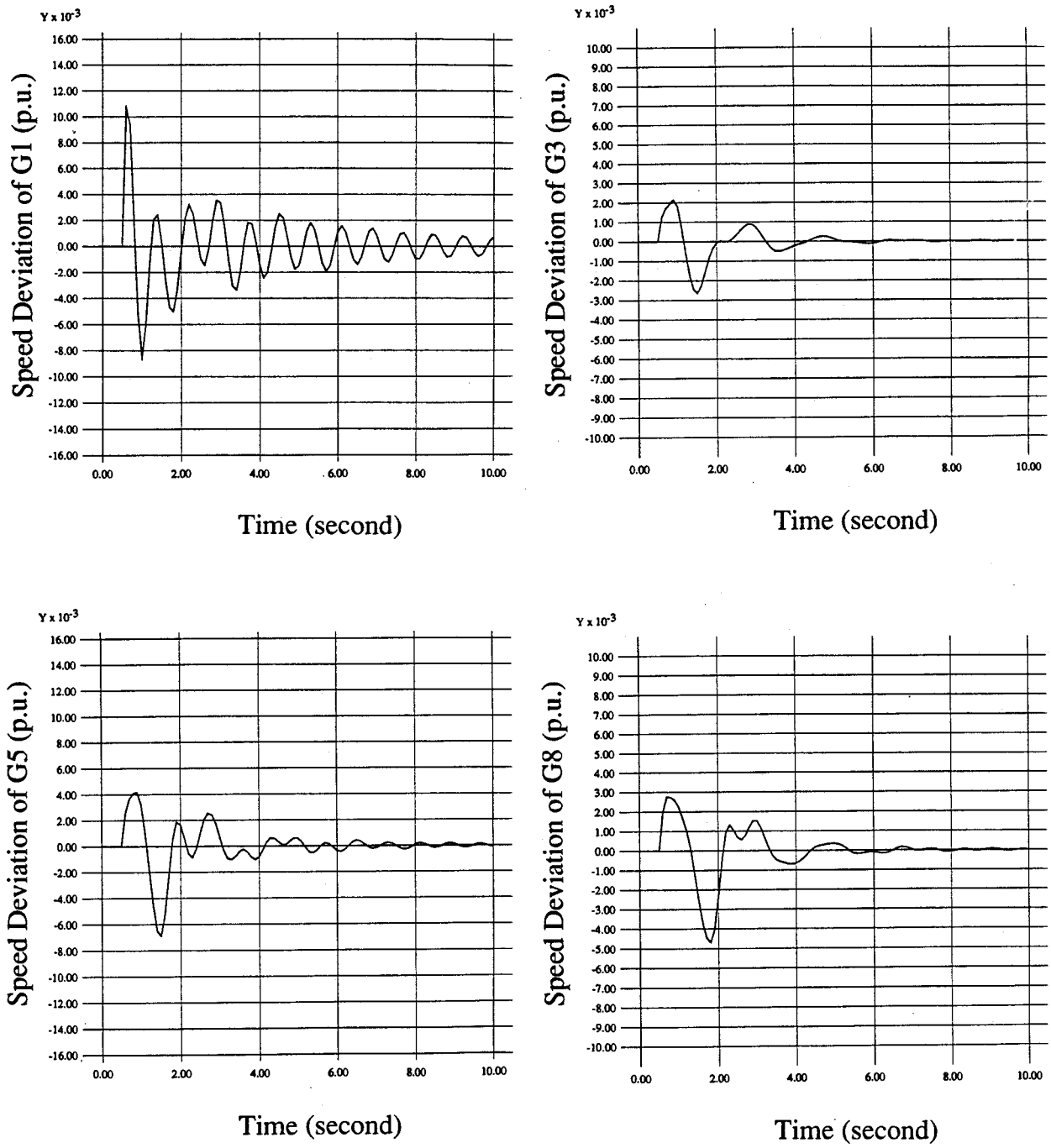

Figure 4.2: Responses to a Short–Circuit near G1 Bus. (b)

Chapter 5

DIRECT MIMO STR FOR MULTIMACHINE SYSTEMS WITH CHANGING OPERATING CONDITIONS

The conventional Power System Stabilizer (PSS) is designed for power system in normal operating state. The system equations for PSS design are linearized around the given operating conditions. For the PSS design, the data of a power system must be complete and the parameters of PSSs are fixed. The fixed stabilizers work properly for the power system only for the given operating conditions. However, the operating conditions of many power systems are constantly changing due to the intentional energy management of the electric plants or unintentional disturbances to the system. If the operating conditions of a power system vary greatly from the given values for which PSSs are designed, the parameters of the fixed PSSs must be retuned. Therefore, it is highly desirable to have a self–tuning stabilizer for some power systems, which can constantly sample the system output, predict the future behavior of the system and automatically self–tune the stabilizer parameters to maintain an optimal performance for power systems.

The self–tuning regulator (STR) has been developed since the early 70's. The minimum variance regulator (MVR) [22] is designed by minimizing the variance of plant output. The generalized minimum variance controller (GMV) [23] is generalized by minimizing both plant output and control. The pole-assignment controller (PAC) ([24]–[26]) allows the prescription of closed-loop poles. The extended horizon controller (EHC) ([27]–[28]) is designed with a time horizon for output predictor. Finally, the generalized predictive control (GPC) [29] is developed with a long–range output predictor and a

control with horizons. A review of the development of these STRs is given in Section 5.1.

In Section 5.2, the principle of Clarke's GPC for indirect single-input–single–output (SISO) STR design is extended to a direct MIMO STR design for power systems. There are two improvements: the initial step control parameters are directly estimated without solving the Diophantine equation and estimating the plant parameters, and the subsequent control parameter is calculated recursively. The computational requirement of GPC is greatly reduced.

In Section 5.3, the method of the new direct MIMO STR is applied to the STR design for the nine–machine power system described in Chapter 3. A set of three STRs is designed for the system. For each STR, the local generator rotor speed and the terminal voltage are chosen as plant output variables and both governor and exciter loops are controlled. The results of the design are evaluated with comprehensive computer simulations for a multimachine system with wide–range changing operating conditions. A comparison between conventional PSSs and the designed STRs is also made.

Many results of this chapter are published [39].

5.1 Review of Self–Tuning Controls

5.1.1 Minimum Variance Regulator (MVR)

In Åström's MVR, the plant is described by a CARMA (Controlled Autoregressive Moving Average) model

$$Ay(t) = q^{-k}Bu(t) + e(t) \tag{5.1}$$

where $y(t)$ is the plant output, $u(t)$ is the control signal, $e(t)$ is a white noise with zero mean, t is the sampling instant, and k is the time delay. A and B are polynomials of the

backward–shift operator q^{-1}

$$\begin{aligned} A = &\ 1 + a_1 q^{-1} + \ldots + a_{na} q^{-na} \\ B = &\ b_0 + b_1 q^{-1} + \ldots + b_{nb} q^{-nb} \end{aligned}$$

To find a predictor for output, a Diophantine equation is defined

$$1 = q^{-k} F + EA \tag{5.2}$$

where E and F are polynomials in q^{-1} of degree $k-1$ and $na-1$, respectively. A k–step–ahead predictor for $y(t)$, which can be obtained from Eq. (5.1) and Eq. (5.2), is

$$y(t+k) = Fy(t) + EBu(t) + Ee(t+k) \tag{5.3}$$

Since $Ee(t+k)$ is the noise in the future, uncorrelated with other RHS terms of Eq. (5.3), the optimal predictor for $y(t+k)$ is

$$\hat{y}\ (t+k|t) = Fy(t) + EBu(t) \tag{5.4}$$

where $\hat{y}\ (t+k|t)$ represents a k–step–ahead optimal predictor from sampled data up to t. For minimizing the variance of plant output, $\hat{y}\ (t+k|t)$ is set to zero. Therefore, a control law becomes

$$u(t) \ = \ -\frac{F}{G} y(t) \tag{5.5}$$

where

$$G = EB$$

The control parameters F and G are directly estimated from Eq. (5.3) without estimating plant parameters A and B. Therefore, MVR is a *direct* self–tuning controller.

Eq. (5.5) shows that polynomial B must have stable roots for $u(t)$ to be bounded. Therefore, the MVR cannot be applied to a plant with unstable B or a non–minimum phase plant.

5.1.2 Generalized Minimum Variance Control (GMV)

The same plant model as Eq. (5.1) is defined for GMV but an auxiliary output is considered

$$\Phi(t) = Py(t) - q^{-k}Ry_r(t) + q^{-k}Qu(t) \tag{5.6}$$

where P, Q and R are weighting polynomials chosen by the designer and $y_r(t)$ is a reference output. To find a predictor for $\Phi(t)$, a Diophantine equation is defined

$$P = q^{-k}F + EA \tag{5.7}$$

The k–step–ahead predictor for $\Phi(t)$, which can be obtained from equations (5.1), (5.6) and (5.7), is

$$\Phi(t+k) = Fy(t) + (Q + EB)u(t) - Ry_r(t) + Ee(t+k) \tag{5.8}$$

Since $Ee(t+k)$ is uncorrelated with other RHS terms of Eq. (5.8), the best predictor for $\Phi(t+k)$ is

$$\hat{\Phi}\,(t+k|t) = Fy(t) + (Q + EB)u(t) - Ry_r(t) \tag{5.9}$$

To minimize the variance of the auxiliary output, $\hat{\Phi}\,(t+k|t)$ of GMV must be zero. Therefore, a control law becomes

$$u(t) \;=\; \frac{Ry_r(t) - Fy(t)}{G} \tag{5.10}$$

where

$$G = Q + EB$$

The closed–loop equation with the control is

$$y(t) = \frac{RB}{BP + AQ}y_r(t-k) + \frac{G}{BP + AQ}e(t) \tag{5.11}$$

The control parameters F and G of this STR are directly estimated from Eq. (5.8). Therefore, GMV is also a direct self–tuning controller.

Eq. (5.11) shows that in order for GMV to deal with an unstable B (non–minimum phase plant), the Q could be taken as a scalar and must be large enough to let the closed–loop poles approach the zeros of AQ when A is stable; and that in order to handle an unstable A (open–loop unstable plant), the values of P must be large enough. Hence, the GMV can control a non-minimum phase or open–loop unstable plant with carefully chosen Q and P. However, GMV is sensitive to varying delay time k unless Q is large.

5.1.3 Pole–Assignment Control (PAC)

Eq. (5.11) shows that the poles of the closed–loop system with GMV control are the roots of polynomial $BP + AQ$. Let

$$BP + AQ = T \tag{5.12}$$

where polynomial T may be prespecified with its roots equal to the desired closed–loop poles. When polynomials P and Q are chosen to satisfy Eq. (5.12), the GMV becomes a PAC.

For self–tuning control, plant parameters A and B of Eq. (5.1) may be estimated and P and Q are then calculated from Eq. (5.12). The drawback of PAC is that Eq. (5.12) cannot be solved if A and B have a common factor.

5.1.4 Extended Horizon Control (EHC)

When the plant time delay k of Eq. (5.1) is uncertain, a more general plant model may be considered

$$Ay(t) = q^{-1}Bu(t) + e(t) \tag{5.13}$$

where time delay k is assumed to be 1. For an actual time delay k, the $k-1$ leading coefficients of B of Eq. (5.13) are zero.

The following Diophantine equation is defined for EHC

$$1 = q^{-T}F + EA \tag{5.14}$$

where T is a time horizon chosen for the design, which is usually larger than the actual plant time delay or the upper limit of a varying plant time delay.

A T–step–ahead predictor for $y(t)$ can be obtained from Eq. (5.13) and Eq. (5.14)

$$y(t+T) = Fy(t) + EBu(t+T-1) + Ee(t+T) \tag{5.15}$$

The optimal predictor for $y(t+T)$ is

$$\hat{y}\,(t+T|t) = Fy(t) + EBu(t+T-1) \tag{5.16}$$

Let polynomial EB ($degree = nb + T - 1$) be written as

$$\begin{aligned} EB = \;& h_0 + h_1 q^{-1} + \cdots + h_{T-1} q^{-(T-1)} \\ & + q^{-(T-1)}(g_1 q^{-1} + g_2 q^{-2} + \cdots + g_{nb} q^{-nb}) \end{aligned} \tag{5.17}$$

A reference output $y_r(t+T)$ is specified in EHC to satisfy

$$\hat{y}\,(t+T|t) = y_r(t+T) \tag{5.18}$$

Substituting Eqs. (5.17) and (5.18) into Eq. (5.16), and choosing the constant control $u(t) = u(t+1) = \ldots = u(t+T-1)$ [27], we obtain a control law

$$u(t) = \frac{1}{\Sigma_{i=0}^{T-1} h_i}(y_r(t+T) - Fy(t) - \Sigma_{i=1}^{nb} g_i u(t-i)) \tag{5.19}$$

For this self–tuning control, control parameters F, h_i and g_i are directly estimated from Eq. (5.15). Therefore, the EHC is a direct self–tuning controller. Since the time horizon T is larger than the actual time delay, the roots of B are not included in the control signal of the EHC. Therefore, EHC can control a non–minimum phase plant. However, simulation experience shows that EHC is unstable for an open–loop unstable plant [29].

5.1.5 Generalized Predictive Control (GPC)

For GPC design, the plant is described by a CARIMA (Controlled Auto–Regressive and Integrated Moving Average) model

$$\begin{aligned} Ay(t) &= q^{-1}Bu(t) + e(t)/\Delta \\ \Delta &= 1 - q^{-1} \end{aligned} \tag{5.20}$$

A train of Diophantine equations is defined

$$1 = q^{-j}F_j + E_jA\Delta \qquad j = 1, 2, \ldots, T \tag{5.21}$$

where the degree of polynomial F_j is na and T is referred to as a maximum output horizon. A set of predictors for output can be obtained from Eq. (5.20) and Eq. (5.21) as

$$y(t+j) = F_jy(t) + E_jB\Delta u(t+j-1) + E_je(t+j) \qquad j = 1, 2, \ldots, T \tag{5.22}$$

Let

$$\begin{aligned} E_jB &= H_j + G_j \qquad j = 1, 2, \ldots, T \\ H_j &= h_0(j) + h_1(j)q^{-1} + \cdots + h_{j-1}(j)q^{-(j-1)} \\ G_j &= q^{-(j-1)}(g_1(j)q^{-1} + g_2(j)q^{-2} + \cdots + g_{nb}(j)q^{-nb}) \end{aligned} \tag{5.23}$$

Besides the maximum horizon T, a minimum output horizon $n1$ and a control horizon nu are defined for selecting the number of optimal predictors from Eq. (5.22). The selected optimal predictors are written in matrix form as

$$\left[\hat{y}\right] = [y_p] + [H]\,[u_c] \tag{5.24}$$

where

$$\begin{aligned} \left[\hat{y}\right] &= \left[\hat{y}\,(t+n1|t), \hat{y}\,(t+n1+1|t), \cdots, \hat{y}\,(t+T|t)\right]^T \\ [y_p] &= [F]\,[y(t), y(t-1), \cdots, y(t-na)]^T \\ &\quad + [G]\,[\Delta u(t-1), \Delta u(t-2), \cdots, \Delta u(t-nb)]^T \\ [u_c] &= [\Delta u(t), \Delta u(t+1), \cdots, \Delta u(t+nu-1)]^T \end{aligned}$$

wherein the j–th rows of matrices $[H]$, $[F]$, and $[G]$ respectively contain the coefficients of polynomials H_j, F_j and G_j, $j = n1, \ldots, T$. A cost function is then defined as follows

$$J = ([\hat{y}] - [y_r])^T([\hat{y}] - [y_r]) + r[u_c]^T[u_c] \tag{5.25}$$

Minimizing J with respect to $[u_c]$ gives

$$u(t) = u(t-1) + [P]([y_r] - [y_p]) \tag{5.26}$$

where $[P]$ is the first row of $(H^T H + rI)^{-1} H^T$.

For the self–tuning control, plant parameters A and B of Eq. (5.20) must be estimated first and F_1 and E_1 is then calculated from Eq. (5.21). To compute F_j and E_j for $j = 2$, $\ldots$, T, a recursive equation is developed. Finally, the control parameters H_j and G_j, $j = 1, \ldots, T$, are obtained from $E_j B$ according to Eq. (5.23). Therefore, the GPC is an *indirect* self–tuning controller. Moreover, control parameters H_j and G_j cannot be obtained directly by a recursive equation. The GPC requires heavy computation.

5.1.6 Summary of STRs

The MVR requires the least computation but cannot handle the non-minimum phase problem (unstable B polynomial). The GMV control can handle the non–minimum phase plant, but it is sensitive to the varying time delay of a plant. The PAC allows the prescription of closed-loop poles, but it cannot cope with a common factor which may occur in the numerator B and denominator A of the plant transfer function. The EHC can handle the non–minimum phase and uncertain system time delay, but may still have difficulty in dealing with the unstable system poles. The GPC is probably the best method of STR design to handle plants with non–minimum phase, common factor, uncertain time delay, and unstable open–loop dynamics. The only drawback of GPC design is the heavy computational requirement.

5.2 A New Direct MIMO STR for Power System

These STR principles have been applied to pulp mills, chemical processes and other industrial processes ([30], [31]). The application of STRs to power systems has also been studied ([32]–[37]), involving only a few of machines. But a larger power system with more machines should be chosen for study since without a reasonable number of machines, the dynamic interactions between machines cannot be thoroughly investigated. In addition, a power system usually has unstable or poorly damped open–loop poles. Also, it is difficult to have the exact information of both system time delay and non–minimum phase when the system operation changes over a wide range. Therefore, the principle of GPC is most attractive for the STR design of power systems. However, the design technique of GPC, especially the computational requirement, must be improved.

In this section, the principle of Clarke's GPC for an indirect SISO STR design is extended to a direct MIMO STR design. A train of modified Diophantine equations and a set of output predictions are described in subsection 5.2.1. A control law from minimization of a cost function of weighted optimal predictors and control signals is derived in subsection 5.2.2. A new recursive equation for control parameter computation is developed in subsection 5.2.3 and a method of direct estimation of the initial step control parameters in subsection 5.2.4. The algorithm of the STR design is summarized in subsection 5.2.5.

5.2.1 Basic Equations and Long-Range Output Prediction

For the MIMO STR design, the vector output of a plant is modeled by

$$[A]\,[y(t)] = q^{-1}\,[B]\,[u(t)] + [e(t)]\,/\Delta \tag{5.27}$$

where

$$
\begin{aligned}
[y(t)] &= [y_1(t), y_2(t)]^T \\
[u(t)] &= [u_1(t), u_2(t)]^T \\
[e(t)] &= [e_1(t), e_2(t)]^T \\
[A] &= \left[I + A_1 q^{-1} + \cdots + A_{na} q^{-na}\right] \\
[B] &= \left[B_0 + B_1 q^{-1} + \cdots + B_{nb} q^{-nb}\right] \\
\Delta &= 1 - q^{-1}
\end{aligned}
$$

In Eq. (5.27), $[y(t)]$ is the plant output vector consisting of rotor speed and terminal voltage at sampling instant t, $[u(t)]$ the control signal vector of excitation and governor loops, $[e(t)]$ the errors, and $[A]$ and $[B]$ are polynomials of the backward-shift operator q^{-1} with 2×2 matrix coefficients. The integrator $1/\Delta$ is introduced to eliminate the static errors. The superscript T indicates the transpose of a vector or matrix.

For a long–range predictor, an output horizon T (maximum output horizon) is assumed and the following Diophantine equation set similar to the original GPC [29], but in matrix form for MIMO design, may be defined.

$$
[I] = q^{-j}\left[F_j'\right] + [E_j]\,[A]\,\Delta \qquad j = 1, 2, \ldots, T \tag{5.28}
$$

where

$$
\begin{aligned}
\left[F_j'\right] &= [F_0'(j) + F_1'(j) q^{-1} + \cdots + F_{na}'(j) q^{-na}] \\
[E_j] &= \left[E_0(j) + E_1(j) q^{-1} + \cdots + E_{j-1}(j) q^{-(j-1)}\right]
\end{aligned}
$$

Here all $F_0'(j), \ldots, F_{na}'(j), E_0(j), \ldots E_{j-1}(j)$ are 2×2 matrices. To simplify the computation of GPC, the Diophantine equation set may be modified as follows. Since $[F_j'] = [I]$ for $q^{-1} = 1$ according to Eq. (5.28), $\left[F_j'\right]$ may be separated into two terms

$$
\begin{aligned}
\left[F_j'\right] &= [I] + [F_j]\,\Delta \\
&= [I] + [F_0(j) + F_1(j) q^{-1} + \cdots + F_{na-1}(j) q^{-na+1}]\,\Delta
\end{aligned}
$$

Therefore, the Diophantine equation set of Eq. (5.28) can be modified as

$$[I] = q^{-j}([I] + [F_j]\,\Delta) + [E_j]\,[A]\,\Delta \qquad j = 1, 2, \ldots, T \tag{5.29}$$

where $[F_j]$ has one less matrix coefficient than $[F_j']$ of the original GPC.

Postmultiplying both sides of Eq. (5.29) by $[y(t)]$, we shall have

$$\begin{aligned}
[y(t)] &= q^{-j}[y(t)] + q^{-j}\,[F_j]\,\Delta\,[y(t)] + [E_j]\,[A]\,[y(t)]\,\Delta \\
&= q^{-j}[y(t)] + q^{-j}\,[F_j]\,\Delta\,[y(t)] + [E_j]\,[B]\,\Delta\,[u(t-1)] + [E_j]\,[e(t)] \\
&\qquad\qquad j = 1, 2, \ldots, T
\end{aligned}$$

The j-step-ahead prediction $[y(t+j)]$ can be obtained from the above equation by shifting time t ahead by j steps

$$\begin{aligned}
[y(t+j)] = \;& [y(t)] + [F_j]\,\Delta\,[y(t)] + [E_j]\,[B]\,\Delta\,[u(t+j-1)] + [E_j]\,[e(t+j)] \\
& j = 1, 2, \ldots, T
\end{aligned} \tag{5.30}$$

$[E_j]\,[B]$ of Eq. (5.30) is of degree $nb + j - 1$ and can be separated into a polynomial $[G_j]$ for the known controls of the past and a polynomial $[H_j]$ for the unknown controls of the future,

$$[E_j]\,[B] = [H_j] + [G_j]$$

where

$$\begin{aligned}
[H_j] &= \left[H_0(j) + H_1(j)q^{-1} + \cdots + H_{j-1}(j)q^{-(j-1)}\right] \\
[G_j] &= q^{-(j-1)}\left[G_1(j)q^{-1} + G_2(j)q^{-2} + \cdots + G_{nb}(j)q^{-nb}\right]
\end{aligned}$$

All $H_0(j), \ldots, H_{j-1}(j), G_1(j), \ldots, G_{nb}(j)$ are 2×2 matrices. Therefore, Eq. (5.30) may

be written

$$
\begin{aligned}
[y(t+j)] = \; & [y(t)] \\
& + [F_o(j)\Delta y(t) + F_1(j)\Delta y(t-1) + \cdots + F_{na-1}(j)\Delta y(t-na+1)] \\
& + [H_o(j)\Delta u(t+j-1) + H_1(j)\Delta u(t+j-2) + \cdots H_{j-1}(j)\Delta u(t)] \\
& + [G_1(j)\Delta u(t-1) + G_2(j)\Delta u(t-2) + \cdots + G_{nb}(j)\Delta u(t-nb)] \\
& + \left[E_o(j) + E_1(j)q^{-1} + \cdots + E_{j-1}(j)q^{-(j-1)}\right][e(t+j)] \\
& \qquad j = 1, 2, \ldots, T
\end{aligned}
\tag{5.31}
$$

There are T equations of (5.31) which may be written in matrix form

$$
[y_f] = [y_p] + [H]\,[u_c] + [E]\,[e] \tag{5.32}
$$

where $[y_f]$ is the predicted output of the future, $[y_p]$ the output and control of the past, $[u_c]$ the control to be determined and $[e]$ the errors of the future. Details are

$$
\begin{aligned}
[y_f] = \; & \left[y(t+1)^T, y(t+2)^T, \cdots, y(t+T)^T\right]^T \\
[y_p] = \; & [C]\,[y(t)] \\
& + [F]\left[\Delta y(t)^T, \Delta y(t-1)^T, \cdots, \Delta y(t-na+1)^T\right]^T \\
& + [G]\left[\Delta u(t-1)^T, \Delta u(t-2)^T, \cdots, \Delta u(t-nb)^T\right]^T \\
[u_c] = \; & \left[\Delta u(t)^T, \Delta u(t+1)^T, \cdots, \Delta u(t+T-1)^T\right]^T \\
[e] = \; & \left[e(t+1)^T, e(t+2)^T, \cdots, e(t+T)^T\right]^T
\end{aligned}
$$

and

$$
[C] = \begin{bmatrix} C(1) & C(2) & C(3) & \cdots & C(T) \end{bmatrix}^T
$$

where $[C]$ is a $2T \times 2$ matrix and $C(1), C(2)$, etc., are 2×2 unit matrices. Other details

are

$$[F] = \begin{bmatrix} F_0(1) & F_1(1) & F_2(1) & \cdots & F_{na-1}(1) \\ F_0(2) & F_1(2) & F_2(2) & \cdots & F_{na-1}(2) \\ F_0(3) & F_1(3) & F_2(3) & \cdots & F_{na-1}(3) \\ \vdots & \vdots & \vdots & \vdots & \vdots \\ F_0(T) & F_1(T) & F_2(T) & \cdots & F_{na-1}(T) \end{bmatrix}$$

$$[G] = \begin{bmatrix} G_1(1) & G_2(1) & G_3(1) & \cdots & G_{nb}(1) \\ G_1(2) & G_2(2) & G_3(2) & \cdots & G_{nb}(2) \\ G_1(3) & G_2(3) & G_3(3) & \cdots & G_{nb}(3) \\ \vdots & \vdots & \vdots & \vdots & \vdots \\ G_1(T) & G_2(T) & G_3(T) & \cdots & G_{nb}(T) \end{bmatrix}$$

$$[H] = \begin{bmatrix} H_0(1) & & & & \\ H_1(2) & H_0(2) & & & \\ H_2(3) & H_1(3) & H_0(3) & & \\ \vdots & \vdots & \vdots & \ddots & \\ H_{T-1}(T) & H_{T-2}(T) & H_{T-3}(T) & \cdots & H_0(T) \end{bmatrix}$$

$[E]$ is similar to $[H]$ except that E replaces H. Note that each element of $[F]$, $[G]$ and $[H]$ is 2×2 matrix and that the upper–right matrix elements above the diagonal of $[H]$ and those of $[E]$ are null. The dimensions of $[F]$, $[G]$, and $[H]$ or $[E]$ are $2T \times 2na$, $2T \times 2nb$, and $2T \times 2T$, respectively.

5.2.2 Control Laws

Consider Eq. (5.32) again. Since the last term of Eq. (5.32) is the disturbance of the future, the first two terms on the RHS of Eq. (5.32) correspond to a set of optimal

predictors. Let it be

$$\begin{aligned}\left[\hat{Y}\right] &= \left[\hat{y}\,(t+1|t)^T, \hat{y}\,(t+2|t)^T, \ldots, \hat{y}\,(t+T|t)^T\right]^T \\ &= [y_p] + [H]\,[u_c]\end{aligned} \tag{5.33}$$

Consider a desirable optimal predictor $[Y]$

$$[Y] = \left[\hat{y}\,(t+n_1|t)^T, \hat{y}\,(t+n_1+1|t)^T, \ldots \hat{y}\,(t+T|t)^T\right]^T \tag{5.34}$$

which is a subset of $\left[\hat{Y}\right]$, or $\left[\hat{Y}\right]$ less the first $2(n_1-1)$ rows, where n_1 is a minimum output horizon, $1 \leq n_1 \leq T$.

Next, since our concern is the increment $\Delta u(t)$ of the present, the increments $\Delta u(t+j)$ of the future for $j \geq n_u$, $1 \leq n_u \leq T$, may be set to zero. Therefore, $[u_c]$ of Eq. (5.32) becomes

$$\left[\bar{u_c}\right] = \left[\Delta u(t)^T, \Delta u(t+1)^T, \cdots, +\Delta u(t+n_u-1)^T\right] \tag{5.35}$$

and the desired optimal predictor may be written

$$[Y] = \left[\bar{y_p}\right] + \left[\bar{H}\right]\left[\bar{u_c}\right] \tag{5.36}$$

where

$$\begin{aligned}\left[\bar{y_p}\right] = &\left[\bar{C}\right][y(t)] \\ &+ \left[\bar{F}\right]\left[\Delta y(t)^T, \Delta y(t-1)^T, \cdots, \Delta y(t-na+1)^T\right]^T \\ &+ \left[\bar{G}\right]\left[\Delta u(t-1)^T, \Delta u(t-2)^T, \cdots, \Delta u(t-nb)^T\right]^T\end{aligned}$$

and

$$\begin{aligned}[\bar{C}] &= [C] \text{ without the first } 2(n_1-1) \text{ rows} \\ [\bar{F}] &= [F] \text{ without the first } 2(n_1-1) \text{ rows} \\ [\bar{G}] &= [G] \text{ without the first } 2(n_1-1) \text{ rows} \\ [\bar{H}] &= \text{the first } 2nu \text{ columns of } [H] \\ &\quad \text{without its first } 2(n_1-1) \text{ rows}\end{aligned} \tag{5.37}$$

To design a long–range optimal predictive control with minimum control effort, the following output reference sequence is chosen

$$[y_r] = \left[y_r(t+n_1)^T, y_r(t+n_1+1)^T, \cdots, y_r(t+T)^T\right]^T \tag{5.38}$$

where

$$[y_r(t+j)] = [y_{r1}(t+j), y_{r2}(t+j)]^T \qquad j = n_1, ..., T$$

Let a cost function be

$$J = ([Y] - [y_r])^T [Q] ([Y] - [y_r]) + \left[\bar{u}_c\right]^T [R] \left[\bar{u}_c\right] \tag{5.39}$$

where $[Q]$ and $[R]$ are weighting matrices. Substituting Eq. (5.36) into Eq. (5.39), minimizing J with respect to $\left[\bar{u}_c\right]$, and solving for $\left[\bar{u}_c\right]$ give

$$\left[\bar{u}_c\right] = (\left[\bar{H}\right]^T [Q] \left[\bar{H}\right] + [R])^{-1} \left[\bar{H}\right]^T [Q] ([y_r] - \left[\bar{y}_p\right]) \tag{5.40}$$

The control signals of the present correspond to the first two elements of $\left[\bar{u}_c\right]$

$$\begin{bmatrix} u_1(t) \\ u_2(t) \end{bmatrix} = \begin{bmatrix} u_1(t-1) \\ u_2(t-1) \end{bmatrix} + [P] \left[\bar{H}\right]^T [Q] ([y_r] - \left[\bar{y}_p\right]) \tag{5.41}$$

where $[P]$ is the first two rows of $(\left[\bar{H}\right]^T [Q] \left[\bar{H}\right] + [R])^{-1}$.

5.2.3 Recursive Computation of Control Parameters

In the original GPC design [29], a recursive equation was developed to calculate parameters $[E_j]$, $[F_j]$ of the Diophantine equation, but not control parameters. Additional calculations of control parameters $[H(j)]$ and $[G(j)]$, $j = 1, 2, \ldots, T$ were required. It was time–consuming even for the SISO control design. In our direct MIMO STR, a recursive

algorithm is developed so that the control parameters $[F(j)]$, $[G(j)]$ and $[H(j)]$ are directly computed from $[F(j-1)]$, $[G(j-1)]$, and $[H(j-1)]$ without solving Diophantine equations.

The recursive formula may be derived as follows. Let j of Eq. (5.31) be replaced by $j-1$ and t of the same equation by $t+1$. In other words, let the time t be shifted one step ahead, we have

$$\begin{aligned}
[y(t+j)] &= [y(t+1)] + \Delta\,[F_o(j-1)y(t+1)] \\
&+ [F_1(j-1)\Delta y(t) + \cdots + F_{na-1}(j-1)\Delta y(t-na+2)] \\
&+ [H_o(j-1)\Delta u(t+j-1) + H_1(j-1)\Delta u(t+j-2) + \cdots H_{j-2}(j-1)\Delta u(t+1)] \\
&+ [G_1(j-1)\Delta u(t) + G_2(j-1)\Delta u(t-1) \cdots + G_{nb}(j-1)\Delta u(t-nb+1)] \\
&+ \left[E_o(j-1) + E_1(j-1)q^{-1} + \cdots + E_{j-2}(j-1)q^{-(j-2)}\right][e(t+j)]
\end{aligned} \tag{5.42}$$

Rearranging the first two terms on the RHS of Eq (5.42) gives

$$\begin{aligned}
[y(t+j)] &= [I + F_o(j-1)]\,[y(t+1)] - [F_o(j-1)y(t)] \\
&+ [F_1(j-1)\Delta y(t) + \cdots + F_{na-1}(j-1)\Delta y(t-na+2)] \\
&+ [H_o(j-1)\Delta u(t+j-1) + H_1(j-1)\Delta u(t+j-2) + \cdots H_{j-2}(j-1)\Delta u(t+1)] \\
&+ [G_1(j-1)\Delta u(t) + G_2(j-1)\Delta u(t-1) \cdots + G_{nb}(j-1)\Delta u(t-nb+1)] \\
&+ \left[E_o(j-1) + E_1(j-1)q^{-1} + \cdots + E_{j-2}(j-1)q^{-(j-2)}\right][e(t+j)]
\end{aligned} \tag{5.43}$$

For j=1, Eq (5.31) may be written as follows

$$\begin{aligned}
[y(t+1)] = \;& [y(t)] \\
&+ [F_o(1)\Delta y(t) + F_1(1)\Delta y(t-1) + \cdots + F_{na-1}(1)\Delta y(t-na+1)] \\
&+ [H_o(1)\Delta u(t)] \\
&+ [G_1(1)\Delta u(t-1) + G_2(1)\Delta u(t-2) + \cdots + G_{nb}(1)\Delta u(t-nb)] \\
&+ [E_o(1)]\,[e(t+1)]
\end{aligned} \tag{5.44}$$

Substituting Eq (5.44) into Eq (5.43) and comparing the results with the like terms of Eq (5.31) give a recursive computation formula of the control parameters as follows

$$F_i(j) = \begin{cases} (F_o(j-1)+I)F_i(1) + F_{i+1}(j-1) & for \quad i = 0,1,\ldots,na-2 \\ (F_o(j-1)+I)F_i(1) & for \quad i = na-1 \end{cases}$$

$$G_i(j) = \begin{cases} (F_o(j-1)+I)G_i(1) + G_{i+1}(j-1) & for \quad i = 1,2,\ldots,nb-1 \\ (F_o(j-1)+I)G_i(1) & for \quad i = nb \end{cases}$$

$$H_i(j) = \begin{cases} H_i(j-1) & for \quad i = 0,1,\ldots,j-2 \\ (F_0(j-1)+I)H_0(1) + G_1(j-1) & for \quad i = j-1 \end{cases} \tag{5.45}$$

$$E_i(j) = \begin{cases} E_i(j-1) & for \quad i = 0,1,\ldots,j-2 \\ (F_0(j-1)+I)E_0(1) & for \quad i = j-1 \end{cases}$$

Note that E parameters are not required for our STR design. The initial step control parameters, $F_i(1)$, $H_i(1)$, and $G_i(1)$, can be estimated from system dynamic responses, which is described in detail in the next subsection.

5.2.4 Direct Estimation of Initial Step Control Parameters

In our STR design, the control parameters $F_i(1)$, $H_i(1)$, and $G_i(1)$ of Eq. (5.45) are estimated directly. Since there are two control loops of a power plant, the excitation and the governor, the i-th row of the [F(1)], [G(1)], and [H(1)] is identified for the i-th loop, $i = 1, 2$. To that aim, j of Eq. (5.31) is replaced with 1 and t is back shifted one step,

resulting in

$$\begin{aligned}\Delta\left[y(t)\right] = \; & [F_o(1)\Delta y(t-1) + F_1(1)\Delta y(t-2) + \cdots + F_{na-1}(1)\Delta y(t-na)] \\ & + [H_o(1)\Delta u(t-1)] \\ & + [G_1(1)\Delta u(t-2) + G_2(1)\Delta u(t-3) + \cdots + G_{nb}(1)\Delta u(t-nb-1)] \\ & + [e(t)]\end{aligned} \tag{5.46}$$

Eq. (5.46) consists of measurement and data of zero mean. Eq. (5.46) may be written

$$\Delta y_i(t) = X(t-1)^T\Theta_i(t) + e_i(t) \qquad i = 1,2 \tag{5.47}$$

where the data vector $X(t-1)$ consists of a sequence of system output and control that are known at time t

$$\begin{aligned}X(t-1)^T \; = \; & [\Delta y(t-1)^T, \Delta y(t-2)^T, \ldots \Delta y(t-na)^T, \\ & \Delta u(t-1)^T, \Delta u(t-2)^T, \ldots \Delta u(t-nb-1)^T]\end{aligned}$$

and

$$\Theta_i(t)^T = \quad \text{the i-th row of} \quad [F_0(1), \ldots F_{na-1}(1), H_0(1), \ldots G_1(1), \ldots G_{nb}(1)] \qquad i = 1,2$$

Note that $F_0(1)$, ..., $F_{na-1}(1)$, $H_0(1)$, $G_1(1)$, ..., $G_{nb}(1)$ are 2×2 matrices. For the estimate of the parameter vector $\Theta_i(t)$ at each sampling, Bierman's UDU version of RLS (recursive least squares) [38] is employed. When these estimated $F_0(1)$, ..., $F_{na-1}(1)$, $H_0(1)$, $G_1(1)$, ..., $G_{nb}(1)$ are available, the subsequent control parameters can be computed recursively using Eq. (5.45) in the previous section.

5.2.5 Algorithm of the STR Design

The algorithm of the direct MIMO STR design is summarized as follows

1. Read new $[y(t)]$ and $[y_r(t)]$ at sampling instant t

2. Estimate [F(1)], [H(1)] and [G(1)] by the RLS— Eq. (5.47)

3. Compute [F(j)], [H(j)] and [G(j)] for $j > 1$— Eq. (5.45).

4. Decide $\left[\bar{F}\right]$, $\left[\bar{G}\right]$, and $\left[\bar{H}\right]$— Eq. (5.37).

5. Compute $[u(t)]$ and activate it—Eq. (5.41).

6. Set $t = t + 1$, go back to step 1 and repeat the process

5.3 Example of Design and Simulation Test of the New STR

In this section, the principle and method of the new direct MIMO STR developed in the previous section are applied to the STR design for the nine–machine system described in Chapter 3. The system is initially unstable. It has been found in Chapters 3 and 4 that the machines 3, 7 and 8 are the strategic plants for stabilizer locations. Three STRs will be designed for these machines.

Some details of the STR design are as follows:

1. The speed deviation $\Delta\omega$ and the terminal voltage v_t of a machine to be equipped with STR are chosen respectively as the output variables y_1 and y_2 of Eq. (5.27). The control signal u_1 of the STR is applied to the excitation loop and u_2 to the governor loop of the machine as Fig. 5.1. A reset block is used to eliminate the effects of u_2 on steady state mechanical torque T_m.

2. The weighting matrix $[Q]$ is fixed as a unit matrix $[I]$ while $[R]$ is fixed as $0.001[I]$ after trial and error. A relatively small [R] provides a better damping to the system output responses while a relatively large [R] provides a smoother control.

3. The selection of n_1, n_u and T is discussed in detail in [29]. They are chosen as 3, 3 and 5 respectively in our design.

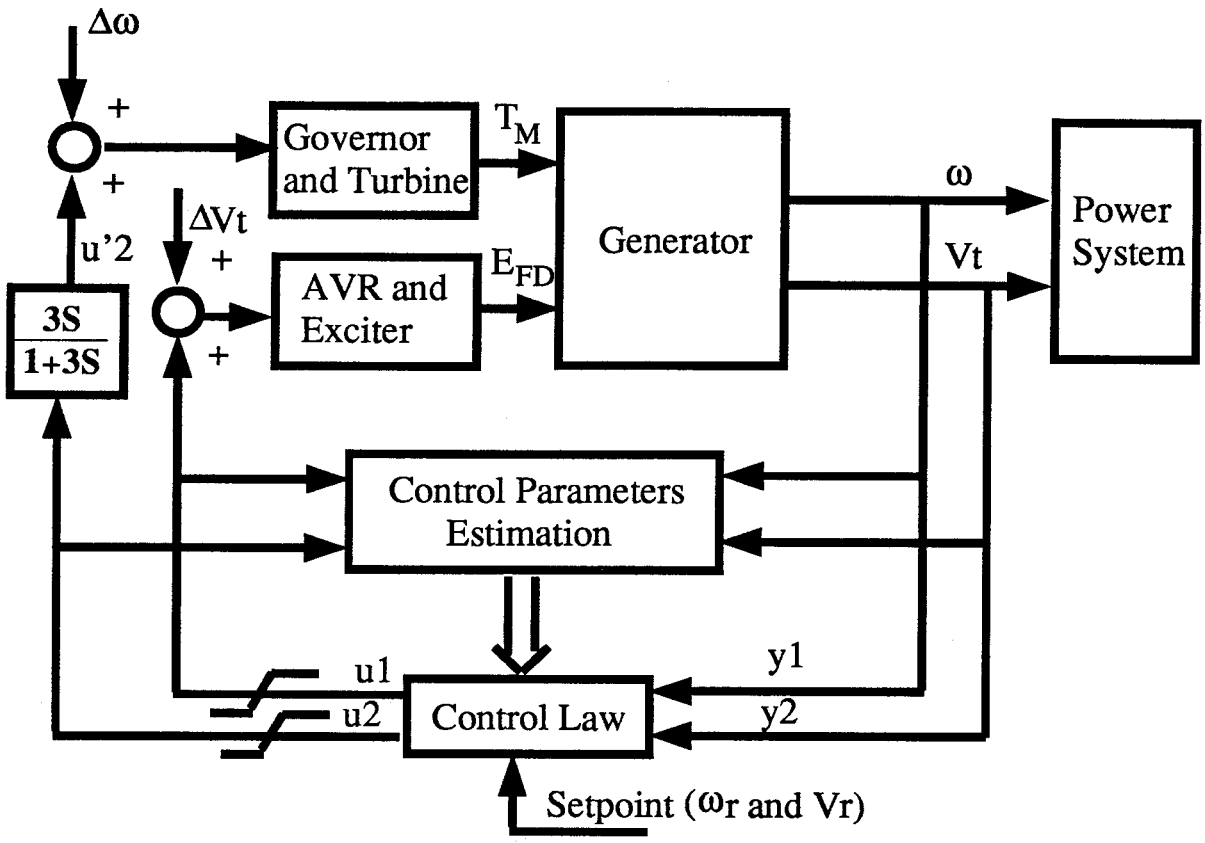

Figure 5.1: Schematic Diagram of the Direct MIMO STR

4. The sampling period is chosen as 60 ms and both na and nb as 5. Further decrease of the sampling period or increase of na does not improve the system dynamic response significantly.

5. A self–adjusting forgetting factor of 0.95 is introduced in the RLS algorithm for the estimate of control parameters. The forgetting factor allows a discount of some old data in the estimation so that the estimator may adapt itself to fast changes of power system operations. The factor is set to 1 when the estimation error $\mid \Delta y_i(t) - X^T(t)\Theta_i(t) \mid$ is less than 0.001.

After the design, the power system with the STRs is given comprehensive simulation tests to determine the merits of STRs. For the simulation tests , nonlinear high order

models are used for each machine, including a 5th order synchronous generator, a 4th order hydro–plant governor and turbine or a 2nd order steam governor and turbine, and a 1st order fast excitation system. A computer simulation program for the multimachine power system is written based on the method in Chapter 2. To simulate the self–tuning control loops according to the algorithm of the new STR, a Fortran program is added to the system simulation program.

Mainly three types of simulation tests are performed: successive step changes in voltage reference, successive step changes in governor gate opening, and three–phase short–circuits at a machine terminal. These tests are repeated for each machine. For comparison, similar tests are repeated for the same nine–machine system but equipped with PSSs designed in Chapter 4. A test of short–circuit and trip–off of the transmission line is also performed. For all tests, the responses such as speed, voltage, electric power, excitation and governor control signal etc. of all machines are recorded and examined. Numerous curves could be plotted but only typical results are shown as Fig. 5.2 through Fig. 5.6.

Fig. 5.2 shows some responses of G3 (machine #3) to the successive step changes in reference voltage of G3 for the system with the designed STRs. To each step change, the STRs adapt very fast to provide damping to the system and the system oscillations subside very quickly. The terminal voltage, the speed deviation, the excitation and the governor control signals are separately plotted.

Fig. 5.3 shows the G3–responses to the successive step changes in governor gate opening of G3 for the system with designed STRs. Again, the STRs are very effective and the system oscillations are damped very quickly.

Fig. 5.4 shows the G3–responses to a three-phase short–circuit for 0.12s near G3 terminal for the system with the designed STRs. The transient stability of the system recovers very fast, which indicates that the designed STRs are very effective. From

Fig. 5.2 to Fig. 5.4 only the responses of G3 are plotted since G3–responses are the most violent ones.

Fig. 5.5 shows the speed deviation responses of several machines to a three-phase short–circuit of a transmission line for 0.12s near Bus 14 and between Bus 14 and Bus 21 for the system with STRs. The short–circuit is removed by tripping off the faulted line, leaving the system operating in a quite different condition. In spite of the two successive severe changes, the transient stability of the system recovers although the settling time is larger than other cases.

Fig. 5.6 compares the responses of G8 for the system with STRs, plotted in solid lines, with those for the system with the PSSs designed in the Chapter 4, plotted in dotted lines, to the same successive step changes in governor opening of G8. It is found that the stability recovers for the system with STRs but not for the system with the PSSs. This is the case which shows that the STRs are superior to the fixed PSSs.

Note that the PSSs presented in Chapter 4, unlike other PSSs, are of a coordinated design ensuring a very stable power system. The capability of the PSSs to stabilize a power system is almost as good as the STRs in most cases. But, when the system operating conditions change to certain new values as in the case of Fig. 5.6, these fixed PSSs cannot stabilize the system properly.

5.4 Conclusions

1. Clarke's principle of indirect SISO STR design [29] is extended to the direct MIMO STR design in this thesis. Two improved design techniques are developed: the direct estimate of the initial step control parameters and the recursive computation of the subsequent control parameters. The computational requirements are reduced. These improvements are general and can be very useful for the STR design of other

industries.

2. The principle and method of the direct MIMO STR are applied to the STRs design of a nine–machine power system. Both excitation and governor loops are controlled and only three machines require the STRs. Tests of successive step changes in voltage reference, successive step changes in governor opening, short–circuits near the machine terminal, and short–circuit and trip–off of the transmission lines all show that the STRs thus designed can effectively stabilize a power system over a wide range of operating conditions.

3. The results in Fig. 5.6 show that when system operating conditions change to some new states, the STRs thus designed still can stabilize the system but the fixed PSSs cannot do so even though they are very well designed. Therefore, further exploration of STR design is necessary to the benefit of power system stability control.

4. The STR design also confirms that only three stabilizers on machines 3, 7 and 8 are sufficient for the stability control of the nine–machine power system.

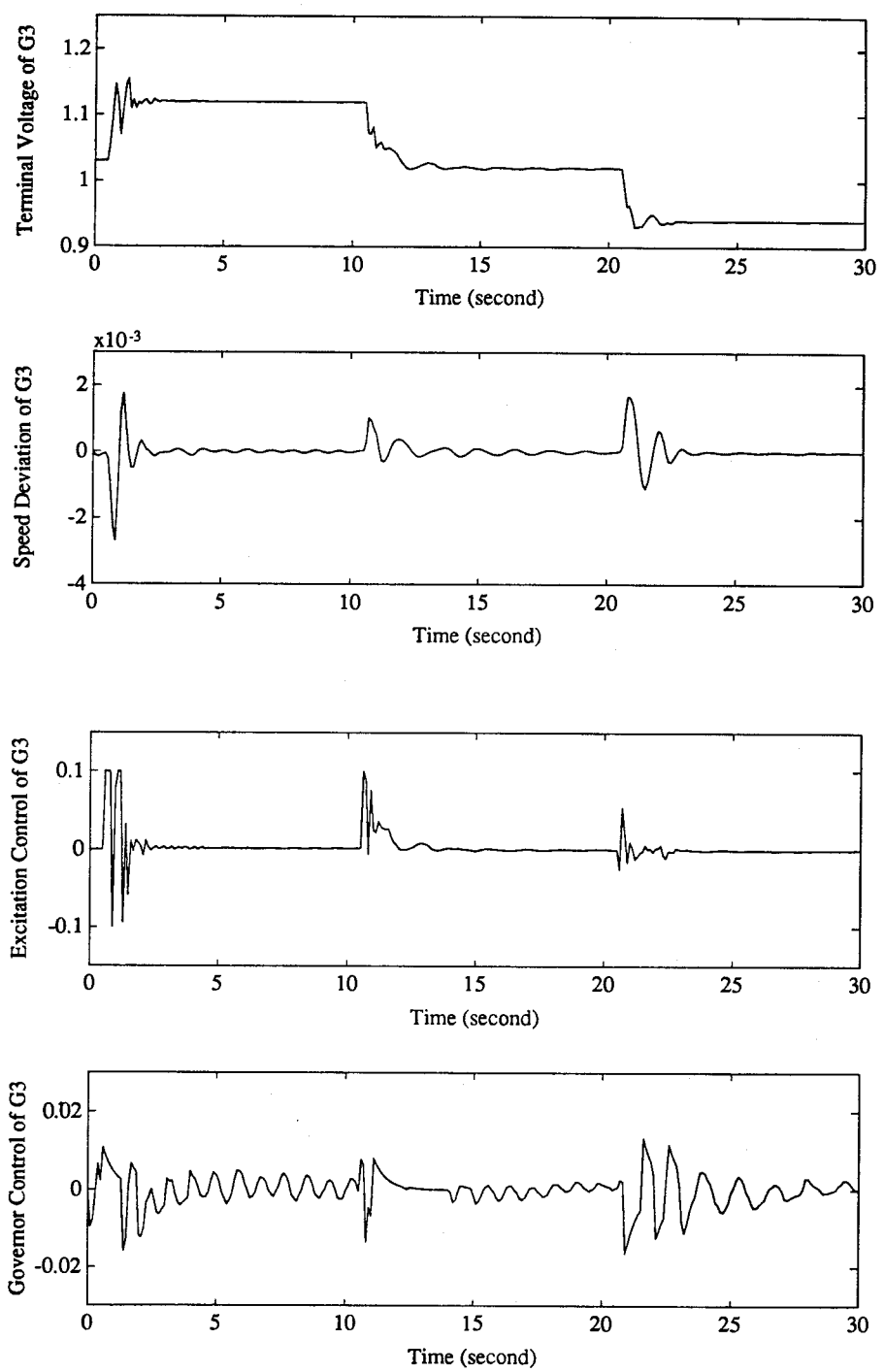

(Sampling period=60 ms)

Figure 5.2: Responses to Step Changes in Reference Voltage of G3

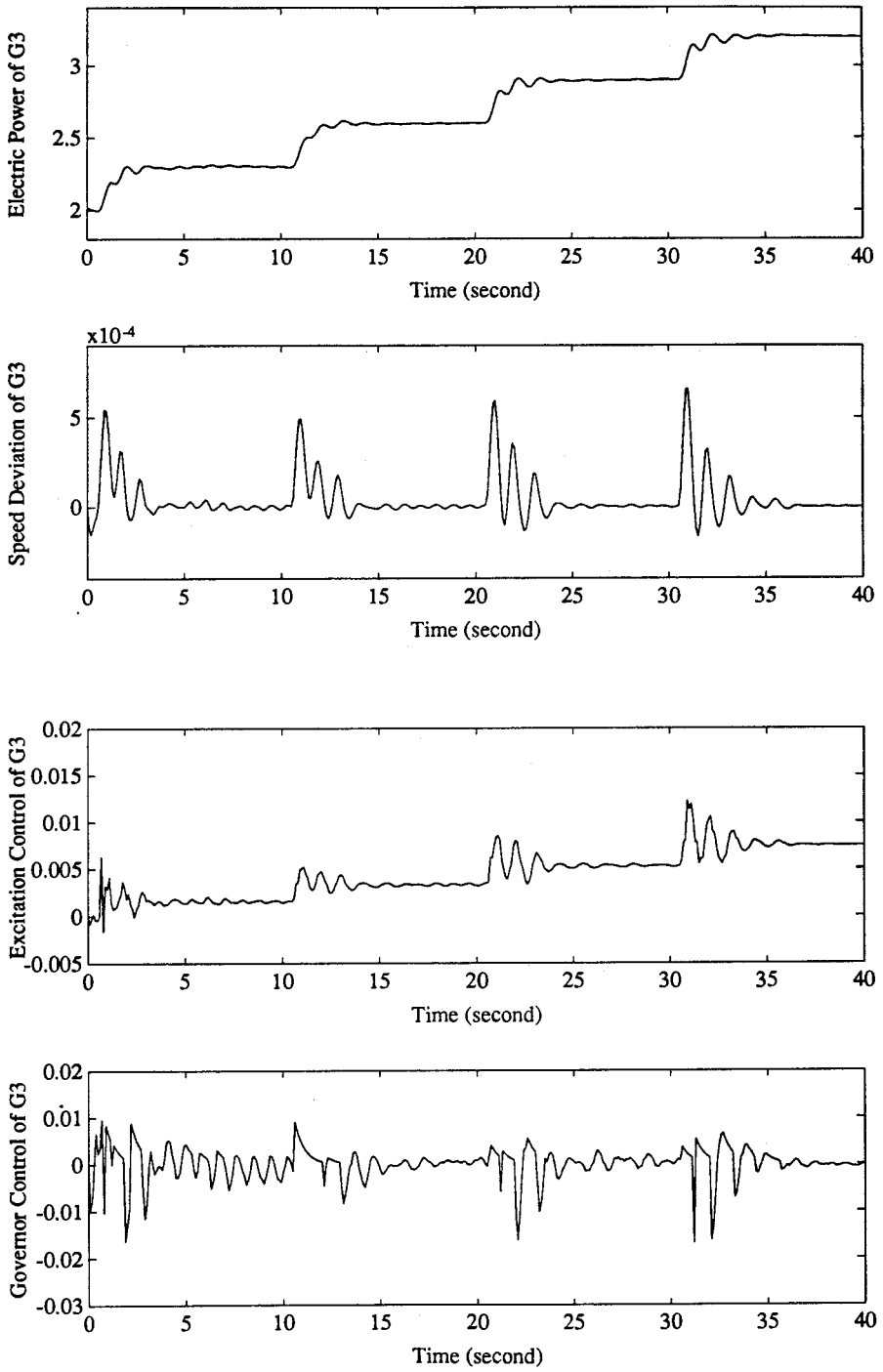

(Sampling period=60 ms)

Figure 5.3: Responses to Step Changes in Gate Opening of G3

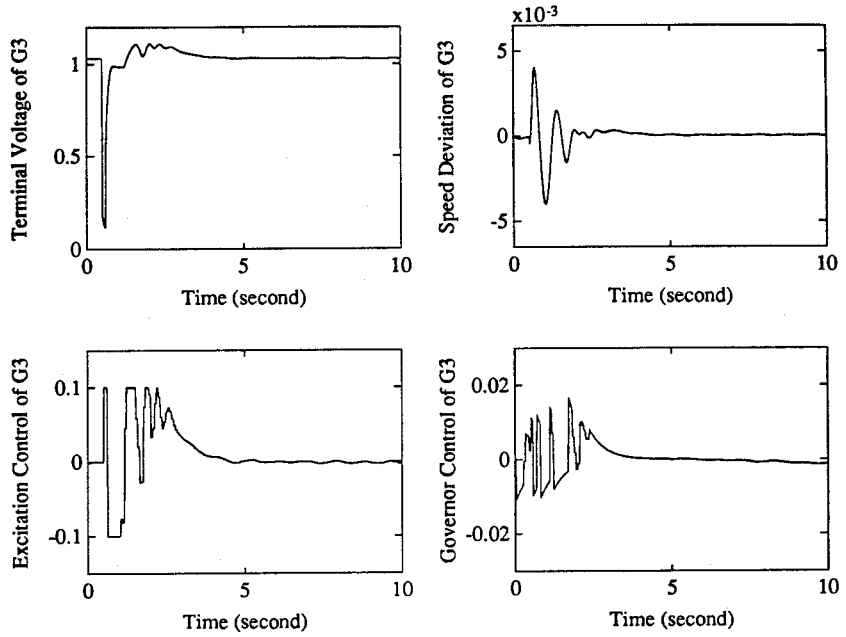

Figure 5.4: Responses to a Short–Circuit near G3 Bus

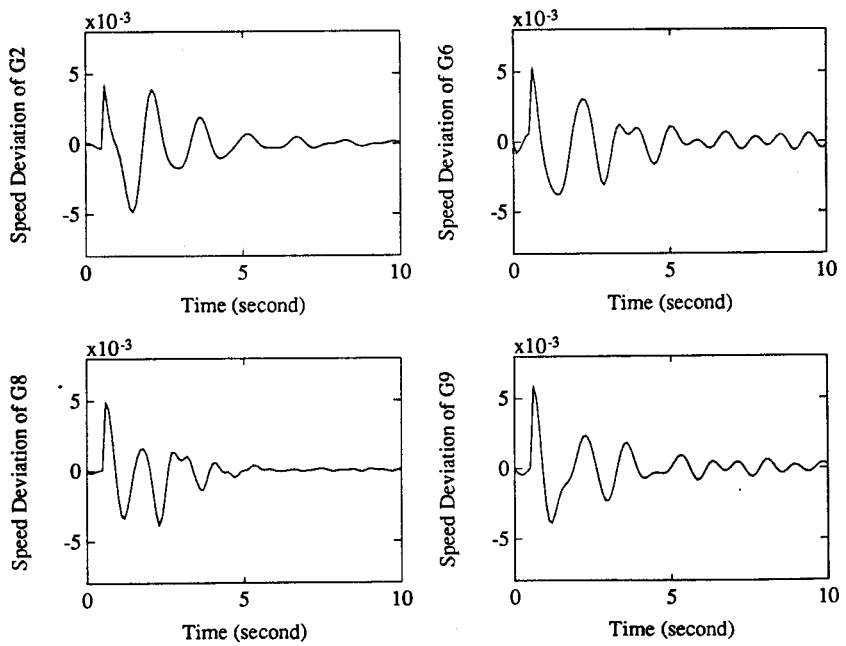

(Sampling period=60 ms)

Figure 5.5: Responses to a Short–Circuit and the Removal of the faulted Line

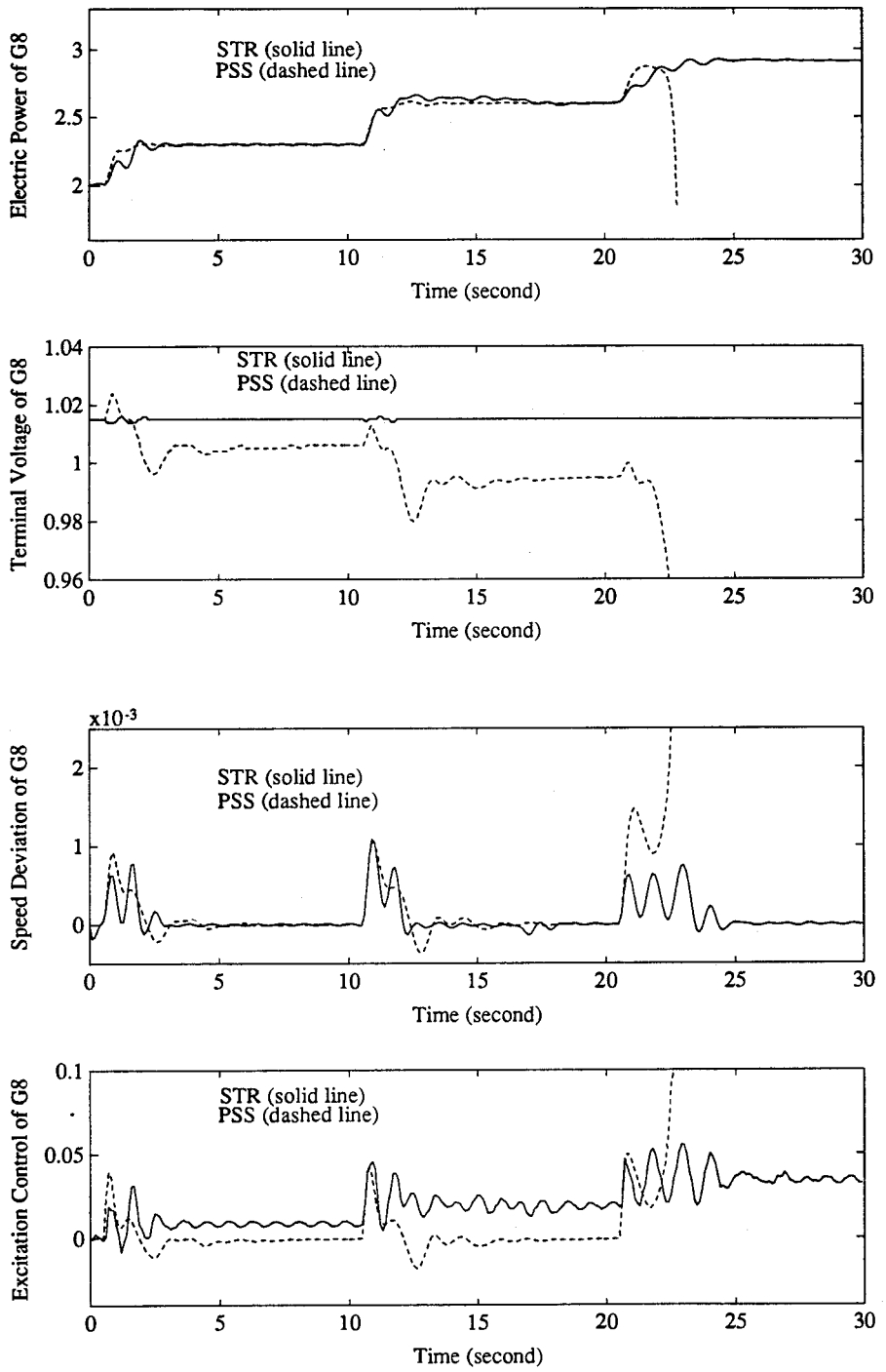

(Sampling period=60 ms)

Figure 5.6: Responses to Step Changes in Gate Opening of G8

Chapter 6

EXCITATION CONTROL OF SHAFT TORSIONAL OSCILLATIONS OF A MULTIMACHINE SYSTEM

6.1 Introduction

Series capacitor compensation is used in transmission lines to increase HVAC transmission capacity of power systems. When electric power is transmitted from a thermal–electric plant over this kind of capacitor–compensated line, series resonance of the line and the generator at subsynchronous frequency may occur. The subsynchronous resonance (SSR) may excite the torsional oscillations of a turbine-generator mechanical system and even cause shaft damage and system interruption. Therefore, stabilizer design to suppress the torsional oscillations of a power system with SSR is an important power system stability control problem.

Since the shaft damage caused by SSR at the Mohave power plant [41], two Benchmark Models have been recommended by IEEE SSR Working Group for SSR studies ([42], [43]). Extensive analysis of SSR has been made, tests and countermeasures for one–machine infinite–bus system, such as the First Benchmark Model (FBM) and the system 1 of the Second Benchmark Model (SBM), have been proposed , and some countermeasures have been implemented ([44]– [46]). PSS control of SSR with filter is also studied [47]. However, a stabilizer for the system 2 of SBM, which has two nonidentical machines with one series–capacitor compensated line, has not yet been developed. This chapter designs a stabilizer through the excitation loop of a generator to damp the multi–mode torsional

oscillations of the system 2 of the SBM.

For SSR analysis and stabilizer design for the system 2 of the SBM, a mathematical model must be developed. This model is different from the conventional model for low–frequency oscillation study which models a turbine–generator system as a single mass spring system and does not recognize the torsional oscillations between various stages of turbines , generator and exciter. For SSR study, however, each of all rotating masses must be modeled by two first–order differential equations because these rotating masses may oscillate with respect to each other when they are excited by SSR. In addition, the damper windings of a synchronous generator are usually ignored in the conventional model for low–frequency oscillation study. But, these damper windings must be included in the model for SSR study because of their effects at high frequencies. Also, the stator armature winding of a generator and the transmission network, which are described by algebraic equations for low–frequency oscillation study, must be remodeled by differential equations for SSR study to find the electric resonance of the capacitor–compensated transmission line and the generator. Since the transmission network and generators are usually described in different coordinate systems, coordinate transformation is necessary for SSR analysis and stabilizer design of the system 2 of the SBM.

Unlike conventional PSS design using only one state variable of a generator as the feedback input of a PSS, more state variables must be used as the feedback to control the multi–mode torsional oscillations of a turbine–generator mechanical system. A linear combination of the local measurable variables is used as feedback in this chapter to design stabilizers for the system 2 of the SBM. To determine which state variables are most effective for the feedback, the participation factor method is used. To determine feedback gains of the decentralized stabilizers, a new direct pole-placement method is developed. With this method, exact pole–placement can be achieved and the feedback gains of stabilizers can be obtained directly without iteration. The results of computer

simulation tests for the systems with and without the designed stabilizers show that the stabilizers thus designed can effectively damp out all torsional oscillations of the system over a wide range of capacitor compensation.

Many results of this chapter are published [50].

6.2 System 2 of the Second Benchmark Model (SBM)

The electrical circuit of system 2 of the SBM is shown in Fig. 6.1 (a) [43]. There are two generator units G1 and G2 connected to a common bus through transformers. The transmission line between the common bus and bus 1 is series–capacitor–compensated. R_t and X_t, respectively, denote the resistance and reactance of a transformer, R_L and X_L the resistance and reactance of a transmission line, and X_C the series capacitance varying from 10% to 90% of X_{L1}.

The mechanical system of unit G1 is presented in Fig. 6.1 (b) [43]. There are four rotating masses of unit G1; the high–pressure turbine (HP), lower–pressure turbine (LP), the generator (GEN) and the exciter (EX), all on one shaft. Each rotating mass and shaft constitutes a torsional mass–spring system. The mechanical system of unit G2 is similar to that of G1 except for no rotating exciter.

6.3 Mathematical Model for the System 2 of SBM

6.3.1 Mechanical System

As previously mentioned, for SSR study, each rotating mass of the mass–spring system of a turbine–generator–exciter set should be modeled by two first–order differential equations. Differential equations for high-pressure turbine, low–pressure turbine, the generator, and the exciter of the first turbine–generator–exciter set in Fig. 6.1 (b) can be

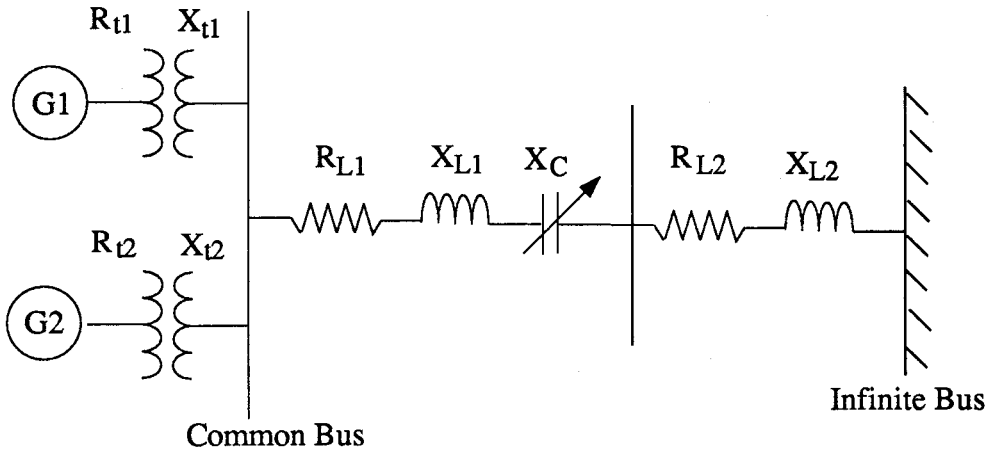

(a) Electrical System

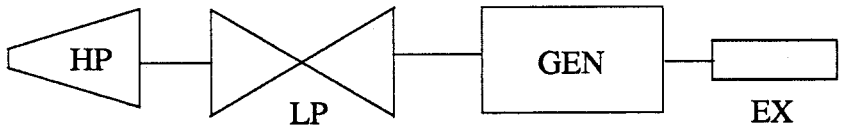

(b) Mechanical System of G1

Figure 6.1: The System 2 of the SBM

written as follows [14]

$$
\begin{aligned}
\dot{\omega}_{H1} &= \frac{1}{M_{H1}}[T_{H1} - D_{H1}\omega_{H1} - K_{HL1}(\theta_{H1} - \theta_{L1})] \\
\dot{\theta}_{H1} &= \omega_b(\omega_{H1} - 1.0) \\
\dot{\omega}_{L1} &= \frac{1}{M_{L1}}[T_{L1} - D_{L1}\omega_{L1} + K_{HL1}(\theta_{H1} - \theta_{L1}) - K_{LG1}(\theta_{L1} - \delta_1)] \\
\dot{\theta}_{L1} &= \omega_b(\omega_{L1} - 1.0) \\
\dot{\omega}_1 &= \frac{1}{M_{G1}}[-T_{e1} - D_{G1}\omega_1 + K_{LG1}(\theta_{L1} - \delta_1) - K_{GX1}(\delta_1 - \theta_{X1})] \\
\dot{\delta}_1 &= \omega_b(\omega_1 - 1.0) \\
\dot{\omega}_{X1} &= \frac{1}{M_{X1}}[-T_{ex1} - D_{X1}\omega_{X1} + K_{GX1}(\delta_1 - \theta_{X1})] \\
\dot{\theta}_{X1} &= \omega_b(\omega_{X1} - 1.0)
\end{aligned}
\tag{6.1}
$$

where the ω's are the rotor speeds in per unit with a base value equal to $\omega_b = 2\pi f$ rad/s, the θ's are the rotor angles, δ is the generator rotor angle, the M's are inertial constants for rotating masses, the K's are the shaft stiffnesses, the D's are dampings, and the T's are the torques applied to masses. Subscripts H, L, G and X, respectively, identify the high– and low–pressure turbines, the generator, and the exciter. Note that turbine torques T_H and T_L are also state variables and their differential equations will be given as Eqs. (6.4) and (6.5) in Section 6.3.2. The generator electric torque output T_e is not a state variable but can be replaced with Eq. (6.14) in Section 6.3.4.

Differential equations for the mass–spring system of the second turbine–generator set are almost the same as those for G1 except that the last two equations and K_{GX} constant of Eqs. (6.1) should be deleted and the subscript 1 should be replaced by 2.

6.3.2 Governor and Turbine

A two-time-constant governor is assumed in Fig. 6.2 (a) where a denotes the speed relay position and g the governor opening [48]. The differential equations for the governor are

$$\dot{a} = \frac{K_G}{1+T_{SR}}(\omega_{ref} - \omega) - \frac{1}{T_{SR}}a \tag{6.2}$$

$$\dot{g} = \frac{1}{T_{SM}}a - \frac{g - g_0}{T_{SM}} \tag{6.3}$$

where g_0 denotes an initial gate opening.

There are two time constants of the steam turbine [48]: T_{CH} for the steam chest and T_{RH} for the reheater and/or the cross-over. The transfer function of the steam turbine is shown in Fig. 6.2 (b). The differential equations for the steam turbine are

$$\dot{T}_H = \frac{F_H}{T_{CH}}g - \frac{1}{T_{CH}}T_H \tag{6.4}$$

$$\dot{T}_L = \frac{F_L}{F_H T_{RH}}T_H - \frac{1}{T_{RH}}T_L \tag{6.5}$$

The fractions F_H and F_L are defined as

$$F_H + F_L = 1 \tag{6.6}$$

6.3.3 Exciter and Voltage Regulator

A two–time–constant excitation system is chosen in Fig. 6.2 (c) where v_R denotes a voltage regulator output and E_{FD} a generator internal voltage [49]. Two differential equations can be written for the excitation system

$$\dot{v}_R = \frac{K_A}{T_A}(v_{ref} - v_t) - \frac{1}{T_A}v_R + \frac{K_A}{T_A}u_E \tag{6.7}$$

$$\dot{E}_{FD} = \frac{1}{T_E}v_R - \frac{1}{T_E}E_{FD} \tag{6.8}$$

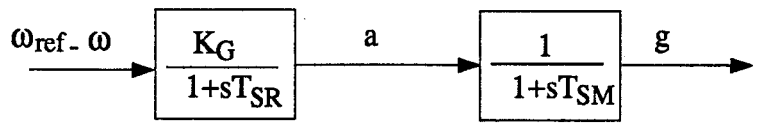

(a) A Two-Time-Constant Governor

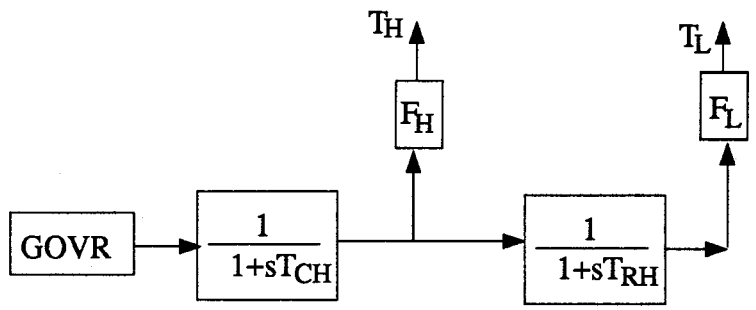

(b) A Two-Time-Constant Steam Turbine

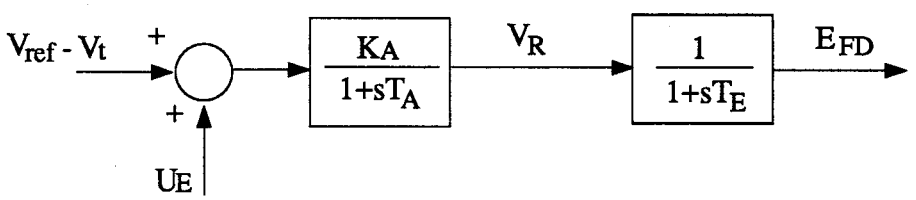

(c) Excitation System

Figure 6.2: Governor, Turbine and Excitation System

where u_E is the supplementary control signal of the stabilizer to be designed and v_{ref} a reference voltage. v_t denotes the generator terminal voltage and can be written as

$$v_t = \sqrt{v_d^2 + v_q^2} \tag{6.9}$$

where v_d and v_q are the d and q components of the v_t and will be described in Section 6.3.4.

6.3.4 Synchronous Generator

For SSR study, it is more convenient to use the generator currents as state variables to model a synchronous generator ([14]). The generator model can be obtained from Park's voltage equations. In Park's equations, the variables of a generator are described by the individual d–q coordinate of the generator. For each generator of system 2 of SBM, besides d and q armature windings on the stator, there are four windings on the rotor: a damper winding D and a field winding F on the d axis and damper windings Q and S on the q axis. Therefore, the Park's equation may be written as follows

$$\begin{aligned}
v_d &= -r_a i_d + \dot{\psi}_d/\omega_b - \omega\psi_q \\
v_q &= -r_a i_q + \dot{\psi}_q/\omega_b + \omega\psi_d \\
v_F &= r_F i_F + \dot{\psi}_F/\omega_b \\
0 &= r_D i_D + \dot{\psi}_D/\omega_b \\
0 &= r_Q i_Q + \dot{\psi}_Q/\omega_b \\
0 &= r_S i_S + \dot{\psi}_S/\omega_b
\end{aligned} \tag{6.10}$$

where v denotes a voltage, i a current, ψ a flux linkage, ω a speed, and r a resistance, all in per unit. Subscripts d, q, F, D, Q, and S identify the respective windings. To use the generator currents as state variables, the flux linkages of Eqs. (6.10) can be substituted

with currents by using the following equations

$$\begin{bmatrix} \psi_d \\ \psi_F \\ \psi_D \end{bmatrix} = \begin{bmatrix} x_d & x_{md} & x_{md} \\ x_{md} & x_F & x_{md} \\ x_{md} & x_{md} & x_D \end{bmatrix} \begin{bmatrix} -i_d \\ i_F \\ i_D \end{bmatrix} \tag{6.11}$$

$$\begin{bmatrix} \psi_q \\ \psi_Q \\ \psi_S \end{bmatrix} = \begin{bmatrix} x_q & x_{mq} & x_{mq} \\ x_{mq} & x_Q & x_{mq} \\ x_{mq} & x_{mq} & x_S \end{bmatrix} \begin{bmatrix} -i_q \\ i_Q \\ i_S \end{bmatrix} \tag{6.12}$$

and Eqs. (6.10) becomes

$$\begin{aligned}
\frac{1}{\omega_b}(-x_d\dot{i}_d + x_{md}\dot{i}_F + x_{md}\dot{i}_D) &= \omega(-x_q i_q + x_{mq} i_Q + x_{mq} i_S) + r_a i_d + v_d \\
\frac{1}{\omega_b}(-x_q\dot{i}_q + x_{mq}\dot{i}_Q + x_{mq}\dot{i}_S) &= -\omega(-x_d i_d + x_{md} i_F + x_{md} i_D) + r_a i_q + v_q \\
\frac{1}{\omega_b}(-x_{md}\dot{i}_d + x_F\dot{i}_F + x_{md}\dot{i}_D) &= -r_F i_F + v_F \\
\frac{1}{\omega_b}(-x_{md}\dot{i}_d + x_{md}\dot{i}_F + x_D\dot{i}_D) &= -r_D i_D \\
\frac{1}{\omega_b}(-x_{mq}\dot{i}_q + x_Q\dot{i}_Q + x_{mq}\dot{i}_S) &= -r_Q i_Q \\
\frac{1}{\omega_b}(-x_{mq}\dot{i}_q + x_{mq}\dot{i}_Q + x_S\dot{i}_S) &= -r_S i_S
\end{aligned} \tag{6.13}$$

where x_d, x_q, x_F, x_D, x_Q, and x_S are the reactances of the respective windings, x_{md} is the mutual reactance of windings on d axis, and x_{mq} is the mutual reactance of windings on q axis. Note that the generator terminal voltage v_d and v_q are not state variables but can be eliminated by using Eq. (6.22) in Section 6.3.5.

The generator electric torque T_e of Eq. (6.1) is not a state variable , but can now be replaced by generator currents:

$$\begin{aligned}
T_e &= i_d\psi_d - i_q\psi_q \\
&= (x_q - x_d)i_d i_q + x_{md} i_f i_q + x_{md} i_q i_D - x_{mq} i_Q i_d - x_{mq} i_S i_d
\end{aligned} \tag{6.14}$$

6.3.5 Transmission Network

In individual machine coordinates d_k–q_k, the terminal voltages of the k-th machine can be expressed in the sum of the voltages across the transformers and the common bus voltages [51]

$$\begin{bmatrix} v_{q1} \\ v_{d1} \end{bmatrix} = \begin{bmatrix} R_{t1} & X_{t1} \\ -X_{t1} & R_{t1} \end{bmatrix} \begin{bmatrix} i_{q1} \\ i_{d1} \end{bmatrix} + \frac{X_{t1}}{\omega_b} \begin{bmatrix} \dot{i}_{q1} \\ \dot{i}_{d1} \end{bmatrix} + \begin{bmatrix} v_{com.q1} \\ v_{com.d1} \end{bmatrix} \tag{6.15}$$

$$\begin{bmatrix} v_{q2} \\ v_{d2} \end{bmatrix} = \begin{bmatrix} R_{t2} & X_{t2} \\ -X_{t2} & R_{t2} \end{bmatrix} \begin{bmatrix} i_{q2} \\ i_{d2} \end{bmatrix} + \frac{X_{t2}}{\omega_b} \begin{bmatrix} \dot{i}_{q2} \\ \dot{i}_{d2} \end{bmatrix} + \begin{bmatrix} v_{com.q2} \\ v_{com.d2} \end{bmatrix} \tag{6.16}$$

where R_t denotes a transformer resistance, X_t its reactance, ω_b the base speed, and $v_{com.d}$ and $v_{com.q}$ respectively the d and q components of the common bus voltage in individual machine coordinates. Now, the two individual coordinates must be interfaced by using a common system coordinate, D–Q coordinate. The position of the infinite bus voltage is chosen as the D axis of the common coordinate which is also the reference axis of the rotor angles of both machines. The relationship between the individual d–q coordinate of the k–machine and the common D–Q coordinate is shown in Fig. 6.3. Therefore, the Eqs. (6.15) and (6.16) can be rewritten as

$$\begin{bmatrix} v_{q1} \\ v_{d1} \end{bmatrix} = \begin{bmatrix} R_{t1} & X_{t1} \\ -X_{t1} & R_{t1} \end{bmatrix} \begin{bmatrix} i_{q1} \\ i_{d1} \end{bmatrix} + \frac{X_{t1}}{\omega_b} \begin{bmatrix} \dot{i}_{q1} \\ \dot{i}_{d1} \end{bmatrix} + [T_1] \begin{bmatrix} v_{com.D} \\ v_{com.Q} \end{bmatrix} \tag{6.17}$$

$$\begin{bmatrix} v_{q2} \\ v_{d2} \end{bmatrix} = \begin{bmatrix} R_{t2} & X_{t2} \\ -X_{t2} & R_{t2} \end{bmatrix} \begin{bmatrix} i_{q2} \\ i_{d2} \end{bmatrix} + \frac{X_{t2}}{\omega_b} \begin{bmatrix} \dot{i}_{q2} \\ \dot{i}_{d2} \end{bmatrix} + [T_2] \begin{bmatrix} v_{com.D} \\ v_{com.Q} \end{bmatrix} \tag{6.18}$$

where

$$[T_1] = \begin{bmatrix} \cos\delta_1 & \sin\delta_1 \\ \sin\delta_1 & -\cos\delta_1 \end{bmatrix} \quad [T_2] = \begin{bmatrix} \cos\delta_2 & \sin\delta_2 \\ \sin\delta_2 & -\cos\delta_2 \end{bmatrix}$$

$v_{com.D}$ and $v_{com.Q}$, respectively, are the D and Q components of the common bus voltage in the D–Q coordinate and δ_1 and δ_2 are the rotor angles of G1 and G2.

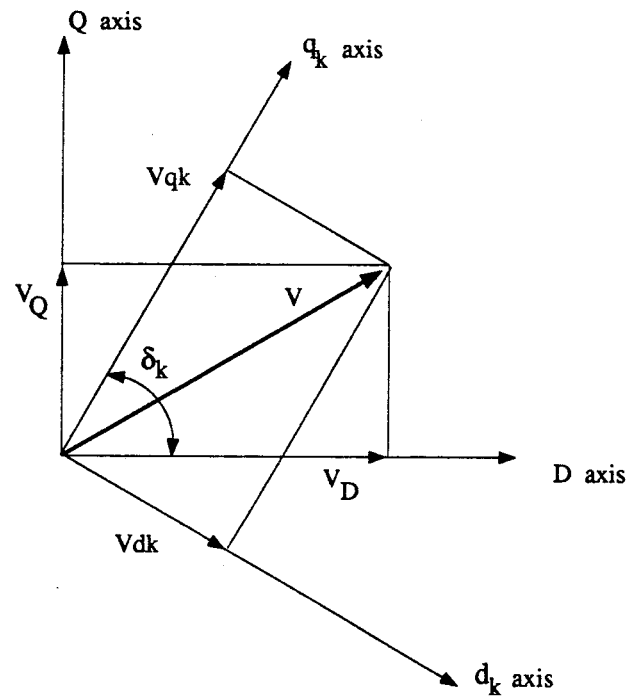

Figure 6.3: Individual Machine and Common System Coordinates

In common D–Q coordinate, the common bus voltages can be expressed in terms of the transmission line, capacitor compensation, and infinite bus voltages as follows:

$$\begin{bmatrix} v_{com.D} \\ v_{com.Q} \end{bmatrix} = \begin{bmatrix} R_L & -X_L \\ X_L & R_L \end{bmatrix} \begin{bmatrix} I_{LD} \\ I_{LQ} \end{bmatrix} + \frac{X_L}{\omega_b} \begin{bmatrix} \dot{I}_{LD} \\ \dot{I}_{LQ} \end{bmatrix} + \begin{bmatrix} E_{CD} \\ E_{CQ} \end{bmatrix} + \begin{bmatrix} v_{OD} \\ v_{OQ} \end{bmatrix} \tag{6.19}$$

where R_L denotes the total line resistance and X_L its total reactance. I_{LD} and I_{LQ}, respectively, are the D and Q components of the line currents; E_{CD} and E_{CQ} the components of the voltage across the capacitor; and v_{OD} and v_{OQ} the components of the infinite bus voltage, all in the common D-Q coordinate.

Next, the D–Q components of the transmission line current may be expressed in terms of the d–q components of individual machine currents as

$$\begin{bmatrix} I_{LD} \\ I_{LQ} \end{bmatrix} = [T_1] \begin{bmatrix} i_{q1} \\ i_{d1} \end{bmatrix} + [T_2] \begin{bmatrix} i_{q2} \\ i_{d2} \end{bmatrix} \tag{6.20}$$

and their derivatives consist of four terms

$$\begin{bmatrix} \dot{I}_{LD} \\ \dot{I}_{LQ} \end{bmatrix} = \frac{d\delta_1}{dt}[T_1'] \begin{bmatrix} i_{q1} \\ i_{d1} \end{bmatrix} + [T_1] \begin{bmatrix} \dot{i}_{q1} \\ \dot{i}_{d1} \end{bmatrix} + \frac{d\delta_2}{dt}[T_2'] \begin{bmatrix} i_{q2} \\ i_{d2} \end{bmatrix} + [T_2] \begin{bmatrix} \dot{i}_{q2} \\ \dot{i}_{d2} \end{bmatrix} \tag{6.21}$$

where

$$[T_1'] = \begin{bmatrix} -\sin\delta_1 & \cos\delta_1 \\ \cos\delta_1 & \sin\delta_1 \end{bmatrix} \quad [T_2'] = \begin{bmatrix} -\sin\delta_2 & \cos\delta_2 \\ \cos\delta_2 & \sin\delta_2 \end{bmatrix}$$

Substituting Equations (6.19), (6.20) and (6.21) into Eq. (6.17), the terminal voltages of G1 in d–q coordinate become

$$\begin{aligned} \begin{bmatrix} v_{q1} \\ v_{d1} \end{bmatrix} &= \begin{bmatrix} R_{t1} + R_L & X_{t1} + X_L\omega_1 \\ -(X_{t1} + X_L\omega_1) & R_{t1} + R_L \end{bmatrix} \begin{bmatrix} i_{q1} \\ i_{d1} \end{bmatrix} + \frac{X_L + X_{t1}}{\omega_b} \begin{bmatrix} \dot{i}_{q1} \\ \dot{i}_{d1} \end{bmatrix} \\ &+ [T_1] \begin{bmatrix} E_{CD} \\ E_{CQ} \end{bmatrix} + [T_1] \begin{bmatrix} v_{OD} \\ v_{OQ} \end{bmatrix} + \frac{X_L}{\omega_b} \begin{bmatrix} C_{12} & -S_{12} \\ S_{12} & C_{12} \end{bmatrix} \begin{bmatrix} \dot{i}_{q2} \\ \dot{i}_{d2} \end{bmatrix} \\ &+ \begin{bmatrix} C_{12}R_L + S_{12}X_L\omega_2 & -S_{12}R_L + C_{12}X_L\omega_2 \\ S_{12}R_L - C_{12}X_L\omega_2 & C_{12}R_L + S_{12}X_L\omega_2 \end{bmatrix} \end{aligned} \tag{6.22}$$

where

$$S_{12} = \sin(\delta_1 - \delta_2) \quad C_{12} = \cos(\delta_1 - \delta_2)$$

$$S_{21} = \sin(\delta_2 - \delta_1) \quad C_{12} = \cos(\delta_2 - \delta_1)$$

Similar equations can be written for the terminal voltage of G2 by simply interchanging the subscripts 1 and 2 of Eq. (6.22).

Finally, the differential equations for the voltages across the capacitor compensation can be written from the current relation

$$\begin{bmatrix} \dot{E}_{CD} \\ \dot{E}_{CQ} \end{bmatrix} = \omega_b \begin{bmatrix} 0 & 1 \\ -1 & 0 \end{bmatrix} \begin{bmatrix} E_{CD} \\ E_{CQ} \end{bmatrix} + \omega_b X_C \begin{bmatrix} I_{LD} \\ I_{LQ} \end{bmatrix} \tag{6.23}$$

where transmission line currents I_{LD} and I_{LQ} are not state variables, but may be replaced by Eq. (6.20).

6.3.6 Summary of Mathematical Model

The complete system model for the SSR study includes 40 nonlinear differential equations as derived in the previous sections. All 40 state variables may be summarized as

$$\begin{aligned}[X]^T = [&\omega_{H1}\ \theta_{H1}\ \omega_{L1}\ \theta_{L1}\ \omega_1\ \delta_1\ \omega_{x1}\ \theta_{x1}\ a_1\ g_1 \\ &T_{H1}\ T_{L1}\ \omega_{H2}\ \theta_{H2}\ \omega_{L2}\ \theta_{L2}\ \omega_2\ \delta_2\ a_2\ g_2 \\ &T_{H2}\ T_{L2}\ i_{d1}\ i_{q1}\ i_{F1}\ i_{D1}\ i_{Q1}\ i_{S1}\ i_{d2}\ i_{q2} \\ &i_{F2}\ i_{D2}\ i_{Q2}\ i_{S2}\ E_{CD}\ E_{CQ}\ E_{FD1}\ E_{FD2}\ v_{R1}\ v_{R2}]\end{aligned}$$

The nonlinear differential equations of the state variables are used for simulation tests. For the control design in the following sections, these nonlinear equations must be linearized with respect to a set of initial values of the state variables. The linearized system state equations will be given as Eq. (6.24) in the next section but the details of the linearized equations are not included. All data of these differential equations are available in the references ([43],[51]).

6.4 A Direct Pole–Placement Method for Control Design

Iterative pole–placement method has been applied to excitation control design for the First Benchmark Model which has only one machine [52]. For the control design of the system 2 of the SBM, which has two machines, a new direct pole–placement method is developed in this thesis. This method does not require any iterations and the resultant stabilizers use only local state variables as feedback signals for decentralized control.

The linearized state equation of a multimachine power system with excitation control u(t) may be written

$$\dot{x} = Ax + Bu \tag{6.24}$$

where x is the $n \times 1$ state vector and u is the $k \times 1$ control vector. A and B, respectively, are the $n \times n$ system matrix and the $n \times k$ control matrix. Assume that there are m unstable eigenvalues to be replaced and that state variables used as control feedback signals have been chosen. Assume further that columns and rows of the system matrix corresponding to the feedback state variables have been moved to the front position. We have

$$\begin{bmatrix} \dot{X}_I \\ \dot{X}_{II} \\ \dot{X}_{III} \end{bmatrix} = [A] \begin{bmatrix} X_I \\ X_{II} \\ X_{III} \end{bmatrix} + [B] \begin{bmatrix} u_1 \\ u_2 \end{bmatrix} \tag{6.25}$$

where X_I contains m local feedback state variables chosen for u_1, the excitation control of the first generator set, and X_{II} contains m state variables for u_2, the control of the second generator set, i.e.,

$$\begin{bmatrix} u_1 \\ u_2 \end{bmatrix} = \begin{bmatrix} K_I & 0 \\ 0 & K_{II} \end{bmatrix} \begin{bmatrix} X_I \\ X_{II} \end{bmatrix} \tag{6.26}$$

where K_I is a $1 \times m$ gain matrix of u_1 and K_{II} that of u_2. Thus, Eq. (6.25) may be rewritten as

$$\begin{bmatrix} \dot{X}_I \\ \dot{X}_{II} \\ \dot{X}_{III} \end{bmatrix} = \left[A + B \begin{bmatrix} K_I & 0 & 0 \\ 0 & K_{II} & 0 \end{bmatrix} \right] \begin{bmatrix} X_I \\ X_{II} \\ X_{III} \end{bmatrix} \tag{6.27}$$

Next, let the unstable mode eigenvalues be shifted to desired values $\lambda_i, i = 1, 2, \ldots, m$, and let the corresponding eigenvectors be $P_i, i = 1, 2, \ldots, m$. For the i-th new eigenvalues,

we shall have

$$\left[A + B\begin{bmatrix} K_I & 0 & 0 \\ 0 & K_{II} & 0 \end{bmatrix}\right][P_i] = [P_i]\lambda_i \tag{6.28}$$

or

$$[P_i] = -[A - \lambda_i I]^{-1}[B]\begin{bmatrix} K_I & 0 & 0 \\ 0 & K_{II} & 0 \end{bmatrix}[P_i] \tag{6.29}$$

Let

$$-\begin{bmatrix} K_I & 0 & 0 \\ 0 & K_{II} & 0 \end{bmatrix}[P_i] = \begin{bmatrix} \alpha_i \\ \beta_i \end{bmatrix} \tag{6.30}$$

where α_i and β_i are constants. Since the value of an eigenvector is not unique, α_i (or β_i) can be chosen by trial and error, but not zero, and both of them are related to P_i.

Substituting Eq. (6.30) into Eq. (6.29), we have

$$[P_i] = [A - \lambda_i I]^{-1}[B]\begin{bmatrix} \alpha_i \\ \beta_i \end{bmatrix} \tag{6.31}$$

where $[P_i]$ is an $n \times 1$ vector. For prescribed eigenvalues λ_i, $i = 1, 2, \ldots, m$, the corresponding eigenvectors P_i can be solved one by one from Eq. (6.31) and all eigenvectors thus obtained can be written in a matrix form as

$$[P] = [P_1 \;\; P_2 \;\; \ldots \;\; P_i \;\; \ldots \;\; P_m] \tag{6.32}$$

where $[P]$ is an $n \times m$ matrix.

By using Eq. (6.30) and Eq. (6.32), we have

$$-\begin{bmatrix} K_I & 0 & 0 \\ 0 & K_{II} & 0 \end{bmatrix}[P] = \begin{bmatrix} \alpha_1 & \alpha_2 & \ldots & \alpha_m \\ \beta_1 & \beta_2 & \ldots & \beta_m \end{bmatrix} \tag{6.33}$$

Let $[P]$ be partitioned as

$$[P] = \begin{bmatrix} P_I \\ P_{II} \\ P_{III} \end{bmatrix} \tag{6.34}$$

where both P_I and P_{II} are $m \times m$ matrices. Then, Eq. (6.33) becomes

$$-\begin{bmatrix} K_I & 0 & 0 \\ 0 & K_{II} & 0 \end{bmatrix} \begin{bmatrix} P_I \\ P_{II} \\ P_{III} \end{bmatrix} = \begin{bmatrix} \alpha_1 & \alpha_2 & \dots & \alpha_m \\ \beta_1 & \beta_2 & \dots & \beta_m \end{bmatrix} \tag{6.35}$$

Therefore, the control gains $[K_I]$ and $[K_{II}]$ can be solved from

$$[K_I] = -[\alpha_1 \ \alpha_2 \ \dots \ \alpha_m][P_I]^{-1} \tag{6.36}$$

$$[K_{II}] = -[\beta_1 \ \beta_2 \ \dots \ \beta_m][P_{II}]^{-1} \tag{6.37}$$

No iterations are required.

The algorithm of the pole–placement method may be summarized as follows:

1. Specify a set of desired new mechanical mode eigenvalues λ_i for closed–loop system and select nonzero elements α_i and β_i, $i = 1, \dots, m$.

2. Let X_I include m feedback state variables chosen for u_1 and X_{II} m variables for u_2.

3. Rearrange the columns and rows of system matrix, if necessary, to form the equation Eq. (6.25).

4. Calculate P_i from Eq. (6.31), for $i = 1, \dots, m$.

5. Form [P] according to Eq. (6.32).

6. Pick out P_I and P_{II} from Eq. (6.34).

7. Obtain K_I and K_{II} from Eq. (6.36) and Eq. (6.37), respectively.

Table 6.1: Torsional Modes

Mode	Frequency of G1	Frequency of G2
1	24.65 Hz	24.65 Hz
2	32.39 Hz	44.9 Hz
3	51.10 Hz	–

6.5 Eigenvalues Analysis of the System without Control

To apply the pole–placement controller design method to the system 2 of the SBM, the eigenvalues of the linearized system model are analyzed in this section to find the unstable mode eigenvalues. Since the unstable eigenvalues are usually associated with the torsional oscillation frequencies of mechanical systems, the torsional modes of mechanical systems are discussed first.

6.5.1 Natural Torsional Oscillating Modes

The natural torsional modes of the turbine–generator–exciter mass-spring system may be found by the eigenvalues of Eqs (6.1) without damping D's and forcing torque T's. There are usually $m - 1$ torsional modes for a m–mass-spring system. These modes are numbered sequentially according to the values of their frequencies. Mode 1 has the lowest torsional oscillating frequency and mode $m - 1$ has the highest one. For the system 2 of the SBM, the torsional modes of mechanical systems of two machines (G1 and G2) were given in [43], and they are also confirmed by our own calculation. These results are listed in Table 6.1. There are three torsional modes for the mechanical system of G1 and two modes for that of G2.

6.5.2 Unstable Mode Eigenvalues

The two generators of system 2 of SBM are assumed operating on full load at a power factor of 0.9. A 40th–order system model derived in previous sections and linearized around the operating conditions is used for eigenvalue analyses. For each given capacitor compensation ratio X_C/X_{L1}, the system model has a set of forty eigenvalues. The capacitor compensation ratio is assumed to vary from 0.05 to 0.9 in 0.05 increments. The eigenvalues of the system for all these compensations are calculated and examined. It is found that a low–frequency mode (M0), the mode 1 of G1 (M11), and the mode 1 of G2 (M12) are unstable, or nearly unstable. The real–part eigenvalue loci of these unstable modes are plotted in Fig. 6.4. The worst situation occurs around a compensation ratio of 0.70. For this compensation ratio, the unstable eigenvalues and their undamped natural frequencies are

Eigenvalues	Natural Frequencies f_n (Hz)	Torsional Modes
$0.9847 \pm j\,155.77$	24.79	M11
$0.0243 \pm j\,155.77$	24.79	M12
$0.3232 \pm j\,6.9752$	1.11	M0

Therefore, the system state equation based on the compensation ratio of 0.7 is singled out for the excitation control design.

6.6 Stabilizer Design for the System 2 of SBM

The objective of the stabilizer design is to place these unstable mode eigenvalues to the desired location using local measurable state variables. First, participation factors of these eigenvalues will be calculated to decide the most effective state variables as feedback input of stabilizers. Then, the state variables will be transformed to some measurable variable for the controller design. Finally, since the gain matrix in the design

is not unique, a gain matrix suitable for the system stability over wide–range capacitor compensation will be sought.

6.6.1 State Variables for Control Feedback

To move the six unstable eigenvalues to prespecified locations by the pole–placement design method, it is necessary to choose six state variables for $[X_I]$ and another six for $[X_{II}]$. Participation factor analysis method is used to determine which of the forty state variables are most sensitive to these unstable modes and should be chosen as the excitation control feedback. It is found that the following state variables are most influential and may be used for feedback design

$$[X_I]^T = [\Delta i_{d1} \;\; \Delta i_{q1} \;\; \Delta\delta_1 \;\; \Delta\omega_1 \;\; \Delta\omega_{L1} \;\; \Delta i_{F1}]$$
$$[X_{II}]^T = [\Delta i_{d2} \;\; \Delta i_{q2} \;\; \Delta\delta_2 \;\; \Delta\omega_2 \;\; \Delta\omega_{L2} \;\; \Delta i_{F2}]$$

The state variables i_d and i_q, the d and q components of the armature current, however, are not directly measurable. They must be replaced by measurable variables. In this design, the electric power output P_e and the generator armature current i_t are chosen. Hence, the desired feedback variables are

$$[Y_I]^T = [\Delta P_{e1} \;\; \Delta i_{t1} \;\; \Delta\delta_1 \;\; \Delta\omega_1 \;\; \Delta\omega_{L1} \;\; \Delta i_{F1}]$$
$$[Y_{II}]^T = [\Delta P_{e2} \;\; \Delta i_{t2} \;\; \Delta\delta_2 \;\; \Delta\omega_2 \;\; \Delta\omega_{L2} \;\; \Delta i_{F2}]$$

They require the following linear transformation

$$\begin{bmatrix} Y_I \\ Y_{II} \end{bmatrix} = [T] \begin{bmatrix} X_I \\ X_{II} \end{bmatrix} \tag{6.38}$$

where T is a 12×12 transformation matrix. Twelve linear algebraic equations are required to form the T matrix. In addition to eight identity equations for the $\Delta\delta$'s, the $\Delta\omega$'s, the

$\Delta\omega_L$'s, and the Δi_F's, the remaining four equations are

$$\begin{aligned} P_{e1} &= i_{d1}v_{d1} + i_{q1}v_{q1} \\ P_{e2} &= i_{d2}v_{d2} + i_{q2}v_{q2} \\ i_{t1} &= \sqrt{i_{d1}^2 + i_{q1}^2} \\ i_{t2} &= \sqrt{i_{d2}^2 + i_{q2}^2} \end{aligned} \tag{6.39}$$

To eliminate v_{d1} and v_{q1} of Eqs. (6.39), Eq. (6.22) may be modified as follows. At the point of system operation, the derivatives of the currents of Eq (6.22), which constructs a very small portion of the voltage across the transformers and the transmission line, can be neglected. The $[T_1][E_{CD} \;\; E_{CQ}]^T$ representing the voltage across X_C of the capacitor compensation will vanish if the total line reactance X_L of Eq (6.22) is replaced by $X = X_L - X_C$. Therefore, Eq (6.22) becomes

$$\begin{aligned} \begin{bmatrix} v_{q1} \\ v_{d1} \end{bmatrix} &= \begin{bmatrix} R_{t1} + R_L & X_{t1} + X\omega_1 \\ -(X_{t1} + X\omega_1) & R_{t1} + R_L \end{bmatrix} \begin{bmatrix} i_{q1} \\ i_{d1} \end{bmatrix} + [T_1] \begin{bmatrix} v_{OD} \\ v_{OQ} \end{bmatrix} \\ &+ \begin{bmatrix} C_{12}R_L + S_{12}X\omega_2 & -S_{12}R_L + C_{12}X\omega_2 \\ S_{12}R_L - C_{12}X\omega_2 & C_{12}R_L + S_{12}X\omega_2 \end{bmatrix} \end{aligned} \tag{6.40}$$

Note that besides i_{d1}, i_{q1}, there are state variables δ and ω of both machines on the RHS of Eqs. (6.40). Now, v_{d1} and v_{q1} of Eqs. (6.39) can be replaced with Eq (6.40). Similar relations can be found for v_{d2} and v_{q2}. Finally, from the results of the linearization of Eqs. (6.39), the transformation matrix $[T]$ may be completed.

Using Eq. (6.38), Eq. (6.25) can be transformed into

$$\begin{bmatrix} \dot{Y}_I \\ \dot{Y}_{II} \\ \dot{X}_{III} \end{bmatrix} = \left[\bar{A}\right] \begin{bmatrix} Y_I \\ Y_{II} \\ X_{III} \end{bmatrix} + \left[\bar{B}\right] \begin{bmatrix} u_1 \\ u_2 \end{bmatrix} \tag{6.41}$$

where

$$\left[\bar{A}\right] = \begin{bmatrix} T & 0 \\ 0 & I \end{bmatrix} [A] \begin{bmatrix} T^{-1} & 0 \\ 0 & I \end{bmatrix} \qquad \left[\bar{B}\right] = \begin{bmatrix} T & 0 \\ 0 & I \end{bmatrix} [B]$$

Now the control vector is chosen as

$$\begin{bmatrix} u_1 \\ u_2 \end{bmatrix} = \begin{bmatrix} K_I & 0 \\ 0 & K_{II} \end{bmatrix} \begin{bmatrix} Y_I \\ Y_{II} \end{bmatrix} \tag{6.42}$$

Note that this is a linear similarity transformation and thus the eigenvalues of the system matrix $\bar{A}$ are the same as those of the original system matrix A. The control design method of Section 6.4 still can be applied to the transformed system by simply replacing A and B matrices by $\bar{A}$ and $\bar{B}$, respectively.

6.6.2 Prespecified Eigenvalues

As already mentioned in Section 6.5.2, there are six unstable eigenvalues among the forty eigenvalues for the system without control. The six eigenvalues consist of three complex conjugate pairs. It is intended to change their damping ratio but not their natural frequencies so that unnecessary control efforts can be avoided. The prespecified eigenvalues are

Specified Eigenvalues	Old Unstable Eigenvalues
$-3.4270 \pm j155.73$	$0.9847 \pm j155.77$
$-3.1155 \pm j155.74$	$0.0243 \pm j155.77$
$-0.8728 \pm j6.9279$	$0.3232 \pm j6.9752$

6.6.3 Feedback Gain Matrices

Since the feedback gain matrices are not unique, it depends on the choice of the α and β constants. The non–zero elements α_i and β_i, $i = 1, 2, \ldots, m$, are all assumed to be

1.00 to begin with. The control gains are directly determined and exact pole–placement for those prespecified eigenvalues is obtained without the need of iteration. However, for stable operation over wide–range capacitor compensation ratio from 0.05 to 0.9, the α and β values of 1.00 chosen for the 0.7 capacitor compensation design should be adjusted. The final values are

$$\begin{bmatrix} \alpha \\ \beta \end{bmatrix} = \begin{bmatrix} 1.00 & 1.00 & 1.00 & 1.00 & 1.00 & 1.00 \\ 1.04 & 1.04 & 0.94 & 0.94 & 1.00 & 1.00 \end{bmatrix}$$

and the control gains become

$$[K_I] = [1.803 \;\; 0.198 \;\; 0.573 \;\; -98.0 \;\; 125.9 \;\; -2.516]$$

$$[K_{II}] = [2.109 \;\; -7.933 \;\; 8.242 \;\; -8.80 \;\; 105.8 \;\; -1.503]$$

The eigenvalues of the six unstable mode have been moved to exact new locations

$$-3.4270 \pm j\,155.73 \quad (f_n = 24.79\ Hz)$$

$$-3.1155 \pm j\,155.74 \quad (f_n = 24.79\ Hz)$$

$$-0.8728 \pm j\,6.9279 \quad (f_n = 1.11\ Hz)$$

Although the control design is for a particular capacitor compensation ratio of 0.7, eigenvalues of the system with the control gains are recalculated for compensation ratio from 0.05 to 0.90 in 0.05 steps. All eigenmodes are stable. Finally, the real–part eigenvalue loci of the low frequency mode (M0), the mode 1 of G1 (M11), and the mode 1 of G2 (M12) for the system with stabilizer, are plotted in Fig. 6.5. Although the worst dampings of M11 and M12 for the system without stabilizers occur at compensation between 0.6 and 0.8 as shown in Fig. 6.4, the best dampings of both M11 and M12 for the system with stabilizer occur at 0.7 as shown in Fig. 6.5, and this is exactly what the system is designed for.

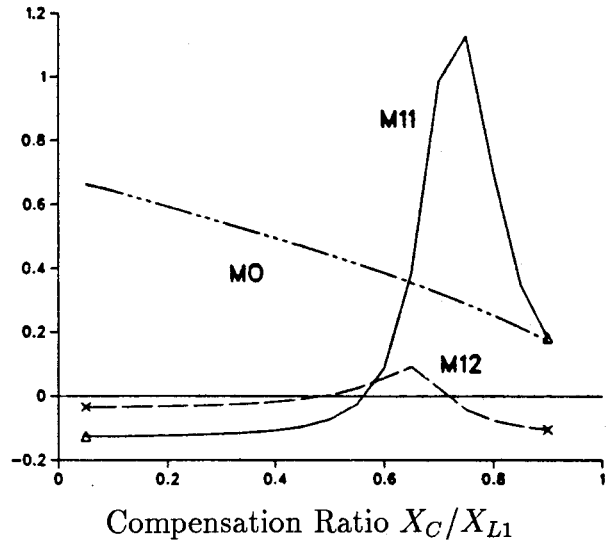

Figure 6.4: Real–Part Eigenvalue Loci of the Torsional Modes of System without Control

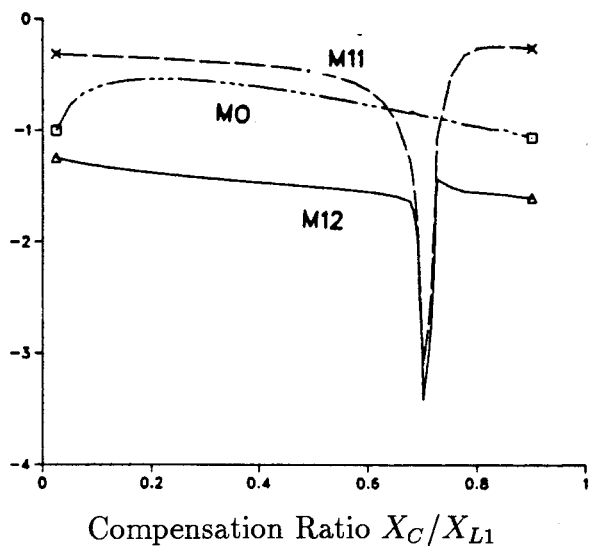

Figure 6.5: Real–Part Eigenvalue Loci of the Torsional Modes of System with Control

6.6.4 Nonlinear Simulation Test

Nonlinear simulations are performed to test the excitation control design in this Chapter. The forty nonlinear differential equations including the governor opening and voltage regulator constraints are used for the computer simulations. Two types of disturbances are simulated: a 10% step torque applied to generator 1 or 2, and a 20% pulsed torque applied to generator 1 or 2 for 0.2 second. All results indicate that the system is stable for the system with control but unstable for the system without control. Since the control is designed for a given state of operation, the system responses to the step torque disturbance are more severe than those to the pulsed torque disturbance. Since the simulation results of the step torque applied to generator 1 or 2 are similar, only the results of the step torque applied to generator 1 are presented in this section. Fig. 6.6 shows the responses to this step torque for the system without control and Fig. 6.7 shows those for the system with control. Multimode oscillations appear in all cases, but the decay is reasonably fast for the system with control. There are high and low frequency components in control signal u_E. While the low frequency component in u_E provides damping to the low frequency oscillations of mode 0, like conventional PSS, and the high frequency components produce effective damping to the high frequency torsional oscillations of mode 1 of both generators.

6.7 Conclusions

1. A mathematical model has been derived for system 2 of the SBM for the SSR studies.

2. A new direct pole–placement method is developed for the stabilizer design of multimachine SSR systems. Only local output signals of individual machines are used as the feedback input.

3. The method has been successfully applied to a stabilizer design for excitation control of torsional oscillations of system 2 of the SBM. Effective feedback signals can be found from participation factor analysis and all unstable mode eigenvalues of the system can be shifted directly to exact new positions without iteration.

4. The stabilizers thus designed can effectively damp out multi–mode torsional oscillations of the system over a wide range of capacitor compensations although the stabilizers are designed for a particular degree of compensation.

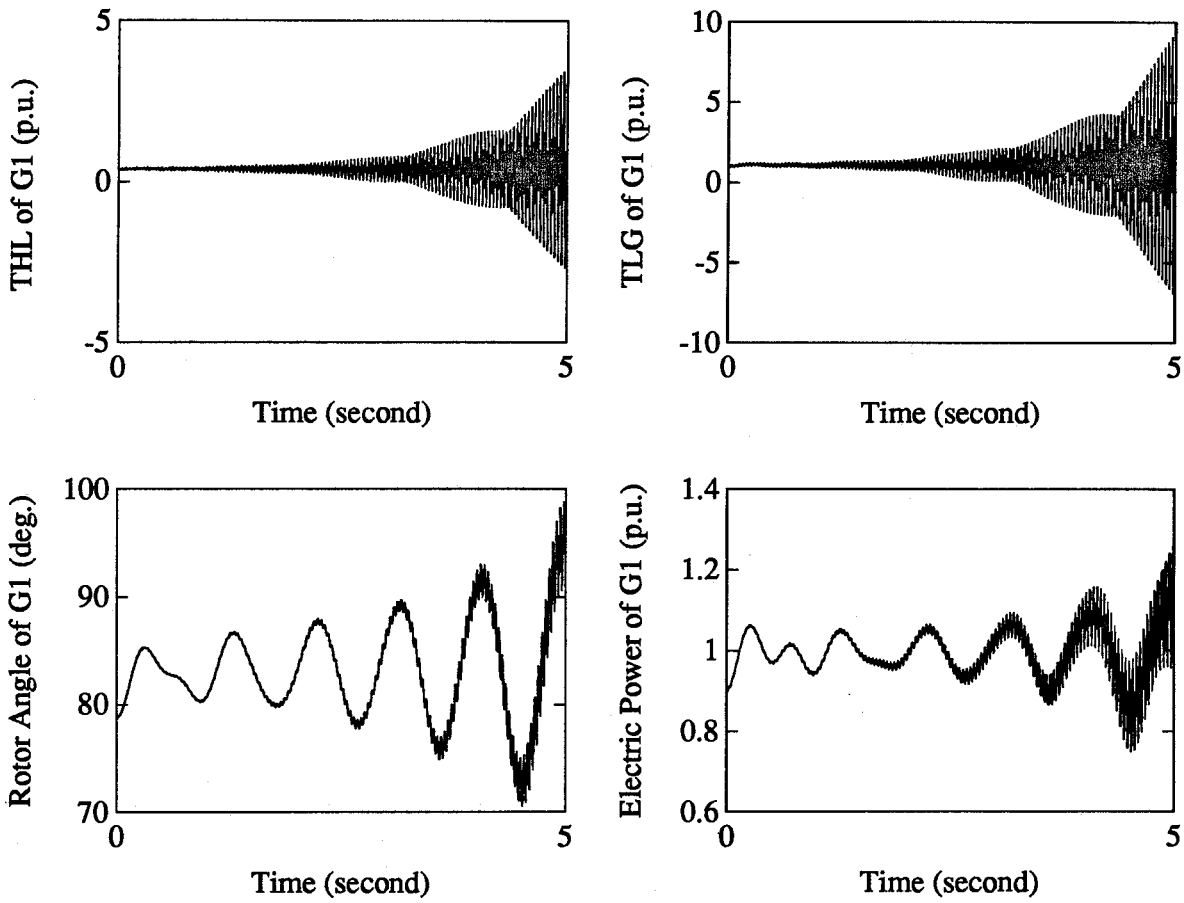

THL: Shaft torque between high and low pressure turbines
TLG: Shaft torque between low pressure turbine and generator

(a) Responses of Generator 1 (G1)

Figure 6.6: Responses to a Step Torque to G1 for the System without Control. (a)

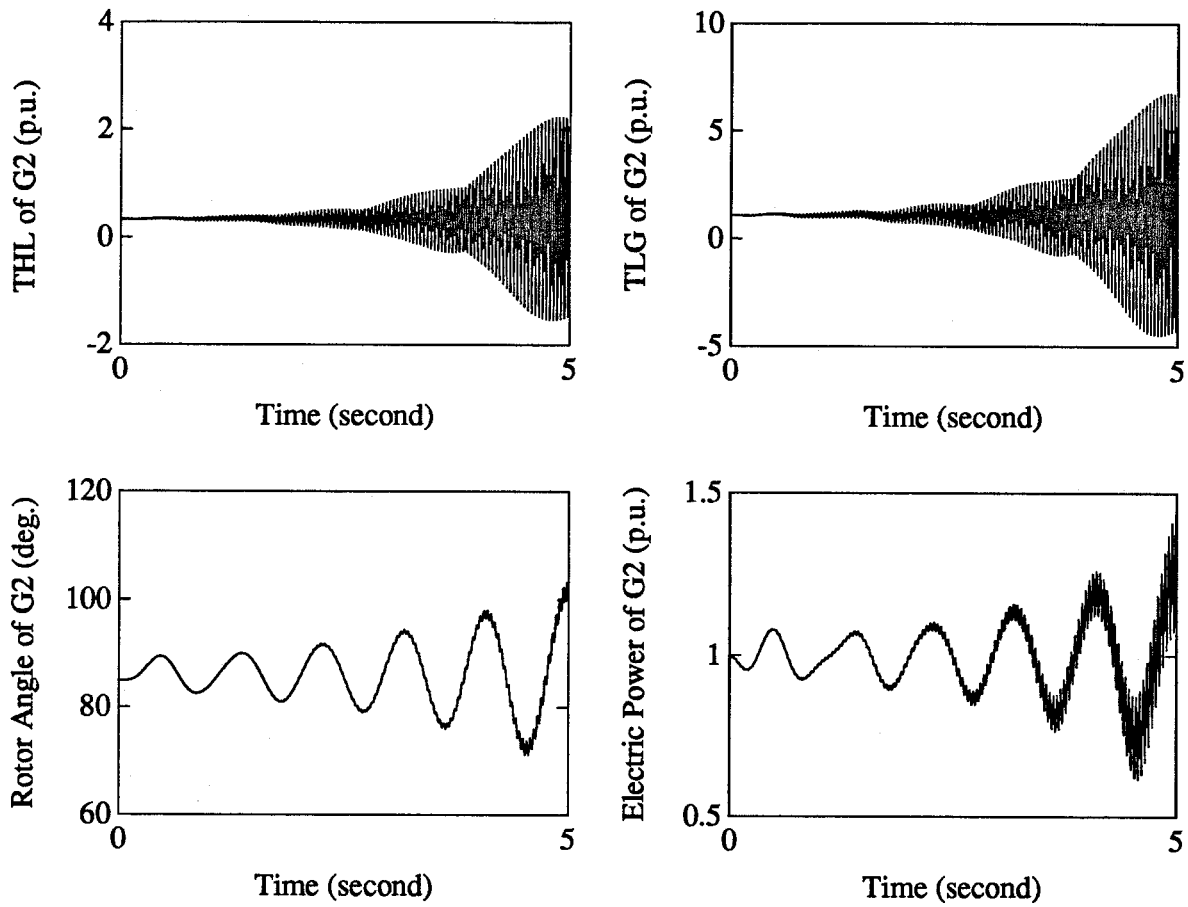

THL: Shaft torque between high and low pressure turbines
TLG: Shaft torque between low pressure turbine and generator

(b) Responses of Generator 2 (G2)

Figure 6.6: Responses to a Step Torque to G1 for the System without Control. (b)

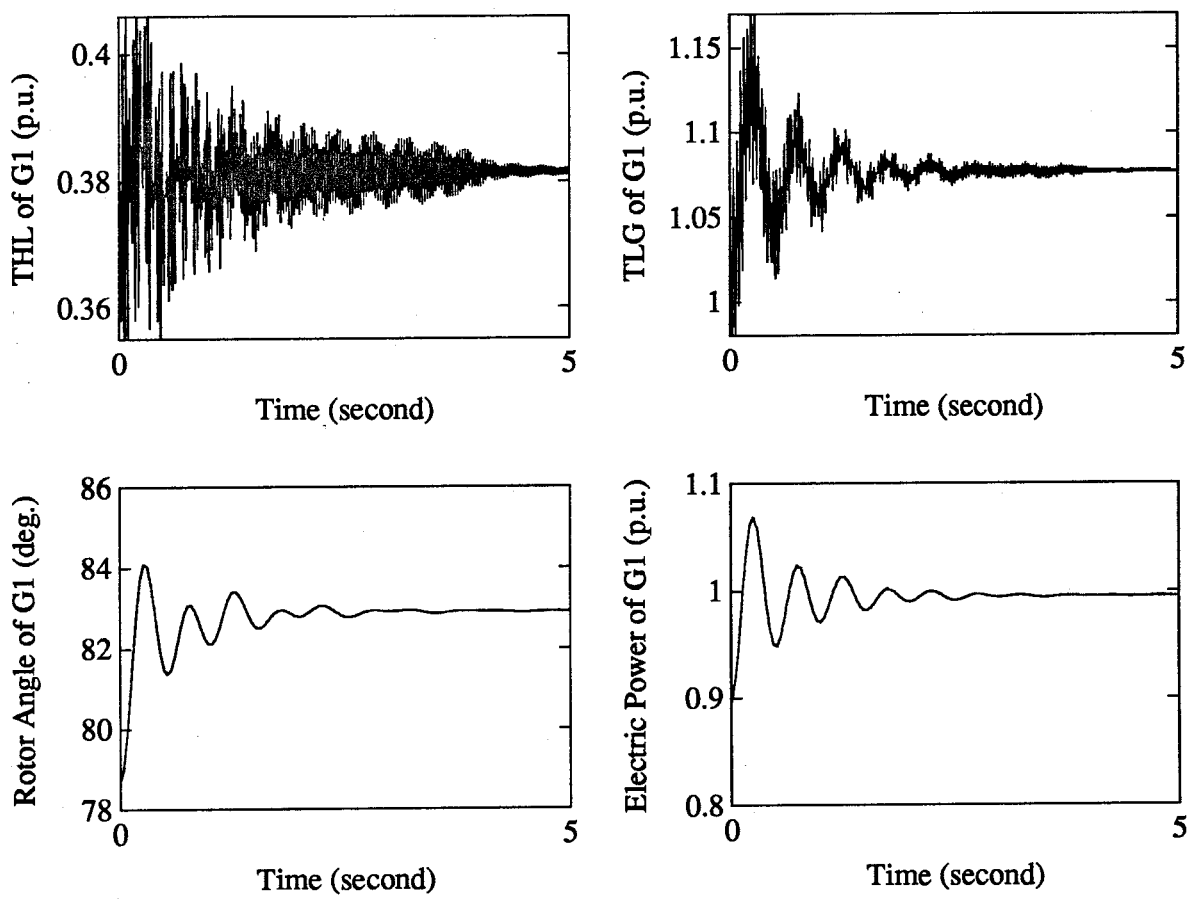

THL: Shaft torque between high and low pressure turbines
TLG: Shaft torque between low pressure turbine and generator

(a) Responses of Generator 1 (G1)

Figure 6.7: Responses to a Step Torque to G1 for the System with Control. (a)

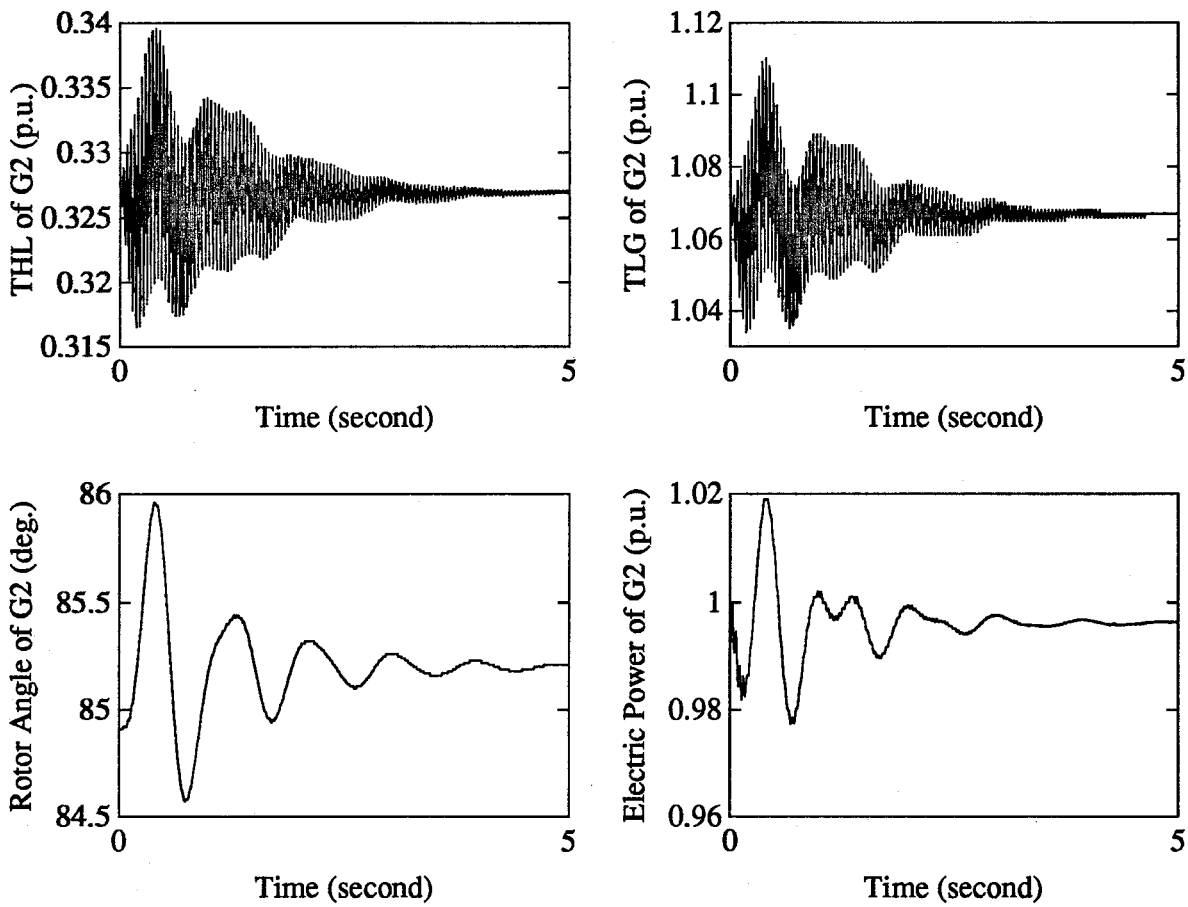

THL: Shaft torque between high and low pressure turbines
TLG: Shaft torque between low pressure turbine and generator

(b) Responses of Generator 2 (G2)

Figure 6.7: Responses to a Step Torque to G1 for the System with Control. (b)

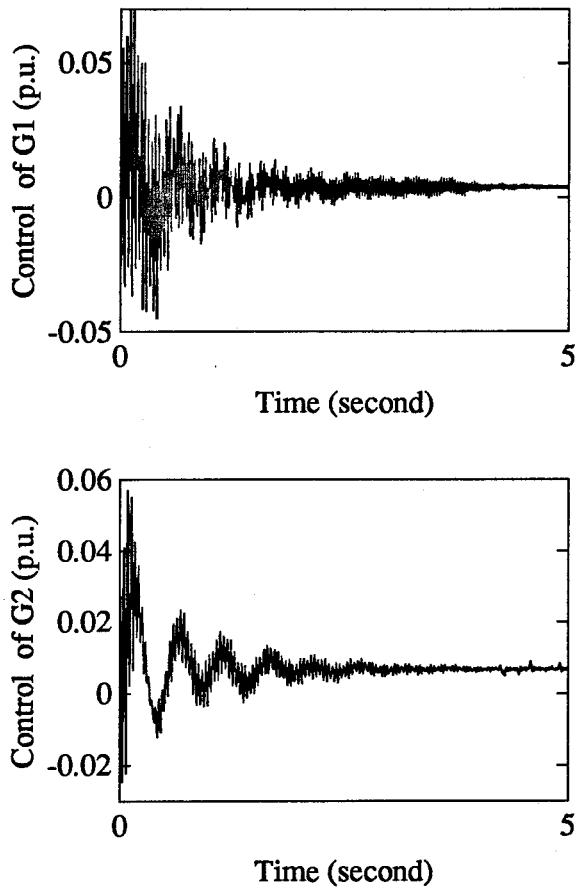

(c) Excitation Control of G1 and G2

Figure 6.7: Responses to a Step Torque to G1 for the System with Control. (c)

Chapter 7

CONCLUSIONS

7.1 New Stabilizer Design Techniques Developed

Three types of stabilizers for dynamic stability control of multimachine power systems are developed in this thesis: the coordinated and decentralized PSS in Chapter 4, the direct MIMO STR in Chapter 5, and the decentralized linear feedback stabilizer in Chapter 6. A number of new design techniques for these stabilizers are developed. They are summarized as follows:

1. Mathematical models for multimachine dynamic stability studies and for high order nonlinear simulations are developed in Chapter 2 and Chapter 6.

2. Participation factors for linear analysis and speed deviation indices (SDI) from nonlinear simulations are used in Chapter 3 for the selection of number and sites of stabilizers. The effectiveness of this method is confirmed by the PSS design in Chapter 4 and the STR design in Chapter 5.

3. A new pole–placement technique is developed in Chapter 4 for decentralized Power System Stabilizer (PSS) design for multimachine power systems with low–frequency oscillations. The PSS transfer functions are explicitly expressed in the final equations for the PSS parameter design. The computation required is much less than the existing methods.

4. A direct self–tuning regulator (STR) for a multimachine system with wide–range changing operating conditions is developed in Chapter 5. Clarke's indirect STR of GPC method is improved so that the initial step control parameters are directly estimated and that the subsequent control parameters are recursively computed. The computational requirement of the original GPC is reduced.

5. A direct pole–placement design technique for decentralized linear feedback stabilizers is developed in Chapter 6 for the stabilization of multimachine multi–mode torsional oscillations. This method is applied to the excitation control design for System 2 of Benchmark II of IEEE. For the design, a mathematical model for the system is also developed.

7.2 Applications and Conclusions

Because of the nature of different types of stabilizers for different kinds of dynamic stability problems, conclusions have been drawn for each topic at the end of each chapter. The final conclusions of applying these new stabilizer design techniques to power systems may be drawn as follows.

1. Both participation factor method of linear analysis and the speed deviation index (SDI) based on nonlinear simulations are helpful in deciding stabilizer number required for a multimachine system and the sites of stabilizer installation. Stabilizers should be installed on machines having relatively larger participation factors of unstable modes or on machines having relatively larger speed deviation indices. For the initially unstable nine–machine system, three stabilizers on machines 7, 8, and 3 are sufficient to ensure the stability of the system although there are four unstable modes and six coherent groups for the open–loop system.

2. The effectiveness of the new pole–placement PSS design technique has been demonstrated by various PSS designs of the two multimachine power systems. Exact assignment of any number of eigenvalues of low–frequency oscillating modes to new specified locations can be achieved for all designs. Non–uniform damping factors can be assigned to the eigenvalues to be changed. Assigning a relatively large damping factor to an unstable mechanical mode can also improve the damping of poorly damped mechanical modes nearby through the dynamic interaction of machines.

3. The principle and method of the direct MIMO STR developed are applied to the STRs design of a nine–machine power system. Comprehensive simulation results show that the STRs thus designed can effectively stabilize a power system over a wide range of changing operating conditions while the stabilizers with fixed parameters may fail to do so. Therefore, further exploration of STR design is necessary to the benefit of power system stability control.

4. The new direct pole-placement method is successfully applied to an excitation control design to damp torsional oscillations of system 2 of the SBM. Effective feedback signals can be found from participation factor analysis and all unstable mode eigenvalues of the system can be shifted directly to exact new positions without iteration. The stabilizers thus designed can effectively damp out multi–torsional–mode subsynchronous oscillations of the system over a wide range of capacitor compensations although the stabilizers are designed for a particular degree of compensation.

7.3 Future Research

Further research shall be done on both analyses and applications. For example, although poles can be shifted to the desired locations with the developed pole–placement method, it needs a method to analytically decide where poles should be shifted for optimal dynamic

stability control. As for the self–tuning control of Chapter 5, the output and control horizons $n1$ and nu are chosen so far by users and the analytical relationship between these chosen horizons and stability conditions are still unclear. The question is how to select the horizons under defined stability conditions. There are also the modeling problems for more complex systems with HVDC, SVC, etc. Furthermore, there are many transient stability control problems such as generator tripping, load shedding, etc. They are beyond the scope of this thesis but should be coordinated with the dynamic stability control of a power system.

Although the stabilizers presented in the thesis prove very effective for dynamic stability control of power systems from computer simulations, more work remains to be done to implement them in real power systems. These include instrumentation, data acquisition, and communication, especially for self–tuning stabilizers.

Bibliography

[1] T.J. Hammons and D.J. Winning, "Comparisons of synchronous–machine models in the study of the transient behaviour of electrical power systems," Proc. IEE 118 (10), pp 1442–1458, 1971.

[2] L.M. Hovey and L. A. Bateman, "Speed regulation tests on hydro station supplying an isolated load," IEEE Trans.on PAS, pp.364–371, Oct. 1962.

[3] Yao-nan Yu, W.Y. Xu, Q. Lu et al. , "Decentralized stabilizers for electric power systems," IMACS 1988 12th World Congress on Scientific Computation Proceedings, Paris, Vol 1, 270-273, July 1988.

[4] H.W. Dommel, Electromagnetic Transients Program Reference Manual (EMTP Theory Book), Department of Electrical Engineering, the University of British Columbia, Vancouver, B.C., Canada, 1986.

[5] F.P. deMello, P.J. Nolan, T.F. Laskowski, and J.M. Undrill , "Coordinated application of stabilizers in multimachine power systems," IEEE Trans. on PAS, pp.892-901, May/June 1980.

[6] Zuze Weng, "Selection of optimal sites in large power system for PSS installation using eigenvector analysis," J.Electr.Engg. (China), NO.4, 1982.

[7] I.J. Perez-Arriaga, G.C. Verghese and F.C. Schweppe, "Selective modal analysis with applications to electric power systems," IEEE Trans.on PAS, Pt.I, pp.3117-3125, Sept. 1982.

[8] G.C. Verghese, I.J. Perez-Arriaga and F.C. Schweppe, "Selective modal analysis with applications to electric power systems," IEEE Trans.on PAS, Pt.II, PP. 3126-3134, Sept. 1982.

[9] Y.Y. Hsu and C.L. Chen, "Identification of optimum location for stabiliser applications using participation factors," IEE Proc. C, Gen., Trans.& Distrib., Vol.134,(3), pp.238-244, 1987.

[10] T.Hiyama, "Coherency-based identification of optimum site for stabiliser applications," IEE Proc. C, Gen., Trans.& Distrib., Vol.130,(2),pp.71-74, 1983.

[11] Yao-nan Yu and Qinghua Li, "Pole-placement power system stabilizers design of an unstable nine-machine System," IEEE Trans.on PWRS, Vol.5, No.2, pp. 353-357, May 1990.

[12] Yao–nan Yu and Qinghua Li, "Coordinated power system stabilizers design of a nine–machine system," Proceedings of the International Conference on Power System Technology, Beijing, Vol.1, pp. 116–121, Sept., 1991.

[13] E.V. Larsen and D.A. Swann, "Applying power system stabilizers," Part I, IEEE Trans. on PAS, pp. 3017-3024, June 1981.

[14] Yao-nan Yu, "Electric Power System Dynamics," (book) Academic Press, New York, 1983.

[15] H.A. Moussa and Yao–nan Yu, "Dynamic interaction of multimachine system and excitation control," IEEE Trans. on PAS, pp. 1150–1158, July/Aug. 1974.

[16] R.J. Fleming, M.A. Mohan and K. Parvatisam, "Selection of parameters of stabilizers in multimachine power systems," IEEE Trans. on PAS, pp. 2329-2333, May 1981.

[17] H.B. Gooi, E.F. Hill, M.A. Mobarak, D.H. Thorne and T.H .Lee, "Coordinated multi-machine stabilizer settings without eigenvalue drift," IEEE Trans. on PAS, pp.3879–3887, Aug. 1981.

[18] S. Lefebvre, "Tuning of stabilizers in multimachine power system," IEEE Trans. on PAS, pp.290–299, Feb. 1983.

[19] C.M. Lim and S. Elangovan, "A new stabilizer design technique for multimachine power systems," IEEE Trans. on PAS, pp.2393–2400, Sept. 1985.

[20] C. L. Chen and Yuan-Yih Hsu, "Coordinated Synthesis of multimachine power system stabilizer using an efficient decentralized modal control (DMC) algorithm," IEEE Trans. on PWRS, pp.543–551, Aug. 1987.

[21] Yao-nan Yu and C. Siggers, "Stabilization and optimal control signals for a power system," IEEE Trans. on PAS, July/August, 1971.

[22] K.J. Åström & B. Wittenmark, "On self–tuning regulators," Automatica, pp.185–199, 9, 1973.

[23] D.W. Clarke & P.J. Gawthrop,"Self–tuning control," Proc.IEE 126 (6), pp.633–640, 1979.

[24] A.Y. Allidina and F.M. Hughes, "Generalised self–tuning controller with pole assignment," IEE Proc.D, 127 (1), pp.13–18, 1980.

[25] P.E. Wellstead, D.L. Prager and P. Zenker, " Pole assignment self–tuning regulator," Proc.IEE 126 (8), pp.781–787, 1979.

[26] D.L. Prager and P.E. Wellstead, "Multivariable pole assignment self–tuning regulator," IEE Proc. Vol.128, Pt.D, No.1, pp.9–18, Jan. 1981.

[27] B.E. Ydstie, L.S. Kershenbaum and R.W.G. Sargent, "Theory and application of an extended horizon self–tuning controller," A.I.Che.J. v.31, no.11, pp.1771-1780, 1985.

[28] K.S. Lee & W.K. Lee, "Extended discrete time multi–variable adaptive control," Int.J.Control, Vol.38, pp.495–514, 1983.

[29] D.W. Clarke, C. Mohtadi and P.S. Tuffs, "Generalized predictive control, pt.1: the basic algorithm," Automatica, 23, pp.137–148, 1987.

[30] G.A. Dumont and P.R. Belanger, "Successful industrial application of advanced control theory to a chemical process," IEEE Control System, I.1, 1981.

[31] L. Keviczky, J. Hetthessy, H. Hilger and J. Kelestori, "Self–tuning adaptive control of cement raw material blending," Automatica, 14, pp.525–533, 198.

[32] Shi–jie Cheng, O.P. Malik and G.S. Hope, "Self– tuning stabilizer for a multimachine power system," IEE Proc. Pt.C, Vol.133, pp.176–188, 1986.

[33] Q.H. Wu and B.W. Hogg, "Adaptive controller for a turbogenerator system," IEE Proc. Pt.D, Vol 135, pp.35–42, 1988.

[34] C.J. Wu & Y.Y. Hsu, "Design of self–tuning PID power system stabilizer for multimachine power system," IEEE Trans.on PWRS, pp.1059–1064, Aug. 1988.

[35] C.M. Lim, "A Self-tuning Stabilizer for excitation or governor control of power systems," IEEE Trans. on EC, pp.152–159, June 1989.

[36] N.C.Pahalawaththa, G.S.Hope & O.P.Malik, "Multivariable self–tuning power system stabilizer simulation and implementation studies," 89 WM 016–7 EC ,1989 IEEE PES Winter Meeting.

[37] Wenyan Gu and K.E. Bollinger, "A self–tuning power system stabilizer for wide–range synchronous generator operation," IEEE Trans. on PWRS, PP. 1191–1199, August 1989.

[38] D.W. Clarke,"Implementation consideration of self–tuning controllers,"- Numerical Techniques for Stochastic Systems (book), F.Archetti and M.Cugiani (Eds), North Holland, 1980.

[39] Yao–nan Yu and Qinghua Li , "MIMO direct self–tuning regulators for a multimachine power system," Proceedings of the International Conference on Power System Technology, Beijing, Vol. 1, pp. 85–91, Sept., 1991

[40] H.A.M.Moussa and Yao–nan Yu,"Optimal power system stabilization through excitation and/or governor control," IEEE Trans.on PAS, pp.1166–1174, 1972.

[41] R.G. Farmer, A.L. Schwalb and E. Katz, "Navajo project report of subsynchronous resonance analysis and solutions," IEEE Trans. on PAS, pp.1226–1232, July/Aug. 1977.

[42] IEEE SSR Working Group, "First benchmark model for computer simulation of subsynchronous resonance," IEEE Trans. on PAS, pp.1565-1572, Sept./Oct. 1977.

[43] IEEE SSR Working Group, "Second benchmark model for computer simulation of subsynchronous resonance," IEEE Trans. on PAS, pp.1057-1066, May 1985.

[44] IEEE SSR Working Group, "A bibliography for the study of subsynchronous resonance between rotating machines and power systems," IEEE Trans. on PAS, pp.216-218, Jan/Feb 1976.

[45] IEEE SSR Working Group, "First supplement (of [44])," IEEE Trans. on PAS, pp.1872-1875, Nov/Dec 1979.

[46] IEEE SSR Working Group, "Second supplement (of [44])," IEEE Trans. on PAS, pp.321-327, Feb. 1985.

[47] A.M. El–Serafi and A.A. Shaltout, "Control of subsynchronous resonance oscillations by multi–loop excitation controller," IEEE PES 1979 Winter Meeting, IEEE Paper A79 076-1.

[48] IEEE Committee Report, "Dynamic models for steam and hydro turbines in power systems," IEEE Trans. on PAS, pp.1904–1915, Nov./Dec. 1973.

[49] IEEE Committee Report, "Computer Representation of excitation systems," IEEE Trans. on PAS, pp.1460–1464, June 1968.

[50] Qinghua Li, Di–zhi Zhao, Yao–nan Yu, "A new pole–placement method for excitation control design to damp SSR of a nonidentical two–machine system," IEEE Trans. on PWRS, pp.1176–1181, August 1989.

[51] Yao–nan Yu, M.D. Wvong, and K.K. Tse,"Multi–mode wide–range subsynchronous resonance stabilization," IEEE PES Summ. Meeting, 1978, IEEE Paper A78 554–8, Los Angeles, July 1978.

[52] Li Wang, Yuan–Yi Hsu,"Damping of subsynchronous resonance using excitation controllers and static VAR: A comparison study," IEEE Trans. on Energy Conversion, pp.6–13, March 1988.